REGULATION OF HOST CELL VESICLE TRAFFICKING AND PROTEIN TRANSLATION BY *LEGIONELLA PNEUMOPHILA* EFFECTORS

by

Alix Kristyn McCloskey

A Dissertation

Submitted to the Faculty of Purdue University

In Partial Fulfillment of the Requirements for the degree of

Doctor of Philosophy

Department of Biological Sciences

West Lafayette, Indiana

December 2019

THE PURDUE UNIVERSITY GRADUATE SCHOOL
STATEMENT OF COMMITTEE APPROVAL

Dr. Zhao-Qing Luo, Chair
Department of Biological Sciences
Dr. Peter Hollenbeck
Department of Biological Sciences
Dr. Daoguo Zhou
Department of Biological Sciences
Dr. Mohamed Seleem
Department of Comparative Pathobiology

Approved by:

Dr. Janice Evans
Head of the Department of Biological Sciences

To my mother Ruth Jean McCloskey, my father Kevin Lee McCloskey, my Aunt Dr. Carol Post, my Uncle Dr. Jeffrey Bolin and my love Dr. Shane Sullivan for the limitless support I have received. Thank you!

ACKNOWLEDGMENTS

I would like to begin by thanking my advisor Dr. Zhao-Qing Luo. Dr. Luo has taught me a vast amount. He has taught me how to be a good experimentalist, how to think critically, how to plan ahead and work efficiently, the importance of communication and the need for accuracy and clarity. He has been incredibly supportive and generous, not to mention tough when he needed to be. Thank you Dr. Luo.

I want to of course thank all the members of the Luo Lab, those past and present. Thank you Dr. Yao Liu for helping me from the very start. Thank you Ninghai for your welcoming and friendly conversations, as well as your useful scientific input and general assistance around the lab. Thank you Victor Roman for your patience, invaluable advice and moral support. Thank you Kayla Perri for putting up with my constant blabbing and your contribution to this very thesis. Thank you Dr. Jiazhang Qiu for your intellectual support and patience while I learned to navigate the lab. Thank you Dr. Canhua Lu for the careful experimental teaching. Thank you Dr. Jiaqi Fu for all your help with the AKTA system. You are invaluable!! Finally, thank you Yan Liu and Chuang Li for the fun times both in lab and out!

An extra special thank you to my aunt and uncle Dr. Carol Post and Dr. Jeff Bolin for the many hours a week you spent giving advice, feeding me food, taking care of my dogs and generally being there for me when I needed you most. I also want to thank my siblings, Myndi Brooks and Galen McCloskey. You two will forever be a part of me and I may not always show it, but I appreciate everything you do and everything you are. I also want to thank my grandma, Becky Post, for being patient, caring and giving throughout my entire life. To all of my family: Jack, Di, Dusty, Jan and all my cousins I would never have accomplished everything I have without your support, guidance and company. Thank you!

Finally, I want to thank my boyfriend, partner and best friend, Dr. Shane Sullivan. Shane, you have been vital to my wellbeing. You have given me unwavering love, support and laughter. You have put up with my ugliest moods and craziest highs and never once showed any inkling of losing your patience. You are a saint! You are my rock and my guiding light. Thank you for everything you have done and everything you will do, because I am sure you will continue to fight the good fight!

TABLE OF CONTENTS

LIST OF TABLES

LIST OF FIGURES

ABSTRACT

Author: McCloskey, Alix, K. PhD
Institution: Purdue University
Degree Received: December 2019
Title: Regulation of Host Cell Vesicle Trafficking and Protein Translation by *Legionella pneumophila* Effectors
Committee Chair: Dr. Zhao-Qing Luo

The intracellular bacterial pathogen *Legionella pneumophila* is the etiological agent of Legionnaires' disease, a severe pneumonia; it has also served as a valuable tool in studying host-pathogen interactions. The study of *L. pneumophila* pathogenesis has led to the discovery of novel biochemical and enzymatic mechanisms and a better understanding of host cell immune responses and signaling. *L. pneumophila* replicates within eukaryotic cells through the use of a type IV secretion system and over 330 effector proteins injected into the host cell. Only approximately 10% of these effectors have been characterized, but regardless of the small fraction, the complexity of *L. pneumophila* infection is clear. A good demonstration of this complexity is the large number of effector activities the bacteria uses to manipulate the small GTPase involved in ER to Golgi trafficking, Rab1. Six different effectors with eight separate activities modulate the activity of Rab1 to aid in the replication of the bacteria. We recently discovered that the protein SetA is yet another effector targeting Rab1. SetA glucosylates Rab1 using a canonical DxD motif and the glucose moiety interferes with both GTP hydrolysis and guanosine nucleotide dissociation inhibitor (GDI) binding. Based on our findings, the role of SetA is likely to aid in maintaining a pool of free Rab1, increasing availability for use by other *L. pneumophila* effectors. Another example of the complexity of *L. pneumophila* pathogenesis is the use of metaeffectors. Metaeffectors are effectors that regulate other effectors, both being produced by *L. pneumophila*. Three mechanisms of metaeffector regulation have been identified: 1) removal of a modification on host proteins placed by the cognate effector, 2) direct modification of the cognate effector or 3) direct binding to the cognate effector. Through the use of Size Exclusion Chromatography (SEC), binding assays with purified proteins and bacterial two-hybrid analysis, we found the mechanism of regulation for the SidI metaeffector Lpg2505 to be inactivation through direct binding. Atypical of previously identified effector characteristics, the binding of SidI by Lpg2505 occurs within the bacterial cell prior to translocation. The expression pattern of both effectors in *L. pneumophila* in

addition to the other findings suggest a temporal role for Lpg2505 activity in which inactivation of SidI occurs after sufficient bacterial replication has occurred.

CHAPTER 1. GENERAL INTRODUCTION

Legionella pneumophila environmental reservoir

Legionella pneumophila is a gram negative, intracellular bacterial pathogen found in freshwater environments where it parasitizes multiple, diverse species of free-living protozoa from genera such as *Acanthamoeba*, *Naegleria*, and *Hartmanella* (Fields, 1996; Fliermans et al., 1981; Rowbotham, 1980). After phagocytosis, *L. pneumophila* replicates within the protozoan cell by manipulating various host processes and acquiring necessary resources. Once sufficient replication has occurred and the nutrients are depleted, the bacteria will lyse the host and egress back into the water environment to continue the infection cycle (Anand, Skinner, Malic, & Kurtz, 1983). The environmental *L. pneumophila* lifecycle is important because the fresh water/protozoan reservoir is the main source for human infection (Berk, Ting, Turner, & Ashburn, 1998; Cirillo et al., 1999; Cirillo, Falkow, & Tompkins, 1994) and the relationship between the protozoan hosts and the bacteria has contributed to the evolution of an incredibly efficient intracellular pathogen (Gomez-Valero & Buchrieser, 2019; Hoffmann, Harrison, & Hilbi, 2014).

Legionnaires' disease

The discovery of *L. pneumophila* as a human pathogen occurred after an outbreak of severe pneumonia during a 1976 American Legion Convention in Philadelphia, thus the pneumonia was appropriately named Legionnaires' disease (LD) (Brenner, Steigerwalt, & McDade, 1979; Fraser et al., 1977; McDade et al., 1977). Since the initial identification of *L. pneumophila* as the etiological agent of LD, nationwide surveillance has recorded multiple outbreaks across the country, which are typically associated with contaminated, aerosolized water sources such as cooling towers, showers, gardens and water fountains ("From the Centers for Disease Control and Prevention. Legionnaires' disease associated with cooling towers--Massachusetts, Michigan, and Rhode Island, 1993," 1994; Hilbi, Hoffmann, & Harrison, 2011; Kanamori, Weber, & Rutala, 2016; Rubin, 2017). Isolated, single-source outbreaks are the most common routes of infection, and although there has been a single report of human to human transmission, this is thought to be an extremely rare occurrence (Correia et al., 2016). Symptoms associated with LD are flu-like, as they most often consist of fever, cough, chills, and sometimes myalgia or arthralgia (Cunha,

Burillo, & Bouza, 2016). Most people infected with *L. pneumophila* clear the infection on their own in just a few weeks. For the immunocompromised, including patients undergoing cancer treatment, post-transplant surgery, or infected with HIV, their immune systems are not sufficient to clear the infection and intervention with antibiotics is necessary (Gudiol, Verdaguer, Angeles Dominguez, Fernandez-Sevilla, & Carratala, 2007; Lanternier et al., 2013; Sandkovsky et al., 2008; Singh, Stout, & Yu, 2004). Levofloxacin, azithromycin and doxycycline are considered standard, initial antibiotic therapies due to their efficient, intracellular bioactivity and effectiveness against *L. pneumophila* (Cunha et al., 2016).

Legionella pneumophila and the host cell

L. pneumophila is an environmental pathogen, with a continuous lifecycle and repeated parasitism of protozoan hosts. Human infection is believed to be "accidental", as humans are a dead end for the bacteria, and subsequently, human infection likely does not inflict high evolutionary pressure. As such, most human infections are mild and short-lived (Khodr et al., 2016). Infections in humans occur after inhalation of the bacteria via aerosolized water droplets. Once in the lungs, the bacteria are phagocytosed by alveolar macrophages. Instead of degradation through the lysosomal pathway, the bacteria immediately begin to alter the course of the phagosome preventing fusion with the lysosome and maturing into a unique, replication-permissive niche termed the *Legionella* containing vacuole (LCV) (Isberg, O'Connor, & Heidtman, 2009). Within minutes, the LCV associates with mitochondria and endoplasmic reticulum (ER)-derived vesicles. Approximately 15 minutes after bacterial uptake, the thickness of the phagosomal membrane reduces and resembles the thickness of the membrane of the ER-derived vesicles associated with the LCV. Several hours after uptake, ribosomes decorate the LCV membrane and the volume of the LCV increases (Tilney, Harb, Connelly, Robinson, & Roy, 2001). The bacteria then replicate within the LCV using nutrients such as amino acids, glucose, glycerol and iron, imported from the host (Eisenreich & Heuner, 2016; O'Connor et al., 2016). *L. pneumophila* has a biphasic lifecycle and once nutrients become limited, the bacteria differentiate from the non-motile vegetative form to a flagellated, stress-resistant infectious form, otherwise known as the transmissive form (Eisenreich & Heuner, 2016). How the bacteria egress from the LCV and later the host cell is not well understood. Evidence for bacterially triggered pore formation followed by pyroptosis, or a requisitioned exocytic pathway after infection in protozoan hosts, have been presented as viable means of release

from the host cell (Chen et al., 2004; Molmeret, Bitar, Han, & Kwaik, 2004; Silveira & Zamboni, 2010).

The *Legionella pneumophila* protein translocation system

The main virulence factor for *L. pneumophila* is the type IV secretion system called Dot/Icm for defect in organelle trafficking/intracellular multiplication. Identification of the Dot/Icm system was achieved by studying *L. pneumophila* mutants that lost the ability to replicate within macrophages and the genomic regions capable of rescuing the defect through complementation. One such mutant developed through multiple passes on suboptimal media was incapable of intracellular growth due to defectiveness in inhibiting phagosome-lysosome fusion. The mutant was also avirulent in animals. After introducing a library of wild-type *L. pneumophila* DNA within a plasmid to the mutant, Marra *et al.* screened for transformants that were able to generate plaques on monolayers of human macrophages at a level comparable to wild-type *L. pneumophila*. They identified the specific genomic region necessary to restore wild-type replication and designated the locus *icm* (Horwitz, 1987; Marra, Blander, Horwitz, & Shuman, 1992). At the same time, another research group found a similar genomic region capable of complementing two different classes of mutants, both defective for intracellular replication. The mutants were identified through a reduction in plaque formation after insertion of a transposable element and subsequent enrichment of thymidine auxotrophs using intracellular survival. The class I mutant was defective in organelle recruitment but was still capable of phagosome-lysosome fusion inhibition. The class II mutants were defective in both. The authors proposed that phagosome-lysosome fusion inhibition alone was not sufficient for intracellular growth, that manipulation of organelle trafficking was also necessary. The authors identified a complementing genomic region able to rescue intracellular replication for both classes of mutants and named the region *dot* (Karen H Berger & Isberg, 1993).

A short time later, Berger *et al.* identified a single open reading frame (ORF) within the *dot* region and designated it *dotA*. They determined that truncated versions of the gene lead to the replication defect phenotype and that the *dotA* product is necessary for intracellular replication within cultured macrophages. They also found that the predicted product had a large hydrophobic region in the C-terminus, leading them to theorize a possible interaction between DotA and lipid bilayers (K. H.

Berger, Merriam, & Isberg, 1994). Another group identified 4 genes within a 4 kb fragment of the *icm* locus that were necessary for intracellular multiplication. The genes form an operon which lays adjacent to, but is transcribed in the opposite direction from, the *dot* locus. They designated the four genes *icmWXY* and *Z* (Brand, Sadosky, & Shuman, 1994). An additional six genes, found within the *icm* locus, were also shown to be required for intracellular replication (*icmTSRQPO*). The predicted products for two (*icmPO*) out of the six genes had significant homology to *Salmonella* proteins involved in plasmid transfer, and when a *L. pneumophila* strain lacking expression of *icmP* or *O* was assayed for plasmid conjugation, the result was a 30-fold reduction in efficiency (G Segal & Shuman, 1997). Over time more *icm* and *dot* genes were analyzed and found to be involved in DNA transfer and to be necessary for replication in macrophages (Gil Segal, Purcell, & Shuman, 1998; Vogel, Andrews, Wong, & Isberg, 1998). A short time later, similarity between the *dot*/*icm* products and the proteins involved in the transfer of the IncI1 plasmid R64 led to the categorization of Dot/Icm as a type IV secretion system (T4SS) (Komano, Yoshida, Narahara, & Furuya, 2000). Ultimately, close to 30 *icm*/*dot* genes have been identified with products functioning as membrane channel proteins, ATPases, chaperones for translocated substrates, etc., (Buscher et al., 2005; Ninio, Zuckman-Cholon, Cambronne, & Roy, 2005; Vincent et al., 2006). A recent study revealed that the Dot/Icm system localizes to the bacterial poles and that the polar export of effectors is critical for a successful infection, a phenomenon not yet found for other pathogen secretion systems (Jeong, Ghosal, Chang, Jensen, & Vogel, 2017). Two additional studies, also very recent, used cryo-EM to visualize the Dot/Icm system *in situ*. Details of the structure, including the channel which directs translocated substrates, the DotB-DotO ATPase complex location and the presence of a plug potentially regulating movement through the secretion system were revealed, representing a large leap in the understanding of the functional dynamics of T4SSs (Chetrit, Hu, Christie, Roy, & Liu, 2018; Ghosal, Chang, Jeong, Vogel, & Jensen, 2017).

Legionella pneumophila effector proteins

Identification of effector genes

It was not until the discovery of RalF by its signature Sec7 motif, identified through bioinformatic analysis of the genome sequence, that the type of molecule transported through the Dot/Icm system

was confirmed (Donaldson & Jackson, 2000; Nagai, Kagan, Zhu, Kahn, & Roy, 2002). RalF is a guanine nucleotide exchange factor (GEF) for the small G-protein ARF1 involved in membrane trafficking from the ER to the Golgi. Although the short period of time (just minutes) needed for *L. pneumophila* to begin to alter the course of the phagosome, in a Dot/Icm-dependent manner, was early evidence that DNA was likely not the molecule being secreted into host cells (Vogel & Isberg, 1999). RalF was found by searching for *L. pneumophila* proteins with homology to eukaryotic ARF1 GEFs, after the discovery that ARF1 localizes to the LCV and that this localization requires the Dot/Icm system. It was shown that RalF was capable of ARF1 activation, that RalF colocalized with ARF1 on the LCV, and that RalF was necessary for ARF1 recruitment to the LCV. The authors also showed that RalF was not necessary for intracellular replication, as the Δ*ralF* mutant grew just as well as the wild-type in cultured macrophages and amoeba (Nagai et al., 2002). The lack of a growth defect is why *ralF* was not discovered in any of the defective intracellular growth mutant screens and was the initial indication that identification of individual effector proteins would require screens that did not rely on an intracellular growth defect.

The discovery of RalF stimulated the identification of additional Dot/Icm substrates using innovative methods that did not rely on a replication defect. One of the earliest such screens led to the identification of over 40 potential effector genes using the T4SS protein DotF as bait in bacterial two hybrid screenings and a bacterial cell-to-cell translocation assay using the *cre*/*loxP* system. Through this study, the genes *sidA-H*, as well as several paralogs of those genes, were identified. When strains containing deletions of the *sid* genes were assayed for intracellular growth, only the Δ*sdeC* mutant showed a discernible defect. This study therefore provided additional evidence that elimination of a single *Legionella* effector rarely causes an intracellular growth defect (Luo & Isberg, 2004).

Two following studies used the easily culturable and genetically tractable *Saccharomyces cerevisiae* as a tool to study the interactions between *L. pneumophila* proteins and a lower eukaryote model. Using the knowledge that elimination of conserved secretory proteins, such as ARF1 and Sar1, lead to growth defects in *S. cerevisiae*, Campodonico *et al.* assayed a strain ectopically expressing the ARF1 GEF *ralF*. When *ralF* was induced, the yeast showed a pronounced growth defect. The authors also ectopically produced the RalF $E_{103}A$ mutant to verify

the toxic phenotype was caused by the GEF activity of RalF and saw growth equivalent to a strain containing only empty vector. The authors then screened a plasmid encoded, random *L. pneumophila* genomic library in yeast looking for clones that no longer grew under inducible conditions. Only ten out of 10,500 clones displayed the toxic phenotype, revealing the level of stringency associated with the screen. The authors focused on one *L. pneumophila* gene, *ylfA*, to validate the approach as a means of identifying Dot/Icm substrates. They found that indeed YlfA was translocated into the host cell during *L. pneumophila* infection and that it could be detected on ER-derived replicative vacuoles. They also used *S. cerevisiae* growth as a readout to study the different domains of YlfA and found that both an N-terminal hydrophobic domain and an adjacent coiled-coil region were necessary for YlfA-dependent growth restriction. This result demonstrated the usefulness of *S. cerevisiae* to analyze the function of *L. pneumophila* effectors (Campodonico, Chesnel, & Roy, 2005). The second study used a chromogenic yeast phenotype readout to measure inhibition of vacuolar traffic based on the ectopic expression of a random *L. pneumophila* library. Through this screen the authors found 3 genes that specifically interfered with the VPS (vacuole protein sorting) system and were named *vipA, vipD* and vip*F* for VPS inhibitor protein. Through a cyclase translocation assay, all three proteins were shown to be Dot/Icm substrates. The authors suggested that the yeast VPS screen could also be useful to study virulence factors of other pathogens known to modulate host cell trafficking (Shohdy, Efe, Emr, & Shuman, 2005).

Another screen took advantage of the previously published genome sequence of the *L. pneumophila* strain Philadelphia-1 (Chien et al., 2004). The authors scanned all identified ORFs using bioinformatic tools such as PSI-BLAST and SMART, looking for amino acid sequences that could be classified as “eukaryotic domains”. They refined their search process by eliminating any genes that had a high prevalence in other prokaryotes. Through this process they found 46 previously uncharacterized genes as well as 16 genes that had already been studied. They confirmed that several of the genes from their screen are translocated into host cells by the Dot/Icm system and up-regulated during stationary growth of the bacteria, specifically during the transmissive phase. In addition, they also provided evidence supporting the theory that the eukaryotic-like domains were acquired through horizontal gene transfer (HGT) (de Felipe et al., 2005).

An additional screen used the presence of particular amino acids found at the carboxy terminus of known Dot/Icm substrates to find other proteins with similar sequences and therefore predicted to be translocated by the Dot/Icm system. The study identified 19 novel effector proteins that were shown to be translocated in a Dot/Icm-dependent manner and solidified the idea that the specific structure of the carboxy terminus of effector proteins acted as a signal for translocation (Kubori, Hyakutake, & Nagai, 2008). Another group developed a comprehensive algorithm incorporating the knowledge gained from effectors already identified. Using the algorithm in a machine learning approach they predicted which *L. pneumophila* ORFs were potential translocated substrates. Once predicted, effectors were validated experimentally, and were then incorporated back into the algorithm to refine the approach. Using this technique, in a 3-phase process, the authors found 40 previously uncharacterized predicted effector proteins. The 40 predicted effectors were named using Lem for *Legionella* effector identified by machine learning (Burstein et al., 2009).

The pool of identified *L. pneumophila* translocated substrates grew substantially with two screens using *L. pneumophila* fusion proteins that generated microscopically visible signals once inside the host cell. Huang *et al.* fused the C-termini of over 400 genes to *sidC* minus the last 100 residues and expressed the fused genes in *L. pneumophila*. The strains were then used to infect primary macrophages in 96-well plates. Each infection was stained with the highly specific anti-SidC antisera and recorded microscopically to quantify the levels of detectable SidC fusion proteins. A total of 49 additional effector proteins were identified using this method (Huang et al., 2011). The second screen fused *L. pneumophila* ORFs, predicted to code for hypothetical proteins, to the C-terminus of β-lactamase and screened for translocated fusion proteins using fluorescence resonance energy transfer (FRET) as a readout. When a fusion protein translocated into the host cell, the β-lactamase would cleave the reporter substrate CCF4-AM, changing the color emitted from green to blue. The authors successfully fused an impressive 798 ORFs to β-lactamase, of which 164 were positive for translocation. The work revealed a substantial addition of 70 novel substrates (Zhu et al., 2011).

Phylogeny of *Legionella* effectors

Through multiple screens, such as those previously discussed, there are now over 330 predicted effector proteins for *L. pneumophila*. This is the largest known effector repertoire for a bacterial

pathogen (Ensminger, 2016). What is even more astonishing is the diversity of effectors across the *Legionella* genus. There are 65 known species of *Legionella*, of which as many as 20 have been associated with human disease, although *L. pneumophila* and *L. longbeachae* are by far the most prevalent (Diederen, 2008; Newton, Ang, van Driel, & Hartland, 2010). Two groups researched the differences in encoded virulence factors among a large portion of the known *Legionella* species. Not surprisingly, the Dot/Icm genes were fairly conserved and present in all 58 species sequenced. What was surprising however, was the vast number of different effector proteins found. Across 58 species and 80 genomes, more than 18,000 unique effector proteins were identified (Gomez-Valero et al., 2019). Amazingly, even though the genus contains a very large number of effectors, only eight were found in all the genomes tested (Lpg0103, Lpg0107, Lpg2300, Lpg2815, Lpg0140, Lpg2832, Lpg3000, Lpg1356), as such, these eight were designated the core effectors (Burstein et al., 2016; Gomez-Valero et al., 2019). In fact, the majority of *Legionella* effectors, approximately 80%, are shared by at most 10 species (Burstein et al., 2016). Both studies cited evidence for interdomain gene transfer and DNA acquisition from eukaryotic hosts. Gomez-Valero *et al.* made a phylogenetic comparison of *Legionella* species capable of replicating in human cells. They found that the species capable of growth within human cells were mixed throughout the different lineages, leading to the conclusion that this capacity was acquired multiple, independent times during the evolutionary history of the genus (Gomez-Valero et al., 2019). Gene synteny is when multiple loci are located in close proximity on the chromosome and are likely evolutionarily and functionally linked. The use of HGT by *L. pneumophila* is believed to have led to the acquisition of multiple syntenic genes (Gomez-Valero et al., 2011). The evolution of syntenic gene pairs within the different sequenced genomes was analyzed by Burstein *et al.* where they identified 19 effector pairs that were either evolutionarily gained or lost together more times than what would be expected by chance. Of these 19 pairs, some had already been shown to work together within the host cell, for example AnkX/Lem3 or SidH/LubX (their functions are described in the following section), but they also identified evolutionarily-linked pairs that were not previously studied, such as SidL/LegA11, Lpg2888/MavP and SidI/Lpg2505 (Burstein et al., 2016).

Syntenic genes in *Legionella*

The idea that syntenic effector genes interacted with each other within the host cell began with the study of SidH and LubX, two substrates of the *L. pneumophila* Dot/Icm system. Kubori *et al.*

discovered that the effector LubX, which is encoded just upstream of the gene for SidH, regulates the activity of SidH within the host cell. LubX is an E3 ubiquitin ligase that through direct interaction with SidH, leads to the polyubiquitination and subsequent degradation of SidH by the host proteasome (Kubori, Shinzawa, Kanuka, & Nagai, 2010). The role of LubX as a regulator of the effector SidH led to the designation of LubX as a metaeffector, the term to describe an effector of an effector. After some time, more effector-metaeffector pairs were identified. Some pairs consist of a metaeffector that regulates the activity of the cognate effector through removal of an effector-placed post-translational modification (PTM) on a host protein. For example, SidD removes the adenosine monophosphate (AMP) moiety ligated to Rab1 by the effector SidM/DrrA (Tan & Luo, 2011). In addition, the metaeffector Lem3 removes the AnkX-dependent phosphorylcholine modification also on Rab1 (Tan, Arnold, & Luo, 2011). The metaeffector LegL1 regulates the cognate effector RavJ by directly binding to the active site and thereby inactivating the enzyme. A fifth example is the deubiquitination of the effector LegC3 by the metaeffector LupA, rendering LegC3 inactive (Urbanus et al., 2016). Recently, the metaeffector SidJ was shown to modify the cognate effectors, proteins of the SidE family, using glutamylation, to effectively shut down their activity. The direct targeting of SidE proteins by SidJ requires the interaction of SidJ with the host protein calmodulin, thereby preventing SidE inactivation prior to translocation into the host cell (Black et al., 2019; Gan, Zhen, et al., 2019).

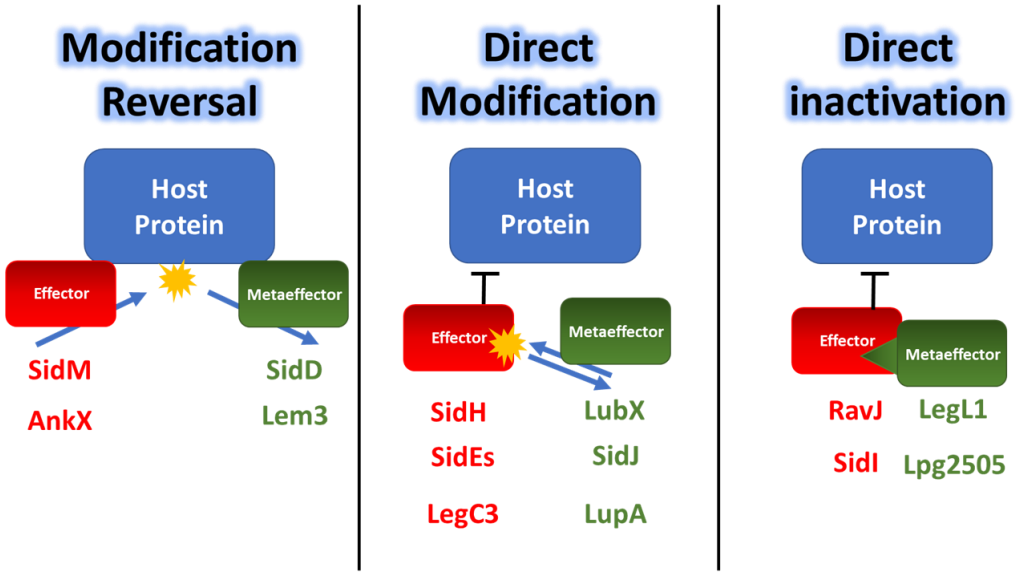

Figure 1-1. Illustration of different types of effector/metaeffector regulatory mechanisms. The metaeffectors SidD and Lem3 regulate through abrogation, by removing the effector-placed host protein modification, restoring normal function of the host protein. LubX and SidJ regulate their cognate effectors' activities by direct modification, adding a ubiquitin and a glutamate residue, respectively. LupA inhibits LegC3 by removing ubiquitin. LegL1 directly inactivates RavJ by binding to the catalytic pocket. SidI is inhibited by the metaeffector Lpg2505 also by direct binding (the relationship is discussed in detail in chapter 3).

Effector redundancy

What is fascinating about the roles of metaeffectors in *L. pneumophila* pathogenesis is that while the removal of most effectors from the chromosome does not lead to any reduction in intracellular replication, it is not uncommon to see a replication defect associated with the removal of a metaeffector (Kubori et al., 2010; Yancheng Liu & Luo, 2007; Shames et al., 2017). This phenomenon highlights the need to maintain a delicate balance when residing within the organism being parasitized. The unique characteristic that most *L. pneumophila* effectors, when removed from the chromosome, do not negatively affect intracellular replication, has made it difficult to assign their roles in bacterial infection. It seems that *L. pneumophila* takes a "shotgun" approach to parasitism and maintains a sort of redundancy in its effector arsenal. It has been proposed that the ability of *L. pneumophila* to replicate in such a diverse group of organisms (multiple species of protists and different types of professional phagocytes) could be possible because of the large and functionally redundant pool of effectors (O'Connor, Adepoju, Boyd, & Isberg, 2011). Being a generalist and having the capacity to replicate within whichever potential host is encountered could be an evolutionary advantage. It is possible that for *L. pneumophila*, groups of effectors may

target general processes common to eukaryotic cells, while the individual effectors target more specifically within certain hosts (Isberg et al., 2009). Distinguishing this type of specificity is difficult in the laboratory, but progress has been made in determining the validity of such a broad-host range explanation for *L. pneumophila*'s redundant effector repertoire.

To better understand the requirements necessary for growth in different environments, such as different hosts, O'Connor *et al.* screened a transposon mutant *L. pneumophila* library looking for regions of the chromosome that were required for growth in bacteriological media. They found that large contiguous regions of the chromosome were dispensable for growth in media. These regions differed from the rest of the genome in GC content, variability between strains, and number of encoded Dot/Icm substrates. Seven total regions were identified using their screen, and even when they deleted six out of the seven regions, the bacteria were still able to grow in media. Surprisingly, a strain missing five out of the seven regions was still able to replicate within primary macrophages. However, when they tested the requirement of the regions for growth in amoebae the results were quite different. Mutants containing different regions and different combinations of regions had differing growth defects in the three different amoebal species tested. Because the efficiency of replication within alternating hosts was dependent on the genes available and that the regions tested were likely acquired through HGT, the authors surmised that the exogenously-sourced, superfluous chromosomal regions probably contribute to the broad host range of *L. pneumophila* (O'Connor et al., 2011).

The same group used the transposon mutant library to infect *Drosophila* cells deficient in various proteins involved in the early secretory system. The deficiency of such proteins was done using RNA interference, a tactic that previously revealed *L. pneumophila* recruits vesicle traffic from multiple sources (Dorer, Kirton, Bader, & Isberg, 2006). They looked for *L. pneumophila* mutants that had similar growth phenotypes in the same knock-down mutant *Drosophila* cells. The genes associated with matching mutants were then clustered together into functional groups. For example, both Δ*lidA* and Δ*legA3* had impaired growth when either Bet5 or Sec22 were depleted, putting them together in the same functional group. Consistent with the idea that effector proteins in separate groups target redundant pathways, when two *L. pneumophila* genes from different functional groups were removed, the strain showed as much as a 60% reduction compared to the

wild-type strain in untreated *Drosophila* cells. A pattern of maintaining sets of effectors with similar functions rather than specific effector proteins was revealed, likely allowing *L. pneumophila* to suitably deal with host variation (O'Connor, Boyd, Dorer, & Isberg, 2012).

Host cell processes targeted by *Legionella pneumophila*

Immune response

Legionella pneumophila, and the *Legionella* genus as a whole, seem to target general host cell processes, typically covering multiple pathways to ensure successful host process manipulation regardless of the type of host. Multiple studies have characterized the functions of specific *L. pneumophila* effectors and the host cell processes in which they act. One of the most significant host processes for any pathogen is the immune response. This is of particular importance for an intracellular pathogen that must maintain host cell health for the duration of its lifecycle.

To learn which host systems are affected by Dot/Icm substrates during *L. pneumophila* infection, total RNA from infected macrophages was used to probe a human gene microarray looking for changes in gene expression after low-dose wild-type infection compared to a *dot/icm* mutant. The major finding was a change in the regulation of genes involved in the mitogen-activated protein (MAP) kinase and NF-κB signaling pathways, which was dependent on a functional Dot/Icm. There are five transcription factors in the NF-κB family, p65 (RelA), p50, p52, Relb and c-Rel, which form stable homo- and hetero-dimers that reside in the host cell cytoplasm. Activation of the pathway leads to loss of dimer formation and the subunits translocate into the nucleus to regulate gene expression. Specifically, p65 has been shown to upregulate antiapoptotic genes (C.-Y. Wang, Mayo, Korneluk, Goeddel, & Baldwin, 1998). When a macrophage cell line was infected with wild-type *L. pneumophila*, staining revealed p65 nuclear localization as early as 3 hours post-infection (hpi) and about half of infected cells showed p65 translocation after 6 hours. No p65 translocation was observed for the *dotA* mutant, at the same MOI, for any time point tested, indicating that the NF-κB activation observed was dependent on Dot/Icm substrates and not just a response to the invading bacteria. In addition, when NF-κB activation was blocked, indications of cell death in infected macrophages were observed as early as 6 hpi, revealing the necessity for NF-κB-dependent host cell survival during *L. pneumophila* infection (Losick & Isberg, 2006). Another

study had similar findings, but in addition, they found that even induced activation of caspase-3, a protease involved in programmed cell death and essential for specific forms of cell dismantling and formation of apoptotic bodies (Porter & Jänicke, 1999), did not affect *L. pneumophila* replication. This was presumably due to the Dot/Icm-dependent anti-apoptotic gene upregulation after NF-κB activation (Abu-Zant et al., 2007).

A short time later, a *L. pneumophila* effector capable of activating the NF-κB signaling pathway was identified. Ge *et al.* screened known effector proteins through ectopic expression in HEK293T cells harboring an NF-κB-inducible *luciferase* reporter. Out of the 100 effector proteins tested, only LegK1 was able to induce NF-κB activation. The level of activation was greater, albeit only slightly, than the well-established inducer TNFα. The authors determined that LegK1 activated the NF-κB signaling pathway by mimicking the role of the IKK complex and phosphorylating some of the members of the IκB family. The IκB family proteins are NF-κB inhibitors that retain NF-κB family members in the cytosol until phosphorylation by the IKK complex. The phosphorylation of the IκB proteins leads to their polyubiquitination and subsequent degradation, freeing NF-κB to then translocate into the nucleus. The belief is, despite triggers for programmed cell death, such as caspase-3 activation, apoptosis of the host cell is delayed long enough for the bacteria to replicate and this delay is dependent on NF-κB activation caused at least in part by the activity of LegK1 (Ge et al., 2009). Through a similar screen another *L. pneumophila* effector, LnaB for *Legionella* NF-κB activator B, which activates NF-κB, was identified. LnaB contains a coiled-coil domain that is necessary for NF-κB activation. The C-terminus of LnaB contains a region that leads to ER localization. However, localization of LnaB to the ER is not required for NF-κB activation as a cytoplasm-residing fragment of LnaB (residues 1-401) is still capable of activating NF-κB. Although the function of LnaB remains unknown, the authors theorize that either the outcome of a host protein interacting with the coiled-coil domain leads to NF-κB activation or LnaB directly interacts with a component upstream in the pathway (Losick, Haenssler, Moy, & Isberg, 2010).

Recently, the *L. pneumophila* effector MavC revealed the complexity of NF-κB regulation during infection. Both LegK1 and LnaB activate the NF-κB pathway, but MavC represses NF-κB activation. It does this by ubiquitinating the E2 enzyme UBE2N through a non-canonical mechanism. Ubiquitination of UBE2N by MavC abolishes the activity of the E2, stopping the

enzyme from forming polyubiquitin chains, and thereby preventing the activation of NF-κB. *mavC* was found to be highly expressed when the bacteria were grown to post-exponential phase and MavC-dependent suppression of NF-κB peaked within the first 30 minutes after bacterial uptake, indicating MavC's likely role in immune response suppression early in infection. There is evidence that in addition to Dot/Icm-dependent NF-κB activation, potentially detrimental activation caused by pathogen-associated molecular patterns (PAMPs) or similar means, occurs during *L. pneumophila* infection (Bartfeld et al., 2009) and the role of MavC may be to counteract such activation (Gan, Nakayasu, Hollenbeck, & Luo, 2019).

The effector protein SdhA was found to also interfere with programmed cell death during *L. pneumophila* infection, but not in a manner involving NF-κB. In 2006 Laguna *et al*. discovered a single effector gene mutant that was severely defective in macrophage replication. Elucidation of the intracellular replication defect revealed a cell death phenotype associated with caspase activation in the host after infection with the Δ*sdhA* strain (Laguna, Creasey, Li, Valtz, & Isberg, 2006). Continued work with the Δ*sdhA* strain revealed more information on how SdhA is involved in regulating host cell death. To better understand the role of SdhA during *L. pneumophila* infection Creasey *et al.* looked for suppressor mutations that rescued the ability of Δ*sdhA* to replicate in macrophages. They identified the effector PlaA, which has significant homology to a *Salmonella* protein SseJ involved in the stability of the Salmonella-containing vacuole. Evaluation of LCV stability for the Δ*sdhA* strain showed increased permeability, leading to exposure of the bacteria to the host cytosol and eventually host cell death activation and bacterial degradation. The authors concluded that SdhA plays a role in LCV membrane stability and through an unknown mechanism, the phospholipase activity of PlaA destabilizes the membrane requiring a balance between the functions of the two effector proteins (Creasey & Isberg, 2012). The cell death caused by exposure of the bacteria to the host cytosol was found to include morphological features typical of pyroptosis, including cell swelling and nuclear condensation. In line with these observations, Ge *et al.* demonstrated that the loss of vacuole integrity due to the absence of SdhA was the cause of the host cell immune response. In addition, they identified the AIM2 inflammasome as a trigger for pyroptosis after detection of bacterial DNA in the cytosol, which explained why there was a minimal defect in amoeba, as a foreign DNA-triggered immune response has not been identified in protozoa (Ge, Gong, Xu, & Shao, 2012).

The effector SidF is also involved in promoting host cell survival. The involvement of SidF in host cell programmed cell death was discovered when an increase in the number of apoptotic cells was seen 14 hpi with the Δ*sidF* strain. The interaction of SidF with two pro-death host proteins was found using a yeast two-hybrid screen. The two host proteins identified, BNIP3 and Bcl-rambo, belong to the Bcl2 protein family and promote cell death by targeting the mitochondria (Cory, Huang, & Adams, 2003). The interaction between SidF and the target proteins was well established and found to be specific, as other, similar pro-death proteins did not interact with SidF. The interaction of SidF with BNIP3 and Bcl-rambo stops their activity. However, it is believed that more than just binding is necessary to halt function, as a SidF fragment that no longer interfered with the pro-death activity was still found to interact with the targets. The specific activity of SidF has yet to be discovered (Banga et al., 2007).

Another method for host cells to defend against intracellular pathogens is autophagy. Autophagy is the process in which cells encase cytosolic cargo in membrane-bound vesicles which then fuse with the lysosome and degrade their contents. Other than targeting pathogens, it is also a means for cells to free up resources (Hayward & Dinesh-Kumar, 2011; Kuballa, Nolte, Castoreno, & Xavier, 2012; Xie & Klionsky, 2007). During autophagy, Atg8 homologues are coupled to the lipid phosphatidylethanolamine on early autophagosome structures. This coupling, or lipidation, of Atg8 homologues can be detected using western blotting (Ichimura et al., 2000). When wild-type *L. pneumophila* was used to infect mammalian cells a reduction in lipidated LC3, an Atg8 homologue, was detected when compared to cells either not infected or infected with a *dotA* mutant. This finding suggested the existence of a Dot/Icm substrate that is capable of suppressing autophagy. To determine the effector or effectors responsible for the suppression, Choy *et al.* tested some of the large chromosomal deletion mutants (O'Connor et al., 2011) and narrowed the possibilities down to 10 effectors. Each effector was then individually tested for autophagy suppression after ectopic expression in HEK293 cells. One effector, RavZ, showed a reduction in lipidated LC3. Furthermore, a Δ*RavZ* mutant, upon infection, displayed the same basal autophagy phenotype as the *dotA* mutant. *In vitro* experiments revealed the function of RavZ to be a cysteine protease that deconjugates Atg8 proteins, separating them from their lipid counterparts and the products afterward had lost the ability to recouple to the lipid (Choy et al., 2012). Another effector protein that targets the host autophagy system was identified by the high degree of similarity to a

eukaryotic sphingosine-1 phosphate lyase (SPL). Just like eukaryotic SPL, *L. pneumophila* SPL (*Lp*Spl) was shown to specifically cleave sphingolipids, preventing them from stimulating autophagy. When a Δ*spl* strain was compared to wild-type *L. pneumophila* during infection in a human macrophage cell line, a significant difference in the number of LC3 puncta accumulation was seen, wild-type infection having much less. This verified that *Lp*Spl indeed plays a role in restricting host autophagy during *L. pneumophila* infection (Rolando et al., 2016).

Ubiquitin signaling

Manipulation of cell signaling is another important tactic for *L. pneumophila* to ensure efficient intracellular replication and it does this through the activity of multiple effectors. Ubiquitination is a major form of cell signaling and is unique to eukaryotic cells. This makes targeting the ubiquitination system a useful and common practice among bacterial pathogens. The recognition of the importance of ubiquitin dynamics during *L. pneumophila* infection began with the observation of polyubiquitinated proteins associated with the LCV and the requirement of host protein degradation machinery for efficient *L. pneumophila* replication (Dorer et al., 2006). Canonical ubiquitination in eukaryotic cells is performed by three separate enzymes, E1, E2 and E3, in order to activate, conjugate and finally ligate ubiquitin to the target protein (Yau & Rape, 2016). As such, pathogens typically encode E3 ligases to target specific host proteins, relying on host E1 and E2 activities for the initial steps (Maculins, Fiskin, Bhogaraju, & Dikic, 2016). Identification of several effector proteins containing the E3 ligase domains, F-box and U-box, stimulated the characterization of such effectors to try to determine their specific roles during infection (Angot, Vergunst, Genin, & Peeters, 2007). LegU1 contains a single F-box domain and was found to ubiquitinate the ER stress chaperone BAT3 and may function to limit the host stress response to the disruption of normal vesicle trafficking due to *L. pneumophila* infection (Ensminger & Isberg, 2010). The effector AnkB also contains an F-box domain and is able to recruit ubiquitinated proteins to the LCV (Price et al., 2009). Later AnkB was found to associate with the focal adhesion protein ParvB. Ectopic expression of AnkB and infection with wild-type *L. pneumophila* compared to a Δ*ankB* strain showed a reduction in the levels of ubiquitinated ParvB. The authors suggested that reducing the ubiquitination of ParvB might suppress the pro-apoptotic function of ParvB (Lomma et al., 2010).

The effector SidC and its homologue SdcA were both found to be E3 ligases but do not contain either an F-box or U-box domain. SidC was found to associate with the cytosolic side of the LCV and involved in recruitment of vesicles from the ER to the LCV (Luo & Isberg, 2004; Ragaz et al., 2008). Determination of the structure of the N-terminus of SidC revealed a potential catalytic triad consisting of a cysteine, histidine and aspartic acid. Experimentation linked the catalytic triad to a unique mechanism of ubiquitin ligation. The E3 ligation activities of both SidC and SdcA were found to be required for recruitment of ER vesicles to, and enrichment of ubiquitinated species on, the LCV, although the exact mechanism of this outcome is not known (Hsu et al., 2014). Another effector GobX, in a manner similar to SidC, was determined to possess a U-box-like domain only after the structure was determined. GobX was in fact proven to be an E3 ligase through detection of self-modification and although GobX localizes to the Golgi, its exact role during *L. pneumophila* infection was not determined (Lin et al., 2015).

A very exciting discovery was made regarding the mechanism of action for the ubiquitin ligase SidE family of effectors. Initially found by studying the mono-ADP-ribosyltransferase (mART) motif of SdeA, the capacity of SidE family proteins to ubiquitinate the host target protein without the need for an E1 or E2 enzyme and using NAD for energy as opposed to the canonical ATP, was established. The mART motif of SdeA led to the production of ADP-ribosylated ubiquitin, a never before seen type of modified ubiquitin and believed to be an essential intermediate in the unique form of sidE family-dependent ubiquitination (Qiu et al., 2016). Further study into the mechanism of SdeA-mediated ubiquitination revealed a second, phosphodiesterase (PDE), domain that works in concert with the mART domain to transform ADP-ribosylated ubiquitin to phosphoribosylated ubiquitin, which is then linked to a host target serine residue through a phosphodiester bond (Bhogaraju et al., 2016). Although it is known that the SidE family proteins target small GTPases associated with the ER, such as Rab33b and Rab1, and that the ubiquitination catalyzed by the SidE proteins affects the GTPase activity, the contribution of this modification to the successful replication of the bacteria is not yet known (Qiu et al., 2016).

Host cell trafficking

Secretory and endocytic pathway interference

Targeting of vesicle trafficking regulators, for example Rab33b and Rab1 by the SidE family effectors is a key trafficking manipulation tactic employed by *L. pneumophila*. The creation of a membrane bound refuge that protects the bacteria from the cytosol and increases in size in order to support the growth and replication of the bacteria, all while avoiding stimulation of the immune response, requires the balanced recruitment of specific host vesicles (Isberg et al., 2009). To acquire the cellular components necessary for efficient replication, *L. pneumophila* recruits vesicle traffic from two main branches, the secretory and the endocytic.

The secretory branch consists of the traffic moving from the ER to the Golgi and finally to either the lysosomes/endosome, the cell surface or secretory vesicles (Rothman & Orci, 1992). As previously mentioned the effector RalF, the first *L. pneumophila* effector reported, activates the small GTPase ARF1, a key component of ER to Golgi traffic, through nucleotide exchange (Nagai et al., 2002). Another important ER to Golgi regulator is the small GTPase Rab1 (Pfeffer, 2001). Although the fraction of total *L. pneumophila* effector proteins characterized to date is small, a multitude have been shown to interact with Rab1, changing the behavior of the small GTPase significantly in favor of bacterial replication. One effector, SidM (a.k.a. DrrA), alters the activity of Rab1 in at least three different ways. Initially SidM was shown to activate Rab1 through GEF activity, recruiting the GTPase to the LCV membrane. In fact, ectopic expression of SidM in mammalian cells was able to outcompete endogenous recruiting elements, disrupting normal ER to Golgi traffic and leading to Golgi fragmentation (Machner & Isberg, 2006; Murata et al., 2006). Shortly thereafter, in addition to the GEF activity, SidM was also found to possess guanosine nucleotide dissociation inhibitor (GDI)-displacement factor (GDF) activity. GDIs retain inactive, GDP-bound GTPases in the cytosol, while GDFs displace GDIs, freeing the GTPases and allowing their integration into membranes. SidM leads to the release of Rab1, and once incorporated into the membrane, will then activate Rab1 through the exchange of GDP for GTP (Machner & Isberg, 2007; Schoebel, Oesterlin, Blankenfeldt, Goody, & Itzen, 2009). Finally, it was discovered that once Rab1 was activated, SidM can catalyze the attachment of an AMP moiety to the tyrosine at

position 77, in the switch II region, preventing access by GTPase activating proteins (GAPs) and locking Rab1 in the active state (Müller et al., 2010).

The continual cycling of vesicles to the LCV is important for the *L. pneumophila* lifecycle (Jonathan C Kagan & Roy, 2002). Removal of active Rab1 from the LCV begins with the effector SidD. SidD is a deAMPylase that specifically removes the AMP group added to Rab1 by SidM (discussed earlier as a metaeffector) (Neunuebel et al., 2011; Tan & Luo, 2011). Once the AMP is removed by sidD, Rab1 can then be accessed by yet another effector, LepB. LepB activates the GTPase activity of Rab1, which hydrolyzes the GTP to GDP, making Rab1 inactive and allowing for the removal of the GTPase from the LCV (Ingmundson, Delprato, Lambright, & Roy, 2007).

AMPylation is not the only modification added to Rab1 during infection. Rab1 is post-translationally modified by multiple *L. pneumophila* effectors. AnkX was found to be a phosphorylcholine transferase capable of attaching a phosphorylcholine (PC) to serine 76 of Rab1. The process of PCylation requires the FIC (filamentation induced by cAMP) motif located at the N-terminus of AnkX. Originally, the FIC domain was believed to only catalyze the addition of AMP, but the activity of AnkX proved the versatility of the motif (Worby et al., 2009). The addition of PC to Rab1 prevents activation by GAPs, such as LepB. The activity of the metaeffector Lem3 (discussed earlier) removes the PC allowing for subsequent GTPase activation (Mukherjee et al., 2011; Tan et al., 2011). Recently we discovered yet another effector that modifies Rab1. The effector SetA, for subversion of eukaryotic vesicle trafficking A, was identified in a screen looking for *L. pneumophila* effectors capable of interfering with vesicle trafficking in yeast. SetA was found to harbor a canonical DxD glucosyltransferase domain and was able to self-modify using UDP-glucose and although the motif was necessary for vesicle trafficking interference, the target of SetA had not been established (Heidtman, Chen, Moy, & Isberg, 2009; Jank et al., 2012). The identification of Rab1 as the primary target of SetA was accomplished through cross-linking mass spectrometry analysis. Detection of glucosylated Rab1 during *L pneumophila* infection was dependent on the presence of the SetA DxD motif, verifying the target as Rab1. Interestingly, primary glucosylation of Rab1 by SetA did not interfere with subsequent AMPylation by SidM or PCylation by AnkX. However, both AMPylation and PCylation interfered with subsequent glucosylation, highlighting the complexity in *L. pneumophila*-mediated Rab1 control (SetA

characterization is discussed in detail in chapter 2) (Z. Wang et al., 2018). The details of effector-mediated temporal or spatial control on the individual Rab1 molecules remains to be determined. The cumulative findings thus far have shown a remarkably high level of complexity.

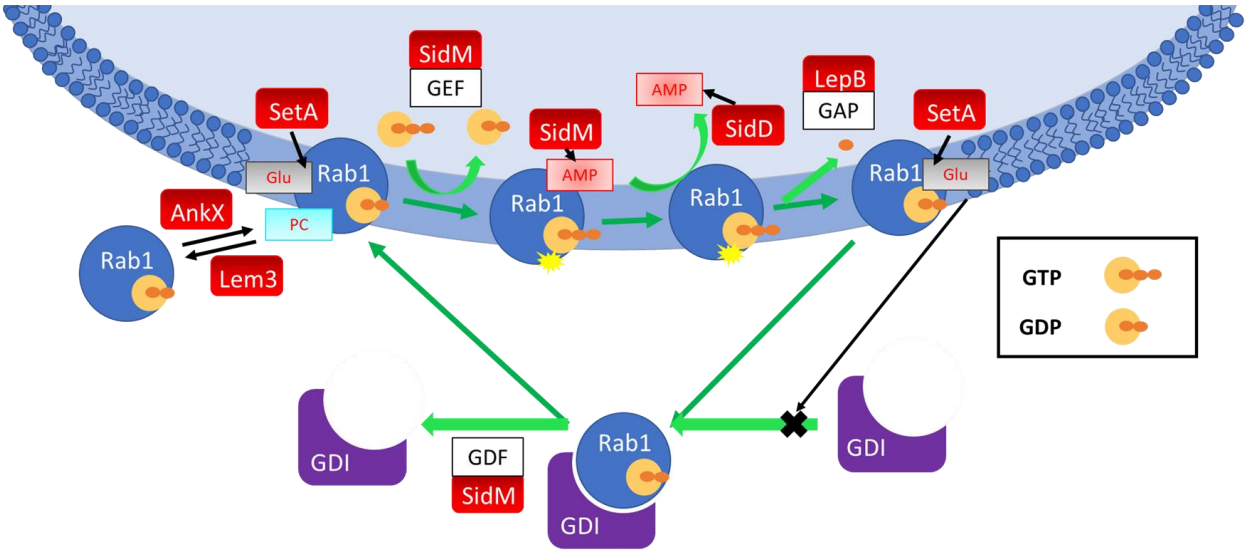

Figure 1-2. Illustration of multi-effector control of Rab1 by *L. pneumophila.* SidM has been shown to have GDI-displacement factor (GDF) activity, guanine nucleotide exchange factor (GEF) activity and the ability to add an AMP to Rab1, locking Rab1 in the active state. SidD is a metaeffector that removes the AMP from Rab1 allowing LepB to activate the GTPase activity of Rab1. AnkX can add a phosphorylcholine (PC) to Rab1 and prevents GTPase activation. Lem3 can remove the PC, allowing for hydrolysis to occur. SetA preferentially glucosylates GDP-Rab1 and shows no interference with GTP exchange but does limit GTPase activity. The glucosylation by SetA also interferes with GDI-Rab1 association.

The endocytic pathway consists of membrane traffic originating at the plasma membrane, either recycled back or sorted to late endosomes and eventually the lysosome or sometimes the trans Golgi network (Gruenberg & Maxfield, 1995). In addition to PCylation of Rab1, AnkX was also found to PCylate Rab35, a GTPase that regulates the sorting of cargo from early endosomes. Initially, PCylated Rab35 was found after infection with wild-type *L pneumophila*, but not when cells were infected with the Δ*ankX* strain. In addition, microinjection of purified AnkX led to enlargement of early endosomes, a phenotype associated with interference of Rab35. These results indicate that AnkX manipulates vesicle trafficking in both the secretory and endocytic pathways (Mukherjee et al., 2011).

Acidification of early endosomes by the Vacuolar H^+-ATPase (v-ATPase) has been implicated as an important step in regulating the endocytic degradative pathway (Hurtado-Lorenzo et al., 2006).

Likely as a means of preventing the LCV from entering the degradative pathway, the effector SidK binds to VatA, a key component of the v-ATPase. The binding of SidK to VatA was shown to inhibit the activity of the v-ATPase and reduce vacuole acidification. Plus, SidK delivery into macrophages impaired the ability of the cells to digest non-pathogenic *Escherichia coli* (Xu et al., 2010).

The effector LegG1 interacts with the host small GTPase Ran, which is involved in endosomal trafficking pathways and microtubule utilization. LegG1 has significant similarity with known Ran GEFs and was shown to activate Ran in cell lysates. However, purified LegG1 was not able to activate Ran during *in vitro* reactions, indicating the need for other cellular components in the activation of Ran. During *L. pneumophila* infection, LegG1-dependent activation of Ran was linked to LCV formation, microtubule stabilization, intracellular replication promotion and even phagocyte migration inhibition (Rothmeier et al., 2013; Simon, Wagner, Rothmeier, Müller-Taubenberger, & Hilbi, 2014).

Retrograde trafficking is part of the endocytic pathway and consists of movement from the late endosomes to the Golgi and the ER. It is a means of recycling components involved in the secretory pathway (Seaman, 2005). Initial experimentation showed that during *L. pneumophila* infection, host cell retrograde trafficking is inhibited. The inhibition was dependent on Dot/Icm substrates and was necessary for intracellular replication. The effector RidL blocks retrograde trafficking at endosome exit sites by interfering with the protein complex responsible for budding off of the endosome. The interference is due to the interaction between RidL and the retromer subunit Vps29 (Finsel et al., 2013). In addition, two recent structural-based studies found that the binding of RidL to Vps29 displaces the Rab7 GAP TBC1D5 from the retromer complex. This, theoretically, frees the GAP, allowing it to perform other functions that potentially aid in the replication of *L. pneumophila*. In fact, when a strain of *Dictyostelium discoideum*, an amoebal model used to study *L. pneumophila* infection, missing the TBC1D5 gene was tested, it was incapable of supporting efficient replication of the bacteria (Bärlocher et al., 2017; Yao et al., 2018).

Finally, avoidance of fusion with endosomes as well as the lysosome is essential for successful *L. pneumophila* infection. Recently, the effector RavD was found to localize to the LCV as well as

surrounding vesicles within 5 hpi. It is believed that RavD is one of multiple effectors responsible for LCV avoidance of endolysosomal maturation. This is because, although the Δ*ravD* strain did not show a significant growth defect, it did show an increase in accumulation of the late endosome/lysosome marker LAMP-1 on the LCV, which does not occur during infection with the wild-type strain (Pike, Boyer-Andersen, Kinch, Caplan, & Neunuebel, 2019). A group screening for bacterial effectors capable of cleaving linear ubiquitin chains found that RavD specifically targets linear Ub chains on the LCV through a unique mechanism involving a Cys–His–Ser catalytic triad (Wan et al., 2019). Together, both studies established the importance of RavD's role during infection.

Lipid metabolism

Lipid metabolism is a process essential for host cell trafficking through signaling, structure and protein interactions (Behnia & Munro, 2005). Efforts to manipulate host lipid metabolism have been described for multiple bacterial pathogens including *L. pneumophila* (Weber, Ragaz, & Hilbi, 2009). Lipid metabolism plays a large role in *L. pneumophila* infection in that specific phosphoinositide (PI) forms anchor effectors to the membrane locations necessary for their function and the PI composition of the LCV aids in recruiting supportive vesicles. The main PI found on the LCV is phosphatidylinositol 4-phosphate (PI(4)P), a phenotype similar to the Golgi, the destination for ER-derived vesicles (Qiu & Luo, 2017). Formation of PI(4)P on the LCV is accomplished through the activities of multiple effectors. SidF, previously mentioned regarding an apoptosis suppression activity, was also found to harbor PI phosphatase activity. Specifically, SidF hydrolyzes the D3 phosphate from $PI(3,4)P_2$ and $PI(3,4,5)P_3$. After injection into the host cell, SidF localizes to the cytoplasmic side of the LCV and presumably, aids in the transformation of the cytoplasmic leaf to a PI(4)P rich membrane (Hsu et al., 2012). The N-terminus of the effector LepB (LepB-NTD), whose Rab1 GAP activity was discussed previously, was determined to function as a PI 4-kinase that adds a phosphate group to the D4 location on PI(3)P, creating $PI(3,4)P_2$, which can then be modified by SidF. In fact, LepB-NTD has a toxic effect when ectopically expressed in yeast and the toxicity is suppressed when SidF is also expressed. It is not entirely clear where the PI(3)P modified by LepB originates. The LCV avoids fusion with the early endosome, which is rich in PI(3)P, so other, unknown sources are likely the major contributors (Dong et al., 2017).

In addition to recruiting certain types of membranes, altering lipid composition allows *L. pneumophila* to avoid fusing with undesirable membranes. SidP is a PI(3)P phosphatase that removes the D3 phosphate group from PI(3)P and PI(3,5)P_2 *in vitro*. The authors believe that the coordinated activities of SidP and SidF work to prevent accumulation of PI(3)P on the LCV, reducing the likelihood of fusion with either the lysosome or endosomes (Toulabi, Wu, Cheng, & Mao, 2013). VipD is a phospholipase that also targets host PI(3)P, through hydrolysis of the lipid as opposed to removal of the phosphate group. VipD localizes to the endosomes through an interaction with the active forms of either Rab5 or Rab22, two small GTPases that regulate endosomal trafficking. Once VipD is associated with the endosomal membrane it effectively removes the PI(3)P and prevents the formation of new PI(3)P by competing with the PI 3-kinase Vps34, for binding to Rab5. The removal of PI(3)P from the endosomal membrane also disrupts the association of multiple endosomal proteins, completely changing the composition of the membranes and shutting down the ability to fuse with other membranes. The authors believe VipD functions near the LCV, thereby preventing the LCV from fusing with any neighboring endosomes (Gaspar & Machner, 2014).

Two more effectors, whose activities work sequentially to alter the lipid composition of the LCV, were characterized by Viner *et al.*: LpdA, which contains a phospholipase D (PLD) domain, converts phosphatidylcholine (PC) to phosphatidic acid (PA) and LecE, through an unknown mechanism, activates the host protein Pah1, which converts PA to diacylglycerol (DAG). The authors theorize that accumulation of DAG on the LCV through the efforts of both LpdA and LecE may prime the membrane for recruitment of different host proteins, including a PI 4-kinase. This, in conjunction with the functions of SidF, LepB and SidP, could ultimately increase the levels of PI(4)P on the LCV (Viner, Chetrit, Ehrlich, & Segal, 2012). This theory, however, needs experimental validation.

Actin cytoskeleton

The actin cytoskeleton plays a vital role in membrane trafficking by providing the forces necessary for membrane budding and movement of the different vesicles (Lanzetti, 2007). Both actin and its regulating protein profilin are known to associate with the LCV (Urwyler et al., 2009). Based on this close interaction, it is not surprising that multiple *L. pneumophila* effectors that act to modify

the host cytoskeleton have been identified. The effector VipA was originally identified by its ability to interfere with organelle trafficking in yeast. VipA is able to polymerize actin microfilaments without the need of any other proteins *in vitro*. Translocated VipA localizes to actin patches and early endosomes, indicating a role in altering actin dynamics to alter host cell trafficking in support of *L. pneumophila* replication (Franco, Shohdy, & Shuman, 2012). Another effector, Ceg14, also targets the host cytoskeleton. Ceg14 displays an opposing activity to VipA and functions to prevent actin polymerization. However, the role of Ceg14 during infection, and the need for opposing effector functions, remains to be determined (Guo, Stephenson, Qiu, Zheng, & Luo, 2014). By targeting an actin nucleator, the ARP2/3 complex, LegK1 contributes to the remodeling of the LCV by preventing access of the LCV to late endosomes and lysosomes (Michard et al., 2015). Finally, RavK is a potent metalloprotease capable of cleaving actin during *L. pneumophila* infection. The localization of RavK during infection could not be determined and therefore the specific actin structures targeted by RavK are unknown, but Liu *et al.* theorized that RavK works locally to reduce the levels of actin around specific organelles (Yao Liu et al., 2017). It is likely that many more actin-targeting effectors will be identified, as the actin cytoskeleton is such an important constituent of the host cell and specifically host organelle trafficking.

Host cell gene expression regulation

Transcription

The targeting of host gene expression by *L. pneumophila* has proven to be important because the manipulation of host gene expression affects all other cell processes. Control of gene expression at the transcriptional level by *L. pneumophila* has been detected through the activities of a handful of effectors. LnaB and LegK1, as examples, regulate transcription by altering the NF-κB pathway (discussed previously) (Ge et al., 2009; Losick et al., 2010). The effectors RomA and LegAS4, homologues from different *L. pneumophila* strains, mimic host gene transcription regulation by methylating multiple histones to suppress expression of immune related genes (T. Li et al., 2013; Rolando et al., 2013; Son et al., 2015).

Recently, two more *L. pneumophila* effectors were found to alter host cell transcription. SnpL, for SUPT5H interaction partner of *Legionella*, was found to localize to the host nucleus and bind the

transcriptional regulator SUPT5H. The interaction between SnpL and SUPT5H led to the upregulation of genes involved in cell division, adhesion and survival. The exact role of SnpL during infection was not determined and very likely more nuclear-localizing *L. pneumophila* effectors exist that together balance host transcription in a temporal manner to optimize bacterial replication (Schuelein et al., 2018). The other effector recently characterized, LegK7, targets a conserved eukaryotic signaling pathway that controls multiple cell processes such as cell-cycle progression, differentiation and apoptosis (Meng, Moroishi, & Guan, 2016). Through phosphorylation of one of the scaffolding proteins, an important pathway constituent, LegK7 alters the activities of downstream transcription factors, which leads to alterations in gene expression, and antagonization of the innate immune response. Moreover, by targeting such an essential component of a conserved eukaryotic pathway, the bacteria ensures success in a greater number of eukaryotic hosts (Lee & Machner, 2018).

Translation

Inhibition of host translation is an extremely important method employed by *L. pneumophila* to ensure efficient replication. Only a small number of effectors which inhibit host translation have been identified so far and the way in which they inhibit translation is only known for one family of the effectors. Lgt1, Lgt2 and Lgt3 are glucosyltransferase enzymes that target the host elongation factor eEF1A. All three enzymes add a glucose moiety to a serine residue in a region important for eEF1A activity. The glucosylation of eEF1A by the Lgt family effectors leads to a large decrease in host protein translation (Belyi et al., 2006; Belyi et al., 2009; Belyi, Tabakova, Stahl, & Aktories, 2008). Another effector, SidI, was also found to interact with eEF1A along with a second elongation factor, eEF1Bγ, one component of the eEF1A GEF. The ultimate outcome of the interactions is a reduction in host translation and although the exact mechanism for SidI-dependent inhibition is not known, isolated mutants that have a large reduction in inhibition were still capable of interacting with the elongation factors, suggesting that SidI has an undetermined enzymatic function (Shen et al., 2009). As previously mentioned, a regulating effector for SidI, Lpg2505, was recently identified and just as the enzymatic activity of SidI remains a mystery so too did the function of Lpg2505 (Shames et al., 2017). In chapter three of this thesis I will discuss the new findings we have made that have helped determine the function of Lpg2505 and the relationship between SidI and its metaeffector. Finally, a fifth effector, SidL was also found to

inhibit host translation and is toxic when expressed in mammalian cells, but the mechanism in which it does this is unknown (Fontana et al., 2011).

Host protein translation inhibition has been associated with multiple, pathogen-supportive changes within the host cell: 1) freeing amino acids for use by replicating bacteria, 2) interference with the cell cycle to ensure bacterial survival, 3) and alteration of the host stress response to promote host cell subsistence. It was discovered that already characterized effectors, the Lgt family and the SidE family, were able to target an important regulator of host amino-acid metabolism, mTORC. De Leon *et al*. found that through the inhibition of protein synthesis by the Lgt family and mTORC interference by the SidE family, the amount of free amino acids would elevate and be available for use by *L. pneumophila,* which is an auxotroph for a number of amino acids (De Leon et al., 2017; Eylert et al., 2010). It was shown by Sol *et al.* that progression of the host cell through the cell cycle, specifically entering into S-phase, is detrimental to replicating *L. pneumophila* and through protein translation inhibition via the 5 effectors described in the previous paragraph, the cell cycle can be arrested (Sol et al., 2019). The study on SidI revealed that in addition to and likely because of the inhibition of host translation caused by SidI, the host heat shock stress response was induced. The stress response leads to an increase in chaperone activity and could benefit *L. pneumophila* by ensuring proper folding of effector proteins as well as the more obvious benefit of keeping the host alive (Shen et al., 2009). In addition, it was found that *L. pneumophila* is able to inhibit a branch of the unfolded protein response (UPR), through the activities of the 5 translation inhibiting effectors, ultimately preventing engagement of downstream innate immune signaling (Hempstead & Isberg, 2015).

Interestingly, *L. pneumophila*'s inhibition of the host translation machinery was also found to stimulate an immune response. The immune response was based on the pathogen's activity as opposed to a molecular pattern. Specifically, protein production inhibition of the NF-κB regulating protein IκB, led to a prolonged activation of NF-κB signaling and an increase in transcription of anti-microbial inflammatory cytokines (Fontana et al., 2011). The number of affected processes, both beneficial and detrimental to the bacteria, caused by the activity of *L. pneumophila* translocated substrates, provides another example of the complexity involved in turning a professional phagocyte into a proliferation-supportive environment.

Summary

This review of *L. pneumophila* pathogenesis, especially the list of effectors discussed in this chapter is not comprehensive, but it does cover the majority of the findings published since the recognition of *L. pneumophila* as a human pathogen. The details presented are a good representation of the breadth of work done on the bacterial pathogen and highlights the impressive level of complexity used by *L. pneumophila* when infecting a diverse range of eukaryotic hosts. So far only slightly greater than 10% of predicted effectors have been characterized (Qiu & Luo, 2017). Many of these effectors have multiple domains and multiple functions, expanding the total enzymatic functionality of the *L. pneumophila* effector pool significantly. Through the study of *L. pneumophila* effectors, novel biochemical mechanisms have been revealed, our understanding of eukaryotic immune systems has expanded and potentially useful tools to study human cell biology have been identified. Much has been gained from the study of *Legionella* species and much more is undoubtedly still to come.

CHAPTER 2. REGULATION OF THE SMALL GTPASE RAB1 FUNCTION BY THE *L. PNEUMOPHILA* GLUCOSYLTRANSFERASE SETA

Abstract

Posttranslational modification of key host proteins by virulence factors is an important theme in bacterial pathogenesis. A remarkable example is the reversible modifications of the small GTPase Rab1 by multiple effectors of the bacterial pathogen *Legionella pneumophila*. Previous studies have shown that the effector SetA, dependent on a functional glucosyltransferase domain, interferes with host secretory pathways. However, the host interactome of SetA was never determined. Here, by using cross-linking mass spectrometry we uncovered Rab1 as the target of SetA during *L. pneumophila* infection. Biochemical studies establish that SetA covalently attaches a glucose moiety to Thr75 within the switch II region of Rab1, inhibiting its intrinsic GTPase activity. Moreover, we found that SetA preferentially modifies the GDP-bound form of Rab1 and that SetA-dependent glucosylation inhibits the interaction between Rab1 and the GDP dissociation inhibitor GDI1, allowing for easier activation of Rab1. Our results indicate SetA is an additional *L. pneumophila* effector capable of regulating Rab1 activity and provide a mechanistic understanding of SetA-dependent inhibition of the host secretory pathways as well as the cellular toxicity seen during ectopic SetA expression in eukaryotic cells.

Introduction

Legionella pneumophila, a gram-negative bacterium, is the etiological agent of a potentially lethal pneumonia called Legionnaires' disease (Fraser et al., 1977). Human infections are typically associated with phagocytosis by alveolar macrophages where *L. pneumophila* resides and replicates within a membrane-bound compartment known as the Legionella-containing vacuole (LCV) (Isberg et al., 2009). The biogenesis of the LCV requires successful modulation of multiple host cell processes, particularly vesicle trafficking and membrane transport, which eventually leads to the formation of an organelle with features closely resembling those of the endoplasmic reticulum (ER) (Jonathan C Kagan & Roy, 2002; Tilney et al., 2001). Crucial for

hijacking host cellular processes, including membrane trafficking, is the Dot/Icm type IV secretion system, which delivers a large cohort of virulence factors, called effector proteins, into host cells (A. Hubber & Roy, 2010; Qiu & Luo, 2017). By engaging in a wide variety of host cellular pathways, these effectors function to construct a niche permissive for intracellular bacterial survival and multiplication (Andrews, Vogel, & Isberg, 1998; Marra et al., 1992). Therefore, functional study of these effectors as well as their roles during infection is a central theme in the field of *Legionella* pathogenesis.

L. pneumophila encodes more than 330 potential effector proteins, representing >10% of its proteome, which suggests that host function modulation is essential to *L. pneumophila* virulence (Ensminger, 2016). Despite extensive efforts over the years, less than 10% of these effectors have been characterized in terms of their biochemical activities and/or interacting host proteins (Ensminger, 2016; Qiu & Luo, 2017). In line with the maturation of the LCV into an ER-like compartment and the importance of vesicle transport between the ER and the Golgi apparatus in this process (Jonathan C Kagan & Roy, 2002), multiple Dot/Icm effectors have been found to target the small GTPase Rab1 (A. Hubber & Roy, 2010; Qiu & Luo, 2017), a protein important for the initial steps in the secretory pathway (J. C. Kagan, Stein, Pypaert, & Roy, 2004). For example, the transition of Rab1 between its GTP-bound active and GDP-bound inactive states is manipulated by two *L. pneumophila* effectors SidM/DrrA and LepB, which function as a guanine nucleotide exchange factor (GEF) and as a GTPase activation protein (GAP), respectively (Ingmundson et al., 2007; Machner & Isberg, 2007; Murata et al., 2006).

Rab1 activity is also controlled by at least three distinct, reversible post-translational modifications catalyzed by sets of Dot/Icm effectors. First, the $GX_{11}DXD$ adenylyltransferase domain of SidM/DrrA catalyzes AMPylation of Rab1 and locks it in the GTP-bound active form (Müller et al., 2010). This modification is reversed by another effector SidD, which together with SidM, temporally regulates the activity of Rab1 (Neunuebel et al., 2011; Tan & Luo, 2011). In addition, AnkX, a Fic domain-containing effector inhibits Rab1 activity by phosphorylcholination (Mukherjee et al., 2011; Tan et al., 2011), a process that is reversed by the dephosphorylcholinase Lem3 (Tan et al., 2011). Rather recently, we found that Rab1 is ubiquitinated by members of the SidE family effectors via a novel mechanism that does not require E1 and E2 enzymes (Qiu et al., 2016).

Despite these extensive manipulations, growing evidence points to the involvement of additional *L. pneumophila* effectors in hijacking host membrane transport (Heidtman et al., 2009; Shohdy et al., 2005). For example, in a large yeast toxicity screen performed by Isberg *et al.*, a cohort of Dot/Icm effectors that interfere with host vesicle trafficking were identified. However, the precise molecular mechanisms and/or host targets of these effectors were not determined. One of the identified *L. pneumophila* effectors was SetA (for subversion of eukaryotic vesicle trafficking A) (Heidtman et al., 2009). SetA contains a functional glucosyltransferase domain with the typical DXD-motif ($D_{134}XD_{136}$), which was found to be essential for its toxicity in yeast and the interference of membrane transport in mammalian cells upon ectopic expression (Heidtman et al., 2009; Jank et al., 2012).

We set out to identify the host glucosylation target(s) of SetA. By using cross-linking high-resolution mass spectrometry, we unveiled Rab1 as a host interacting protein of SetA. Importantly, we found that during *L. pneumophila* infection, SetA directly glucosylates Thr_{75} within the switch II region of Rab1. This site is in close proximity to residues AMPylated (Tyr_{80}) and phosphorylcholinated (Ser_{79}) by SidM and AnkX, respectively (Mukherjee et al., 2011; Müller et al., 2010; Tan et al., 2011). Moreover, we found that glucosylation of Rab1 inhibits its GTPase activity *in vitro* and GDP-loaded Rab1 is a preferable substrate of SetA-catalyzed modification. Glucosylation of Rab1 inhibits its interaction with the regulatory protein GTP disassociation inhibitor 1 (GDI1), while at the same time, binding to the bacterial GEF SidM and GTP loading is not impacted.

Results

Small Rab GTPases were identified as potential substrates of SetA by cross-linking mass spectrometry.

Heidtman *et al*. identified SetA as a *L. pneumophila* Dot/Icm substrate that inhibits yeast growth, likely by disrupting vesicle trafficking (Heidtman et al., 2009). Such phenotypes were found to be strictly dependent on a predicted glycosyltransferase domain located in the N-terminus of SetA. Later, Jank *et al.* further established that SetA harbors mono-O-glucosyltransferase activity by using UDP-glucose as a sugar donor (Jank et al., 2012). Despite these analyses, the

mechanism underlying the effect of SetA ectopic expression was not known because its cellular target(s) had yet to be identified. In order to determine its eukaryotic glucosylated substrate(s), we ectopically expressed SetA in mammalian cells and analyzed the interacting host proteins by combining *in vivo* formaldehyde cross-linking and affinity purification-mass spectrometry (**Fig. 2-1A**). SopD2, a type III effector of *Salmonella Typhimurium*, was included as a positive control for our approach as it has been shown to interact with multiple small Rab GTPases (D'Costa et al., 2015; Spanò, Gao, Hannemann, Lara-Tejero, & Galán, 2016; Teo et al., 2017). The efficiency of cross-linking reactions was monitored by immunoblotting analyses. Upon optimization of this procedure, cross-linked proteins of high molecular weight (higher than the bait proteins) were readily detected; these proteins were not detected in non-cross-linked controls, suggesting the effectiveness of this method **(Fig. 2-1B**). Comparative analyses of cross-linked samples and controls led to the identification of most known SopD2-interacting proteins (e.g., Rab7, Rab8 and Rab10 in the left panel of **Fig. 2-1C**). In cross-linked SetA samples, but not in the controls, we detected multiple Rab GTPases (i.e., Rab1, Rab5c and Rab7) (**Fig. 2-1C**, the right panel). Together with previous findings on the disruption of host vesicle trafficking, our cross-linking mass spectrometry analyses suggest that Rab GTPases are valid host cell target candidates for SetA. The identification of host targets arguably is the greatest challenge in the study of effector function, probably due to the low enzyme-substrate affinity. The success of identifying Rab small GTPases as potential targets for SetA by cross-linking indicates that this method can be a valuable tool to study other effectors.

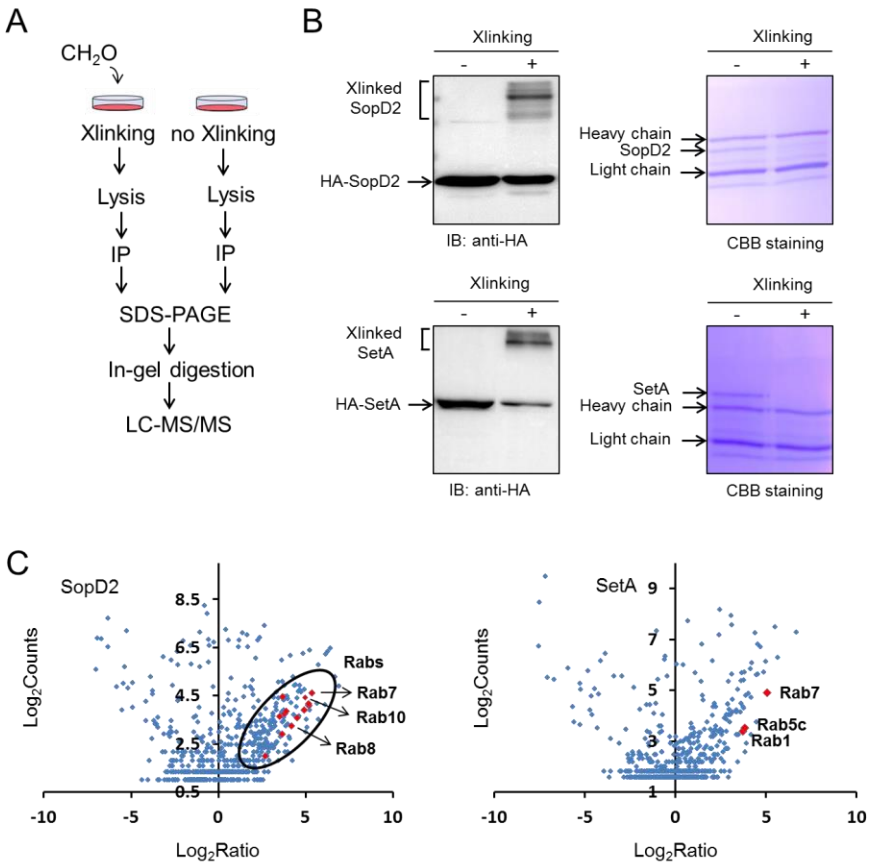

Figure 2-1. Identification of host binding proteins of bacterial effectors by a cross-linking (Xlinking) mass spectrometry strategy. (A) A schematic diagram of the overall workflow that combines *in vivo* formaldehyde cross-linking, affinity purification and mass spectrometry to identify SetA-interacting proteins. HEK293T cells producing HA-tagged SetA were treated with 1% formaldehyde and then lysed prior to immunoprecipitation of cross-linked protein complexes by an HA-specific antibody. The precipitates were further separated by SDS-PAGE before in-gel digestion with trypsin and LC-MS/MS analyses. (B) Monitoring of formaldehyde cross-linking reactions by immunoblotting analyses. A *Salmonella* type III effector SopD2 was included as a positive control. The Coomassie-stained gels containing cross-linked bands were processed for mass spectrometric analyses. Corresponding gel bands from non-cross-linked controls were also analyzed. (C) Scatter plots of protein ratios as a function of their relative abundance (denoted by MS/MS spectral counts). The ratio was calculated as spectral counts in cross-linked samples divided by those in non-cross-linked controls and then normalized against protein molecular weight. Large ratios indicate preferential detection in cross-linked samples, representing potential interacting substrates. Red dots correspond to detected Rab proteins in cross-linked samples. (Experiments performed by Wang, Z. *et al.* of Peking University)

Ectopic expression of SetA caused glucosylation of Rab1 in mammalian cells.

Next, we examined whether the Rab GTPases identified above are glucosylation targets of SetA. We co-expressed 3xFLAG-tagged Rab1 in HEK293T cells with either wild-type (WT) SetA or its catalytically inactive mutant $SetA_{D134,136A}$. With nearly full coverage of the Rab1 sequence,

we detected seven mono-glucosylated peptides (**Fig. 2-2A**), suggestive of multiple modification sites catalyzed by SetA. By quantitative mass spectrometry, we determined the extent (i.e., percentages) of glucosylation for these modified peptides. Our data reveal that peptide -F_{73}RTITSSYYR$_{82}$- was highly (~75%) modified (**Fig. 2-2B**). This fragment is in the switch II region of Rab1 and contains the modification sites for both SidM and AnkX-dependent AMPylation and phosphorylcholination (Mukherjee et al., 2011; Müller et al., 2010; Tan et al., 2011). In contrast, the percentage of modification for most of the other modified peptides was below 5% (**Table 2-1**). In addition, we examined Rab5c and Rab7 co-expressed with SetA and found only a small (<5%) fraction of the peptides was glucosylated (**Table 2-1**). These findings suggest that among the identified small GTPases, Rab1 is likely to be the preferred substrate of SetA.

Moving forward, we focused our analysis on SetA-mediated glucosylation of Rab1. The doubly pronated peptide (m/z = 728.36) showed a mass shift of 162.05, corresponding to the attachment of one glucose molecule. In contrast, such an increase in mass was not observed in the peptide samples from Rab1 co-expressed with the enzymatically inactive mutant SetA$_{D134,136A}$ (**Fig. 2-2B**). We then sought to pinpoint the exact site of modification within this peptide. Due to extensive neutral loss of sugar moieties in traditional MS/MS (i.e., collision-induced dissociation), we fragmented the modified peptide by electron transfer dissociation (ETD) (Lu et al., 2014). MS/MS analysis unambiguously determined the glucosylated site to be Thr$_{75}$ (**Fig. 2-2C**). Taken together, these data suggest that production of SetA in mammalian cells caused mono-glucosylation of Rab1 at Thr$_{75}$, a site in the vicinity of the modification sites (Se$_{r79}$ and Tyr$_{80}$) of AnkX and SidM, respectively (Mukherjee et al., 2011; Müller et al., 2010; Tan et al., 2011). As expected, SetA-mediated modification of Rab1 required its glucosyltransferase activity.

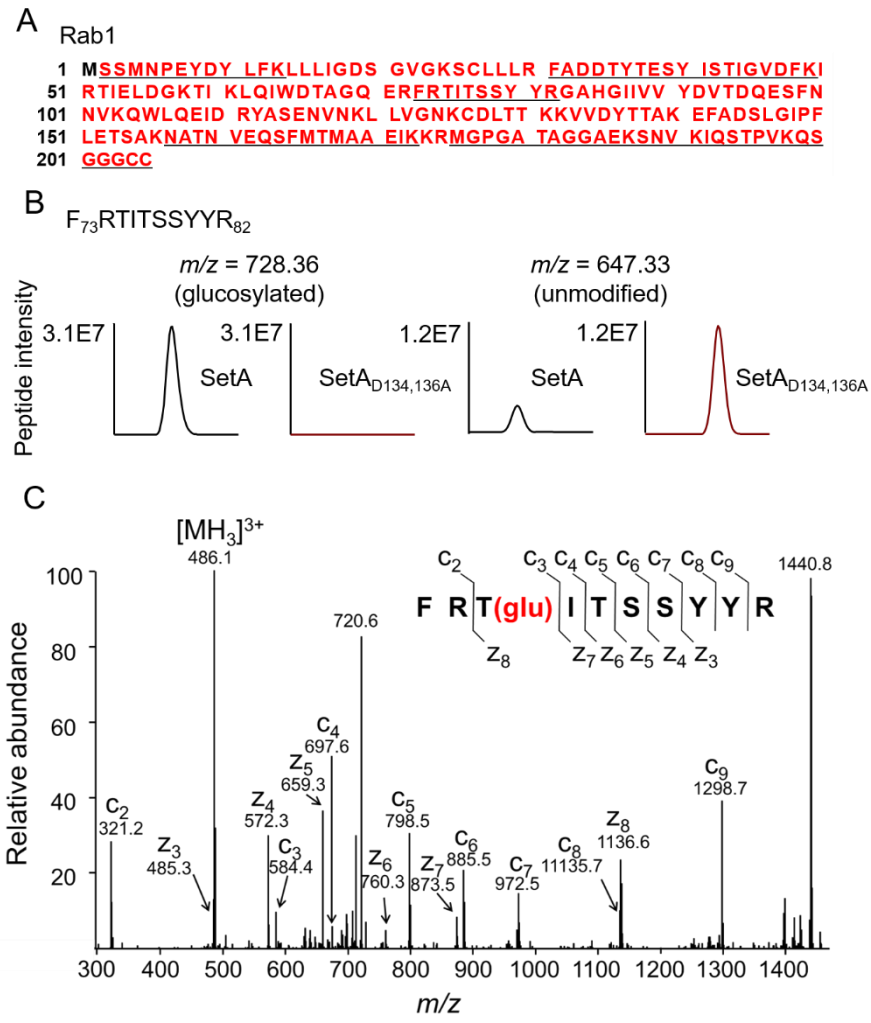

Figure 2-2. Extensive glucosylation of Rab1 upon co-expression with SetA in mammalian cells. 3×FLAG-Rab1 was isolated from HEK293T cells co-transfected with either wild-type SetA or its catalytically inactive mutant $SetA_{D134,136A}$. Immunoprecipitated Rab1 was then digested with trypsin and analyzed by LC-MS/MS. (A) Detected Rab1 sequence shown in red in LC-MS experiments. The glucosylated peptide sequences are underlined. (B) MS detection of Rab1 peptide $F_{73}RTITSSYYR_{82}$ that was covalently modified with one molecule of glucose. Extracted ion chromatograms of the doubly protonated peptide are shown with peak intensities indicating the relative amounts of either the modified (m/z = 728.36) or unmodified (m/z = 647.33) peptides. (C) Determination of modification sites by electron transfer dissociation (ETD) analysis. The MS/MS spectrum of modified $F_{73}RTITSSYYR_{82}$ is shown. The fragment ions c3 to c9 have a mass increase of 162.1 corresponding to the addition of one glucose while z3 to z7 fragments lack such a mass shift, suggesting glucosylation of Thr_{75}. (Experiments performed by Wang, Z. *et al.* of Peking University)

Table 2-1. The modification rates of the glucosylated peptides from Rab1, Rab5c and Rab7.

		Peptide intensity			
Protein	**Peptide sequence**	**Modified**	**Unmodified[1]**	**Unmodified[2]**	**%Modification[3]**
Rab1	(73-82)FRTITSSYYR	3.7E8	5.3E7	2.1E8	75.0
	(31-49)FADDTYTESYISTIGVDFK	6.7E6	3.5E6	5.6E6	38.0
	(2-13)SSMNPEYDYLF	7.7E5	4.8E6	6.1E6	5.0
	(188-205)SNVKIQSTPVKQSGGGCC	5.1E6	4.8E7	3.5E7	5.0
	(188-198)SNVKIQSTPVK	5.3E6	5.5E7	4.9E7	3.0
	(176-187)MGPGATAGGAEK	1.2E7	3.3E8	4.6E8	1.0
	(157-173)NATNVEQSFMTMAAEIK	1.5E5	5.4E7	8.6E7	0.1
Rab5c	(83-92)YHSLAPMYYR	7.0E5	2.3E8	2.3E8	0.1
Rab7	(11-31)VIILGDSGVGKTSLMNQYVNK	1.2E5	2.4E6	3.4E6	2.0
	(22-31)TSLMNQYVNK	3.9E5	3.0E7	2.5E7	0.4
	(39-48)ATIGADFLTK	6.4E5	1.6E8	1.1E8	0.1
	(158-171)EAINVEQAFQTIAR	3.1E5	1.4E8	1.2E8	0.1

[1]: Intensity of unmodified peptides in the Rab samples prepared from cells expressing WT SetA.

[2]: Intensity of unmodified peptides in the Rab samples prepared from cells expressing the inactive SetA mutant.

[3]: Percentages are calculated as the ratio of the intensity drop of unmodified peptides in samples prepared from cells expressing WT SetA. When the modifications are minimal, the intensity of modified peptides was normalized first and then divided by that of unmodified peptides in the Rab samples prepared from cells expressing the inactive SetA mutant. (Experiments performed by Wang, Z. *et al.* of Peking University)

Rab1 was glucosylated by purified SetA.

Next, we asked whether SetA was capable of directly modifying Rab1 by glucosylation. We first examined the glucosyltransferase activity of SetA by incubating purified recombinant His_6-SetA or its catalytically inactive mutant His_6-$SetA_{D134,136A}$ with UDP-glucose. LC-MS readily detected auto-glucosylation products of SetA. The glucosylated peptide $L_{509}SNQLNRHTFFNQR_{612}$ (m/z = 646.32, z=3) was present in samples from wild-type SetA but

not the catalytically inactive mutant (**Fig. 2-3A**). We then performed a glucosylation assay by incubating purified GST-Rab1 and UDP-glucose with His_6-SetA or His_6-$SetA_{D134,136A}$. Glucosylated Rab1 peptide $F_{73}RTITSSYYR_{82}$ was detected in reactions containing SetA but not $SetA_{D134,136A}$ **(Fig. 2-3B**). In comparison to co-expression experiments performed above, we observed relatively lower efficiency of modification (15%), probably due to less than ideal conditions used during the biochemical assays. Taken together, these results establish that SetA is a glucosyltransferase that directly modifies Rab1.

SetA specifically glucosylated Rab1 during *L. pneumophila* infection.

To further validate Rab1 as the physiological substrate of SetA, glucosylation during *L. pneumophila* infection was examined. To monitor the modification status of Rab1 during bacterial infection, we infected HEK293T cells expressing 4xFLAG-Rab1 with relevant *L. pneumophila* strains. Signals of the glucosylated peptide -$F_{73}RTITSSYYR_{82}$- were detected in cells infected by wild-type but not the Lp02Δ*setA* mutant (**Fig. 2-3C**). Importantly, introduction of a plasmid expressing SetA into the Δ*setA* strain restored its ability to modify Rab1 (**Fig. 2-3C**). In contrast, and although expressed at similar levels (**Fig. 2-3D**), $SetA_{D134,136A}$ was unable to complement the ability of strain Lp02Δ*setA* to glucosylate Rab1 (**Fig. 2-3C**). Consistent with higher expression and secretion levels of SetA produced from a multi-copy plasmid (**Fig. 2-3D**), the rate of Rab1 glucosylation in cells infected with the complementation strain was substantially (>more than 10 times) higher than that in wild-type infected cells (**Fig. 2-3C**). Taken together, these findings show that Rab1 is the target of SetA glucosylation during *L. pneumophila* infection.

Because our previous experiments had revealed that ectopic expression of SetA leads to modifications of Rab5c and Rab7 in mammalian cells and that SetA can directly glucosylate Rab7 *in vitro*, we examined whether these two GTPases are modified by SetA during *L. pneumophila* infection. Signals from modified peptides belonging to Rab5c or Rab7 were not detected even in cells infected with the strain overexpressing SetA (**Fig. 2-4**). Thus, Rab1 is the specific substrate of SetA during *L. pneumophila* infection.

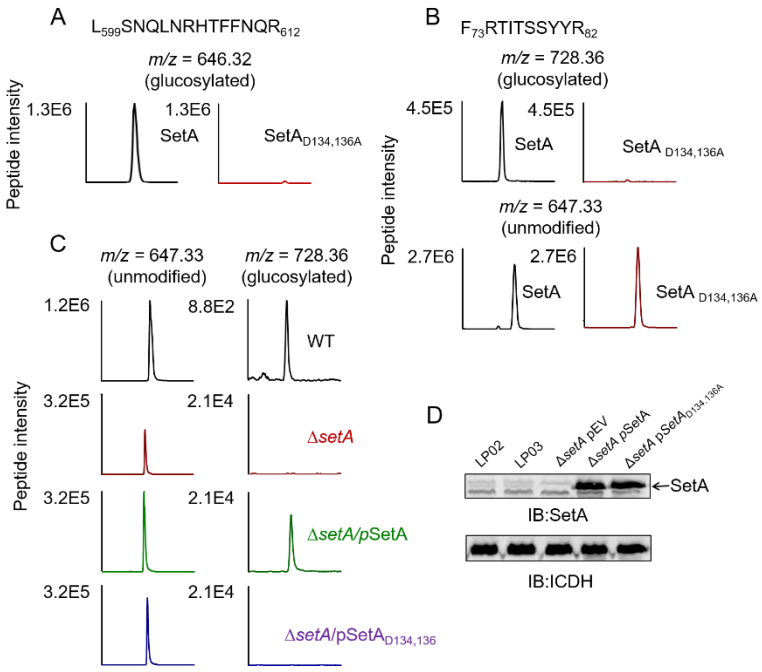

Figure 2-3. Glucosylation of Rab1 in biochemical reactions and during *L. pneumophila* infection. (A) Auto-glucosylation of SetA. Glucosylated SetA peptides were detected in wild-type SetA but not in its enzymatically inactive mutant. The extracted ion chromatograms of doubly protonated L_{599}SNQLNRHTFFNQR_{612} (m/z = 646.32) are shown. (B) *In vitro* glucosylation assays with UDP-glucose as a precursor. Equal amounts of purified Rab1 were incubated with either His_6-SetA or its enzymatically inactive mutant $SetA_{D134,136A}$. Gel-separated Rab1 was digested for further LC-MS/MS analyses. Extracted ion chromatograms of Rab1 peptide F_{73}RTITSSYYR_{82} with glucosylation (m/z = 728.36) and without modification (m/z = 647.33) are shown. (C) Glucosylation of Rab1 by SetA during *L. pneumophila* infection. FLAG-tagged Rab1 was isolated from host cells infected by the indicated *L. pneumophila* strains and analyzed by LC-MS/MS. The extracted ion chromatograms of Rab1 peptide F_{73}RTITSSYYR_{82} are shown. (D) The expression levels of SetA in different *L. pneumophila* strains. Lp02: wild type; Lp03: dotA-; Δ*setA*pEV: the Lp02Δ*setA* strain carrying an empty vector; Δ*setA*pSetA: the Lp02Δ*setA* strain carrying a plasmid that expresses SetA; Δ*setA*p$SetA_{D134,136A}$: the Lp02Δ*setA* strain carrying a plasmid that expresses the enzymatically inactive mutant $SetA_{D134,136A}$. (Mass spectrometry analysis performed by Wang, Z. *et al.* of Peking University)

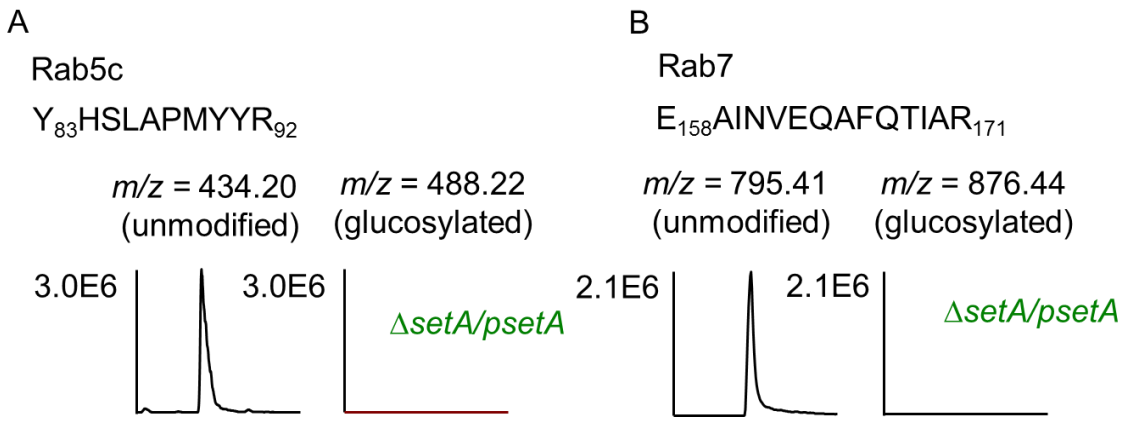

Figure 2-4. Undetectable levels of Rab5c and Rab7 glucosylation during L. pneumophila infection of host cells. (A) The extracted ion chromatograms of Rab5c peptide Y83HSLAPMYYR92 are shown. The peak intensities indicate the relative amounts of Rab5c peptides with potential glucosylation (m/z = 434.20) or without modification (m/z = 488.22). FLAG-tagged Rab5c was isolated from host cells infected by Legionella Δ*setA*/pSetA strain and analyzed by LC-MS/MS. (B) The extracted ion chromatograms of Rab7 peptide E158AINVEQAFQTIAR171 are shown. The peak intensities indicate the relative amounts of Rab7 peptides with potential glucosylation (m/z = 876.44) or without modification (m/z = 795.41). (Mass spectrometry analysis performed by Wang, Z. *et al.* of Peking University)

SetA preferentially modified the GDP-bound form of Rab1 and the modification affected its interactions with GDI1 but not SidM.

Rab1 oscillates between a GTP-bound and a GDP-bound form through its activity cycle (Bhuin & Roy, 2014; Bourne, 1988). To determine the effects of the modification, we examined whether SetA has a preference for Rab1 in one of these two forms. We first ectopically expressed SetA in HEK293T cells together with either $Rab1_{Q70L}$, a mutant that mimics the GTP-bound form (Nuoffer, Davidson, Matteson, Meinkoth, & Balch, 1994) or $Rab1_{S25N}$, a mutant that assumes the GDP-bound conformation (Tisdale, Bourne, Khosravi-Far, Der, & Balch, 1992). Immunoblotting assays confirmed that both SetA and Rab1 were produced at similar levels between cells transfected to express these two mutants. Each form of Rab1 was then affinity purified for analysis by LC-MS to determine the rates of modification. Our results reveal that Rab1 in the GDP-bound form exhibited a markedly higher ratio of modification than that of its GTP-bound form (**Fig. 2-5A**). Furthermore, we evaluated the *in vitro* modification rates by loading purified Rab1 with either GDP or the non-hydrolyzable GTP analogue GTPγS. After incubation with SetA, LC-MS analyses revealed a higher modification rate (2-3 fold) of Rab1:GDP than that of Rab1:GTP (**Fig. 2-5B**). Collectively, these results indicate that SetA preferentially modifies the GDP-bound form of Rab1.

In the regulation of vesicle trafficking, Rab proteins are cycled between the cytosol and intracellular membranes depending on their activation state (Grosshans, Ortiz, & Novick, 2006). In the inactive GDP-bound form, Rabs bind to a GDP dissociation inhibitor (GDI) and are maintained in the cytosol. In the active GTP-bound form, Rabs are associated with membranes, where they interact with effectors to promote vesicle fusion and trafficking (Cherfils & Zeghouf, 2013). As SetA preferentially modifies the GDP-bound form of Rab1 and other Rab1 modifications performed by *L. pneumophila*, AMPylation and phosphorylcholination, inhibit Rab1 binding to a GDI (Oesterlin, Goody, & Itzen, 2012), we wondered whether glucosylation of Rab1 had a similar effect. We expressed HA-Rab1 in mammalian cells together with either FLAG-SetA or FLAG-SetA$_{D134,136A}$ and quantified the relative abundance of the endogenous GDI1 co-precipitated with Rab1 by selected reaction monitoring (SRM) analyses. Immunoprecipitation of the potential Rab1-GDI1 complex showed markedly less GDI1 binding to glucosylated Rab1 than the unmodified protein prepared from cells producing the SetA mutant (**Fig. 2-5C**).

Activation of Rab1 requires the exchange of GDP for GTP with the aid of a GEF protein. The Dot/Icm effector SidM is a GEF that directly binds to Rab1 and recruits it to the LCV (Ingmundson et al., 2007; Machner & Isberg, 2006, 2007; Murata et al., 2006). We tested whether glucosylation of Rab1 affects its interaction with SidM. We compared the binding affinity of SidM to glucosylated Rab1 and its native form. Purified recombinant SidM was incubated with lysates from cells expressing Rab1 together with either SetA or the catalytically inactive mutant. Immunoprecipitation of the potential Rab1-SidM complex showed indistinguishable binding of SidM to glucosylated Rab1 and unmodified controls prepared from cells producing the SetA mutant (**Fig. 2-6**). Together, these results suggest that glucosylation of Rab1 affects its interaction with GDI1 but not SidM, which is similar to the impact of AMPylation or phosphorylcholination on this GTPase (Mukherjee et al., 2011; Müller et al., 2010; Oesterlin et al., 2012).

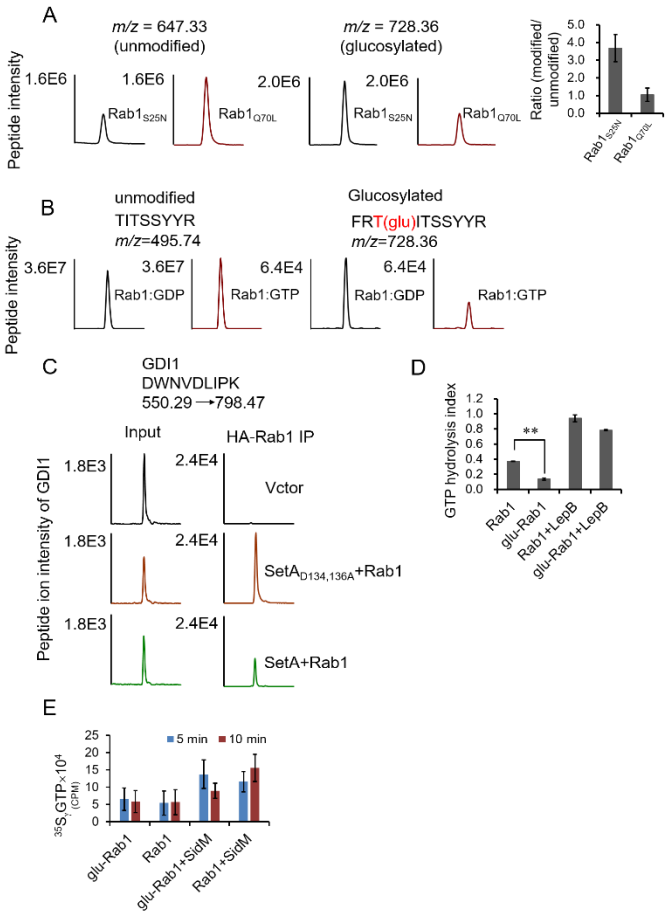

Figure 2-5. Preferential glucosylation of GDP-locked Rab1 over the GTP-bound form and the influence of this modification on Rab1 function. (A) SetA co-expressed with $Rab1_{Q70L}$ (GTP-locked Rab1) or $Rab1_{S25N}$ (GDP-locked Rab1) in HEK293T cells. The glucosylation of these two forms of Rab1 was detected by LC-MS/MS. The left panels are the extracted ion chromatograms of doubly protonated peptide F_{73}RTITSSYYR$_{82}$ with peak intensities representing the relative amounts of the modified or unmodified peptides. The right bar graphs plot the intensity ratio of the modified peptide over the unmodified one for both GTP- and GDP-locked Rab1 samples. (B) Wide type Rab1 was purified and loaded with GDP or GTP. The *in vitro* glucosylation of Rab1:GDP or Rab1:GTP was monitored by LC-MS. The left and right panels are the extracted ion chromatograms of doubly protonated peptide T_{75}ITSSYYR$_{82}$ and F_{73}RTITSSYYR$_{82}$ with peak intensities representing the relative amounts of the unmodified and modified peptides respectively. (C) Glucosylation of Rab1 affected its interaction with GDI1. HA-tagged Rab1 was co-expressed with FLAG-SetA or its catalytically inactive mutant $SetA_{D134,136A}$ in HEK293T cells. Samples from cells transfected with an empty vector were included as negative controls. The relative abundance of the endogenous GDI1 co-precipitated with Rab1 was quantified by selected reaction monitoring (SRM) analyses with the transition of 550.29→798.5 (DWNVDLIPK). (D) Inhibition of Rab1 GTPase activity by SetA-mediated glucosylation. 1 mM unmodified Rab1 or glucosylated Rab1 were incubated with GTP for 2 h with or without the addition of 0.1 mM LepB. The GTPase activity was assayed by measuring the level of free phosphate released by Rab1-mediated hydrolysis. The GTP hydrolysis index was calculated as follows: (OD620 of the experimental samples – OD620 of the blank)/ OD620 of the Rab1 associated with LepB. (E) Impact of Rab1 GTP loading by SetA-mediated glucosylation. GDP-loaded GST-Rab1 or glucosylated GST-Rab1 was incubated with 35SγGTP with or without SidM for the indicated time. Radioactivity associated with the protein was determined by a scintillation counter. Data are from three independent experiments (A, D, E) with error bars denoting standard deviation. *p<0.05, **p<0.01. (Mass spectrometry analysis and GTP hydrolysis assay performed by Wang, Z. *et al.* of Peking University)

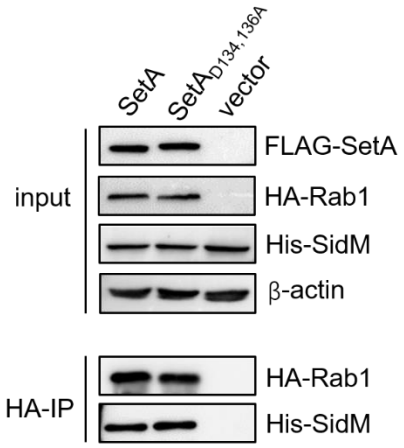

Figure 2-6. Unaltered binding of SidM to Rab1 upon its glucosylation. HA-tagged Rab1 was co-expressed with SetA or its catalytically inactive mutant $SetA_{D134,136A}$ in HEK293T cells. Samples from HEK293T cells transfected with an empty vector were used as negative controls. The cell lysates were further incubated with purified His_6-SidM (2 μg). The binding efficiency of purified His_6-SidM to Rab1 was assessed by immunoprecipitation. The levels of Rab1 and precipitated SidM were probed by immunoblotting analyses. (Experiment performed by Wang, Z. *et al.* of Peking University)

Glucosylation of Rab1 inhibited its GTPase activity but did not interfere with GTP loading.

Next we investigated the functional consequences of SetA-mediated glucosylation on its GTP hydrolysis activity. To obtain large amounts of modified proteins, GST-Rab1 was overexpressed in *E. coli* together with His_6-SetA or His_6-$SetA_{D134,136A}$. LC-MS measurements of the affinity purified Rab1 showed that >70% of the protein was glucosylated when co-expressed with SetA. Both the modified and unmodified versions of Rab1 were purified and incubated with GTP in reactions with or without the bacterial GAP LepB (Ingmundson et al., 2007). Compared to non-modified controls, glucosylated Rab1 exhibited markedly lower GTPase activity (**Fig. 2-5D**). As expected, in reactions that received LepB, the GTP hydrolysis activity was significantly higher. Nevertheless, the modified Rab1 exhibited significantly lower efficiency of GTP hydrolysis compared to its native counterpart (**Fig. 2-5D**).

To better understand the inhibition of Rab1 GTPase activity upon glucosylation, we examined the ability of the modified Rab1 to load GTP with or without SidM catalysis. Spontaneous GTP loading by glucosylated Rab1 did not detectably differ from its unmodified counterpart. There was also no detectable difference in the level of bound GTP between the

modified and unmodified versions when the reaction was catalyzed by SidM (**Fig. 2-5E**). Thus, glucosylation inhibits the GTPase activity of Rab1 but not its ability to associate with GTP.

Some modifications on Rab1 interfere with further effector-induced modifications.

The residue Thr_{75} glucosylated by SetA is close to the sites modified by AnkX and SidM (Ser_{79} and Tyr_{80}, respectively) (Mukherjee et al., 2011; Müller et al., 2010). We set out to determine whether primary glucosylation of Rab1 interferes with subsequent AMPylation or phosphorylcholination due to potential steric hindrance. To address this, we purified GST-Rab1 from *E. coli* expressing either SetA or the catalytically inactive $SetA_{D134,136A}$ and further incubated the proteins with either SidM or AnkX and searched for potential secondary modifications (i.e., double modifications on the same protein). In all cases, the rates of modification were monitored by LC-MS measurements of relevant peptides. Double modifications on Rab1 (simultaneous glucosylation with either AMPylation or phosphorylcholination) were readily observed, as evidenced by the detection of the doubly modified peptides -F_{73}RT(glu)ITSS(pc)YYR_{82}- and -F_{73}RT(glu)ITSSY(pc)YR_{82}- under collision-induced dissociation. Quantitative mass spectrometric analyses indicated that approximately 74% of glucosylated Rab1 was further AMPylated upon incubation with SidM, yielding dual modified proteins; this rate did not differ significantly from reactions with unmodified Rab1 (~80%) (**Fig. 2-7A**). Similar results were obtained for glucosylated Rab1 used for subsequent phosphorylcholination (93% vs 95%) (**Fig. 2-7B**).

Additionally, we investigated whether primary AMPylation or phosphorylcholination would impact subsequent glucosylation. Purified Rab1 was first incubated with either SidM or AnkX prior to the addition of SetA and UDP-glucose. LC-MS analyses detected markedly lower glucosylation rates for AMPylated or phosphorylcholinated Rab1 (**Fig. 2-8**). In fact, peptides modified by both phosphorylcholination and glucosylation were not detectable under our experimental conditions. Taken together, these findings suggest that primary glucosylation of Rab1 does not interfere with subsequent AMPylation or phosphorylcholination while AMPylation or phosphorylcholination does affect secondary glucosylation.

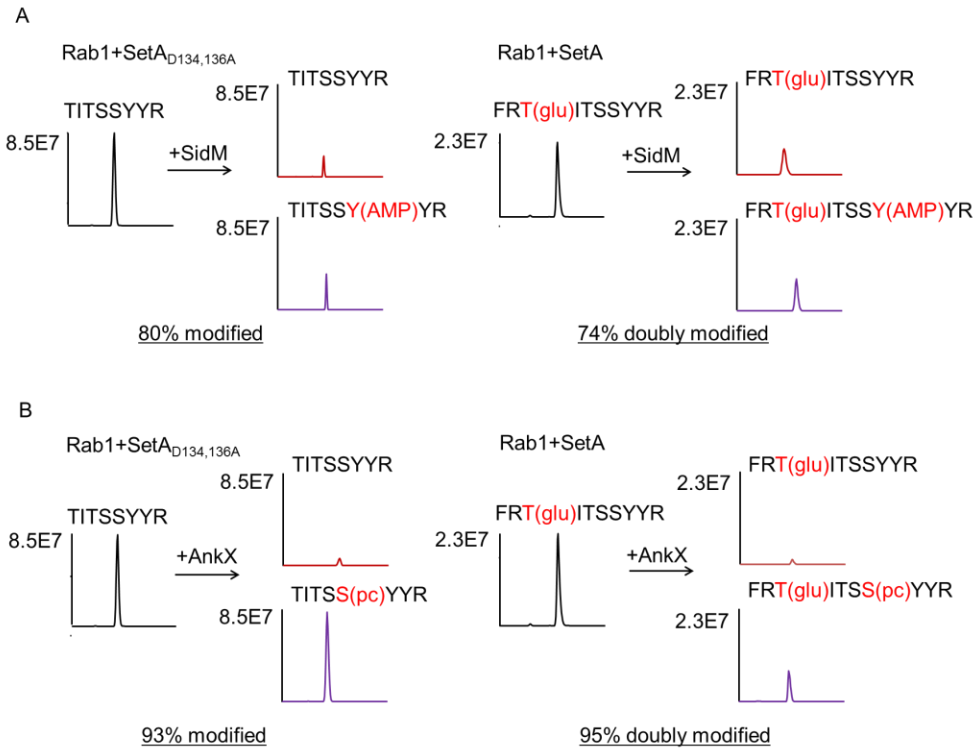

Figure 2-7. Primary glucosylation of Rab1 on Thr$_{75}$ did not interfere with subsequent AMPylation or phosphorylcholination. Purified GST-Rab1 from *E. coli* expressing SetA or its catalytically inactive mutant was incubated with either SidM or AnkX for potential AMPylation or phosphorylcholination. The modification status of Rab1 was analyzed by LC-MS/MS. The extracted ion chromatograms of different peptides (with or without modifications) are shown. The rates of AMPylation or phosphorylcholination of unmodified $T_{75}ITSSYYR_{82}$ and glucosylated $F_{73}RTITSSYYR_{82}$ were assessed by monitoring the peak intensities of various peptide forms before and after *in vitro* reactions. (A) The rates of AMPylation of unmodified $T_{75}ITSSYYR_{82}$ and glucosylated $F_{73}RTITSSYYR_{82}$. (B) The rates of phosphorylcholination of unmodified $T_{75}ITSSYYR_{82}$ and glucosylated $F_{73}RTITSSYYR_{82}$. (Mass spectrometry analysis performed by Wang, Z. *et al.* of Peking University)

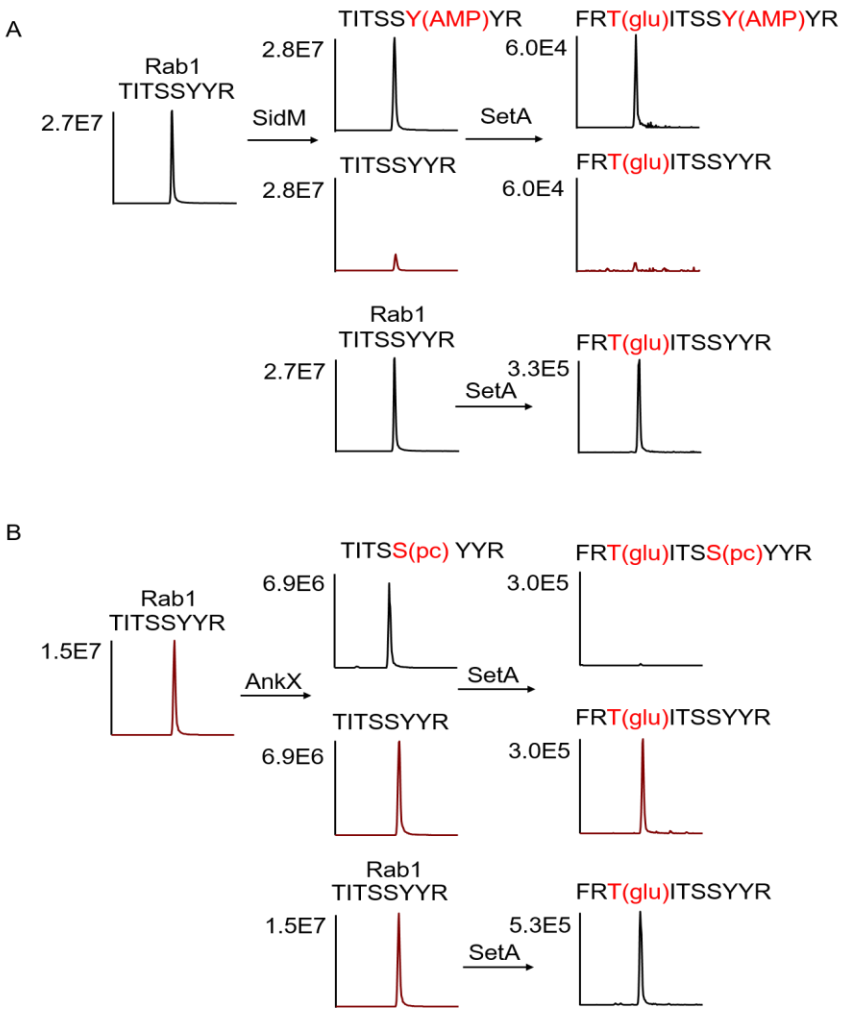

Figure 2-8. Primary AMPylation or phosphorylcholination of Rab1 adversely impacted subsequent glucosylation. Purified GST-Rab1 was incubated with either SidM or AnkX for potential AMPylation or phosphorylcholination. Half of the reaction mixtures were used for further glucosylation by adding SetA and UDP-glucose. The same amounts of Rab1 were used for control experiments. The modification status of Rab1 was analyzed by LC-MS/MS. The extracted ion chromatograms of different peptides (with or without modifications) are shown. (A) The intensity of Rab1 peptides with primary AMPylation and secondary glucosylation and those peptides with only glucosylation. (B) The intensity of Rab1 peptides with primary phosphorylcholination and secondary glucosylation and those peptides with only glucosylation. (Mass spectrometry analysis performed by Wang, Z. *et al.* of Peking University)

Discussion

To establish an intracellular niche permissive for its replication, *L. pneumophila* utilizes a large number of effectors to hijack host vesicle trafficking pathways (Qiu & Luo, 2017). Among these, SetA inhibits yeast growth by targeting vesicle trafficking in a manner that requires a

glucosyltransferase domain containing the conserved DXD motif, which possesses mono-O-glucosyltransferase activity using UDP-glucose as a sugar donor (Heidtman et al., 2009; Jank et al., 2012). Glycosylation is increasingly recognized as an important strategy used by bacterial pathogens to subvert host cell functions. Clostridium difficile toxins A (ToxA) and B (ToxB), for instance, glucosylate Rho GTPases, leading to a redistribution of the microfilament system (Just, Selzer, et al., 1995; Just, Wilm, et al., 1995). In addition, the *Escherichia coli* type III effector NleB catalyzes arginine GlcNAcylation of host death receptors to disrupt TNF signaling in infected cells (S. Li et al., 2013; Pearson et al., 2013). *L. pneumophila* itself also encodes three other effectors (Lgt1, 2 and 3) with glucosyltransferase activity. Unlike SetA, these effectors function to inhibit host protein synthesis by targeting the elongation factor eEF1A (Belyi et al., 2006; Belyi et al., 2008), likely to liberate amino acids for bacterial consumption (De Leon et al., 2017).

Rab GTPases cycle between an inactive GDP-bound form and an active GTP-bound form to recruit different downstream effectors responsible for vesicle formation, movement, tethering and fusion (Grosshans et al., 2006; Zerial & McBride, 2001). Mass spectrometry analyses revealed that multiple residues of Rab1 were glucosylated when SetA was overexpressed (**Fig. 2-2A**). Quantitative mass spectrometric analysis showed that modification on Thr_{75} had the highest rate when Rab1 was co-expressed in mammalian cells (**Fig. 2-2B**). In addition, in reactions with purified proteins, Rab1 was effectively modified by SetA, again mostly on Thr_{75} (**Fig. 2-3B**). Further, only the modification of this site was detectable in Rab1 purified from cells infected by *L. pneumophila* (**Fig. 2-3C**). Thus, Thr_{75} is the major site of SetA-mediated Rab1 modification. This residue is located in the highly conserved switch II region of GTPases, which is involved in binding to various regulatory proteins. Levin *et al.* found that Thr_{75} is phosphorylated by TAK1, a kinase involved in innate immunity (Levin, Hertz, Burlingame, Shokat, & Mukherjee, 2016). In addition, when infected by the *L. pneumophila* mutant Δ*ankX*Δ*sidM*, the level of Rab1 phosphorylation was lower than those in uninfected cells or cells infected by the Δ*dotA* mutant (Levin et al., 2016), suggesting additional effector(s) may target Rab1 and influence TAK1-mediated phosphorylation. We reason that SetA may be one of these effectors, competing with TAK1 for available substrates. Clearly, the bacterium competes with the host to control the activity of Rab1. Phosphorylation on Thr_{75} reduces the binding affinity of Rab1 to GDI1 (Levin et al., 2016). Glucosylation on Thr_{75} also led to diminished interaction between Rab1 and GDI1 (**Fig. 2-**

5C). This may promote Rab1 incorporation into the membrane of the LCV, consistent with the finding that SetA is associated with the LCV shortly after *Legionella* uptake (Jank et al., 2012). Nevertheless, the Δ*setA* mutant did not exhibit a detectable difference in the retention of Rab1 on the LCV (**Fig. 2-9**), arguing against a role of SetA-mediated glycosylation in altering the cellular localization of Rab1.

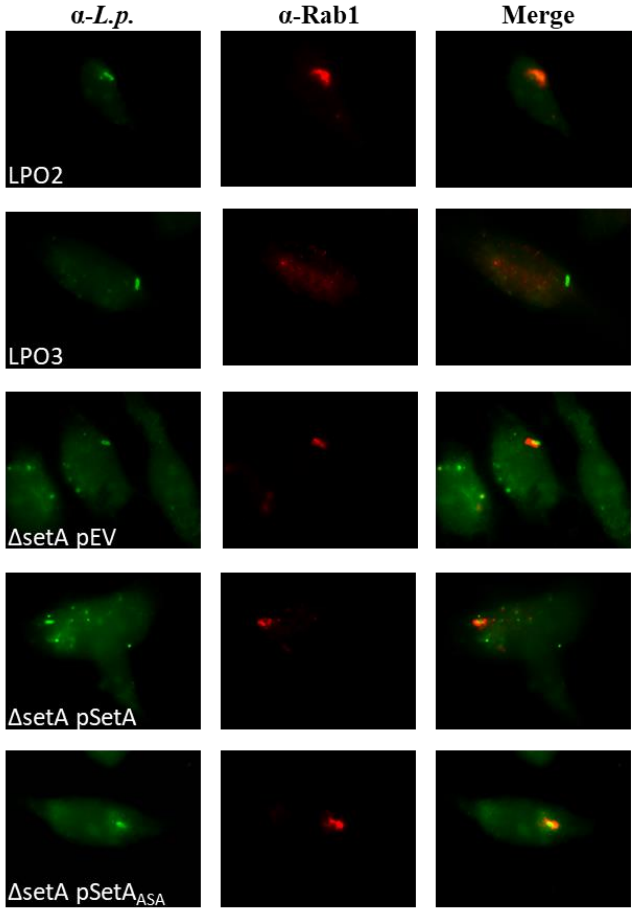

Figure 2-9. The absence of a catalytically active SetA has no bearing on the association of Rab1 with the LCV during *L. pneumophila* infection. BMDM were infected with the indicated strains at a MOI of 0.5. At 1 hpi, the cells were fixed and immunostained with antibodies against *L. pneumophila* and Rab1. There was no discernible difference in the level of Rab1 localization with the LCV between the strains, with the exception of LP03, the *dotA* mutant negative control.

Our results indicate that glucosylation inhibits the GTPase activity of Rab1 but does not affect its ability to receive GTP (**Fig. 2-5D and E**), which is in line with the observation that SetA prefers the GDP-bound form of Rab1. Thus, the activity of SetA appears to increase the pool of the GTP-bound, active form of Rab1. In this regard, SetA may function synergistically with other

effectors such as SidM to ensure that active Rab1 is associated with the LCV for a certain duration during *L. pneumophila* infection.

Of note is that despite the close proximity of the major glucosylation site on Rab1 to residues modified by the *L. pneumophila* effectors SidM and AnkX, modification of Thr_{75} by SetA does not detectably interfere with subsequent AMPylation of Tyr_{80} or phosphorylcholination of Ser_{79} (**Fig. 2-7A and B**). This observation suggests that steric hindrance is not necessarily an issue for simultaneous Rab1 modifications by multiple effectors. However, we did find that secondary glucosylation was impaired by AMPylation or phosphorylcholination (**Fig. 2-8**). We reason that the first modification may induce some conformational changes, minimizing SetA's accessibility of the targeted Rab1 residue. We did not detect MS signals corresponding to any doubly modified Rab1 molecules purified from cells infected with wild type *L. pneumophila*, suggesting that these modifications are not extensive enough for detection or simultaneous modifications may not occur on the same molecule during infection at least at the time points measured during our study.

Our findings that SetA targets Rab1 by glucosylation provide a molecular mechanism for its blockage of the host secretory pathways as well as cellular toxicity to yeast and mammalian cells, effects which are also seen for SidM and AnkX (Tan et al., 2011; Tan & Luo, 2011). The toxicity likely results from the lock of Rab1 in its active GTP-bound form, or from the disruption of its interactions with other cellular binding partners or a combination of both. The activity of SetA adds an additional layer of complexity to the regulation of Rab1 function during *L pneumophila* infection. It is possible that host cells also regulate Rab1 activity by glucosylation at Thr_{75}. For the study of *L. pneumophila* virulence, a future challenge is to dissect the potential interplays among these modifications and how each of them is temporally and spatially regulated to ensure a successful infection.

CHAPTER 3. THE MECHANISM OF THE REGULATION OF SIDI ACTIVITY BY ITS METAEFFECTOR LPG2505

Abstract

Legionella pneumophila is an intracellular pathogen and as such, requires precise control of its virulence in order to replicate efficiently. To that end, *L. pneumophila* produces many (at least 330) effectors which target a wide variety of host proteins and systematically manipulate specific host processes such as immune response, vesicle trafficking and gene expression. The *L. pneumophila* genome also encodes effectors of those effectors, called metaeffectors, to regulate the effector activities and prevent overtaxing of the host. Only a handful of effector/metaeffector pairs have been characterized thus far. The known regulatory mechanisms include, abrogation of host protein modifications, direct modification of the effector and direct binding to the catalytic pocket of the cognate effector. We sought to characterize the regulatory function of the already established SidI metaeffector Lpg2505. Through the use of affinity pulldowns, size exclusion chromatography (SEC) and bacterial two-hybrid assays, we established that the regulatory activity of Lpg2505 is through direct binding to SidI, leading to the inhibition of its activity. Such interaction occurs within *L. pneumophila* without the need of a host trigger and an excess of Lpg2505 interferes with translocation of SidI into the host. The crystal structure of Lpg2505 suggests no enzymatic activity for Lpg2505 and aided in identifying a region of Lpg2505 potentially important for binding to and inhibiting SidI function. Finally, the levels of SidI and Lpg2505 expression indicate a temporal control based on changes in the production of the proteins.

Introduction

The intracellular replication of *L. pneumophila* begins with modulation of host processes and formation of the *Legionella* containing vacuole (LCV) (Isberg et al., 2009). This is achieved by injecting over 330 predicted effector proteins directly into the cytosol through a type IV secretion system (TIVSS). These predicted effector proteins target processes such as immune response, vesicle trafficking, cell signaling and gene expression (Qiu & Luo, 2017).

One such host process targeted by *L. pneumophila* is protein translation. Interference with host cell translation is thought to aid in bacterial replication by freeing nutrients, such as amino

acids, suppressing cell cycle progression and modulating immune response gene expression (De Leon et al., 2017; Qiu & Luo, 2017; Sol et al., 2019). There have been five *L. pneumophila* effectors identified to date that inhibit host protein translation. The Lgt family (Lgt1, Lgt2, Lgt3) glucosylate the elongation factor eEF1A, resulting in loss of eEF1A activity (Belyi et al., 2008). The effector SidL was found to inhibit host translation in an *in vitro* assay and expression of SidL in *L. pneumophila* reduces host translation during infection in macrophages. However, the mechanism of such inhibition by SidL has not been determined (Fontana et al., 2011). Finally, SidI has been shown to bind to the elongation factors eEF1A and eEF1Bγ, and through this interaction, greatly impairs host translation. Similar to SidL, how SidI disrupts the elongation process remains to be determined (Shen et al., 2009).

Extensive targeting of entire cellular processes can be detrimental to the host and counter-proliferative for an intracellular pathogen. To effectively replicate within the host cell *L. pneumophila* must maintain a balance between its own needs and the fitness of the host. To help maintain this balance, *L. pneumophila* will secrete secondary effectors that regulate the activities of effectors already acting on the host. These secondary effectors are termed metaeffectors, for effectors of effectors, and the genes of effector/metaeffector pairs are often encoded near one another and share a linked evolutionary history, a relationship known as synteny.

A handful of different regulatory mechanisms have been discovered for *L. pneumophila* metaeffectors. One form of regulation is by removal of an effector-mediated PTM on a host protein. For example, the metaeffector SidD, encoded next to and in a divergent orientation from the effector SidM (DrrA), regulates the activity of SidM by removing the AMP moiety added to Rab1 by SidM (Tan & Luo, 2011). Another form is exemplified by the effectors LubX and SidH. LubX is encoded upstream of SidH and regulates the activity of SidH through direct ubiquitination followed by host proteasome degradation (Kubori et al., 2010). SidJ is another metaeffector that regulates cognate effectors through direct modification. SidJ targets members of the SidE effector family by adding a glutamate to the residue necessary for ADP-ribosyltransferase activity, thereby suppressing the function of the SidE effectors (Black et al., 2019; Gan, Zhen, et al., 2019). A third regulatory method is direct inactivation through binding. In a yeast screen to identify effector/metaeffector pairs, Urbanus *et al.* discovered a few new pairs, one in where the metaeffector, LegL1 antagonizes the effector RavJ by binding directly to and blocking the active site. With a 1:1 stoichiometry, LegL1 and RavJ represented the first reported effector/metaeffector

pair that form a stable complex. However, the details of how the RavJ/LegL1 complex forms during *L. pneumophila* infection, or if LegL1 has an enzymatic function, have not been uncovered (Urbanus et al., 2016).

Here we show that, in a manner similar to RavJ/LegL1, the previously identified SidI metaeffector Lpg2505 (Burstein et al., 2016; Shames et al., 2017) regulates the activity of SidI by directly binding to SidI. We show that this interaction occurs within *L. pneumophila* prior to translocation and demonstrate that an excess of Lpg2505 negatively effects translocation of SidI into the host. Finally, we determined the structure of Lpg2505 and through this identified a region of Lpg2505 that is necessary for the interaction with SidI.

Results

SidI and Lpg2505 show typical effector-metaeffector relationship.

Previously, a screen performed by Shames *et al.* identified a gene which was necessary for efficient *L. pneumophila* intracellular replication, *lpg2505* (Shames et al., 2017). The authors found that the replication defect seen for the Δ*lpg2505* strain was dependent on the presence of a functional SidI. When the operon including *sidI* was removed from the chromosome of the Δ*lpg2505* strain, replication within bone marrow-derived macrophages (BMDMs) was comparable to that of wild-type *L. pneumophila*. Replacement of *sidI* with the inactive mutant $sidI_{R453P}$ in the Δ*lpg2505* strain also led to replication comparable to wild-type. In addition, they showed that toxicity of SidI to yeast was suppressed by Lpg2505 (Shames et al., 2017).

I began evaluating the relationship between SidI and Lpg2505 by first assessing the expression profiles of both respective genes during growth in broth. After a 1:20 dilution SidI was detectable almost immediately. After 12 hours the amount of SidI was reduced and by 21 hours it was no longer detectable. This result coincides with the notion that as an inhibitor of host cell translation, the activity of SidI would free up nutrients necessary for bacterial use during the exponential phase. Typical of a metaeffector, the amount of detectable Lpg2505 increased after the expression of SidI began to reduce, at approximately 12 hours, and peaked at 18 hours (**Fig. 3-1A**). This sequential expression pattern is in accordance with the notion that Lpg2505 is a regulator of SidI, counteracting its activity after the most active time of *L. pneumophila* growth.

Interestingly, low level detection of Lpg2505 was seen throughout the growth cycle, made evident by comparison to the Δ*lpg2505* strain.

I then performed a saponin fractionation assay to determine if the pattern of translocation for both proteins coincided with the pattern of expression in broth. Neither translocated SidI nor translocated Lpg2505 could be detected at various time points during infection even when I enriched for the proteins by IP with antibodies specific to the two proteins (data not shown). SidI is a potent host-cell translation inhibitor, therefore it is not surprising that the amount translocated during infection may be too low to detect using this method.

Replication defect of Δ*lpg2505* strain is not due to immune response by host cell.

To evaluate why the Δ*lpg2505* strain is defective for intracellular replication, whether it is due to poor growth of the bacteria or a response of the host cell, I analyzed the formation of the LCV by relevant *L. pneumophila* strains in bone marrow-derived macrophages (BMDM) at 14 hpi by quantifying the number of bacterial cells within the vacuoles. The majority of the cells infected with the wild-type strain Lp02 harbored large vacuoles containing 1-10 cells per vacuole and approximately 15% had vacuoles containing greater than 10 bacterial cells. In contrast, approximately 80% of the cells infected by the Δ*lpg2505* strain had small vacuoles containing only 1 or 2 cells per vacuole, a result similar to the BMDM cells infected with the *dotA* mutant LP03 (**Fig. 3-1B**). For all three strains the host cells appeared healthy with no indications of stress. The smaller LCVs found in the cells infected with the Δ*lpg2505* strain, and the lack of any host-cell stress phenotype, indicate that the reduced replication for *L. pneumophila* missing *lpg2505* is not likely due to an immune response by the host cells.

Incubation of SidI with Lpg2505 rescues SidI-dependent translation inhibition, but delayed addition of Lpg2505 does not.

To determine if Lpg2505 regulates SidI by counteracting the translation inhibition activity I used an *in vitro* translation assay with *luc* mRNA as the readout (Promega #L4960). I evaluated the level of protein translation in the presence of different combinations of SidI and Lpg2505. Shen *et al.* reported that as little as 2ng of SidI was sufficient to reduce the level of translated Luciferase by more than 80% (Shen et al., 2009). I compared the levels of translated *luciferase* in the presence of 50ng SidI and found that after incubation with Lpg2505, SidI had almost completely lost its

ability to inhibit the translation of *luciferase* (**Fig. 3-1C**). To determine if Lpg2505 was acting on eEF1A and reversing a potential SidI-dependent modification on the elongation factor, I added a saturating amount of Lpg2505 to a reaction preincubated with SidI and already displaying an inhibitory phenotype. Surprisingly, the addition of Lpg2505 after SidI-mediated inhibition had occurred did not restore translation, nor did it increase, even slightly, the production of Luciferase (**Fig. 3-1C**). These results suggest that Lpg2505 does not act to undo the activity of SidI on the elongation factors.

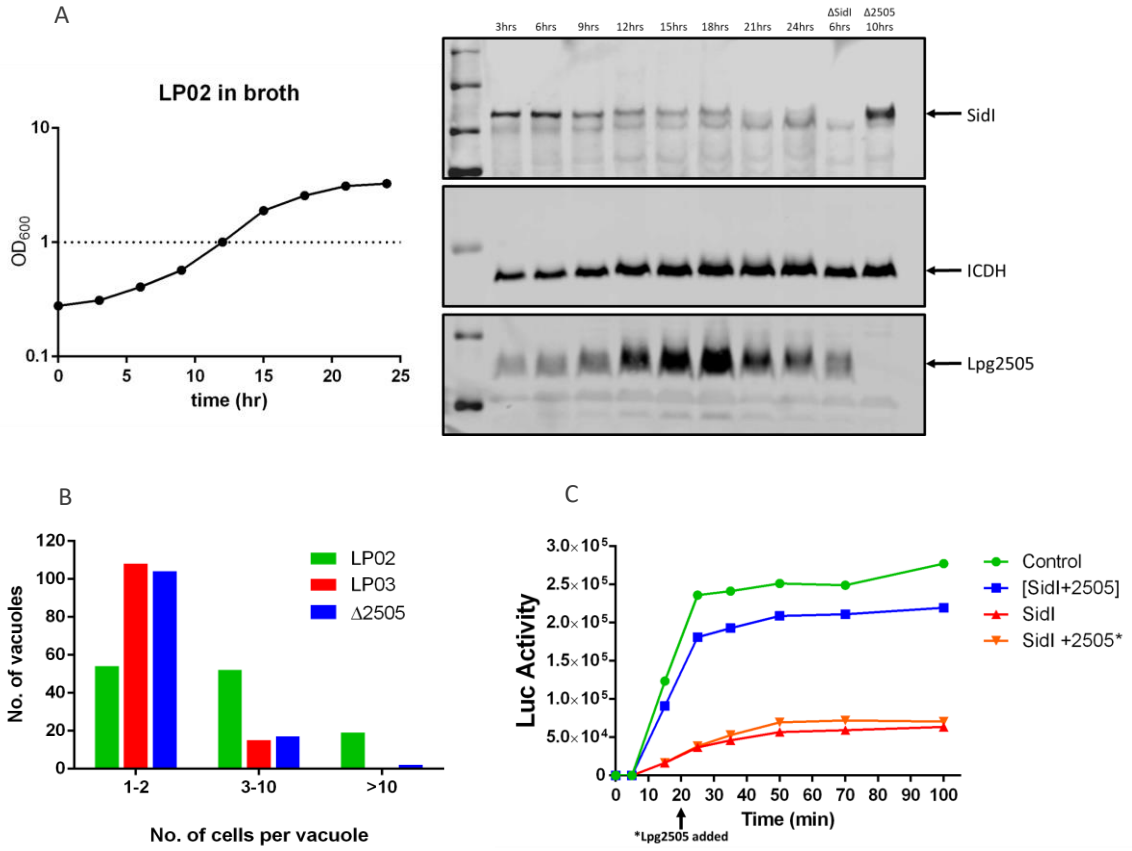

Figure 3-1. SidI and Lpg2505 show typical effector-metaeffector relationship. (A) Growth curve and western blot showing the changes in detectable SidI and Lpg2505 through broth growth cycle. An overnight culture of Lp02 was subcultured at a ratio of 1:20, and OD_{600} values were taken every 3 hours along with a sample of the cells for protein level evaluation using SDS-PAGE and immunoblotting. Anti-serum against isocitrate dehydrogenase (ICDH) was used as a loading control. (B) Bone marrow derived macrophages were infected with the indicated strains, washed 2 hpi to remove extracellular bacteria, and fixed at 14 hpi to enumerate the number of cells per vacuole. Total counted macrophages per strain was >120. (C) *In vitro luc* translation assay to evaluate Lpg2505-dependent regulation of SidI. SidI alone, SidI preincubated with Lpg2505 or rescue of SidI translation inhibition by a late addition of Lpg2505 were tested using a rabbit reticulocyte lysate (RRL) kit and Luciferase control RNA purchased from Promega. Luminescence of each reaction was measured every 10 minutes for 100 minutes. For the late addition reaction, Lpg2505 was added after the 20-minute luminescence reading was taken.

Structure of Lpg2505 does not have an easily identifiable enzymatic site.

To better understand how Lpg2505 works to inhibit SidI, my collaborator, Dr. TaoTao Chen, determined the crystal structure of the protein to a resolution of 2.6 Å. The structure of Lpg2505 does not show significant homology with any other known protein structure. It has a compact shape consisting of 16 alpha-helices. There is no predictable catalytic binding pocket, indicating Lpg2505 likely does not have an enzymatic activity (**Fig. 3-2A**). However, the crystal structure did predict the formation of a symmetric homodimer for Lpg2505. The dimer is formed through the interactions of helices α1, α2 and α5 from one molecule with helices α8, α9, α10 and α16 from another molecule (**Fig. 3-2B**). Lpg2505 dimer formation was confirmed using size-exclusion chromatography (SEC). Purified untagged Lpg2505 produced two separate peaks in SEC, one at approximately the predicted molecular weight (mw) (34 kDa) and another at approximately double the predicted mw (68 kDa) (**Fig. 3-2C**). Based on the predicted dimerization interfaces, we theorized that a bulky N-terminal tag may interfere with the ability of Lpg2505 to form a dimer. Indeed, when we tested His_6-SUMO-Lpg2505, using the same conditions, only a single peak at approximately the predicted mw (47 kDa) was produced (**Fig. 3-2C**). When I tested the N-terminally tagged version for SidI inhibition in the *in vitro* translation assay I saw translation activity rescue comparable to the untagged version (**Fig. 3-2D**). Thus, it is likely that the dimer is an artifact resulting from crystallization, a common phenomenon known as crystal stacking (Gan, Zhen, et al., 2019). Consistent with this notion, the dimer form does not have biological significance in terms of inhibiting the function of SidI. Interestingly, the structure revealed that one region of Lpg2505 involved in the dimer interface does indeed play a role in SidI inhibition (addressed in a later section).

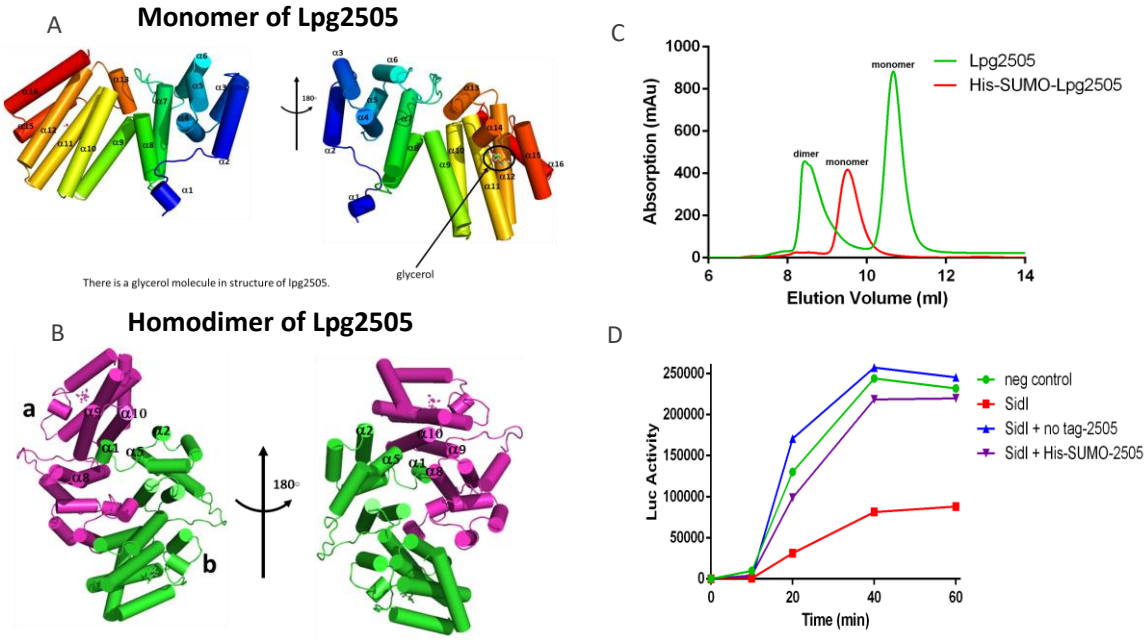

Figure 3-2. Crystal structure of Lpg2505 shows the formation of a dimer and no indication of an enzymatic activity. (A) Monomer of Lpg2505 showing compact form with 16 α-helices. (B) Homodimer of Lpg2505 showing the helices involved in the dimer interface. (C) SEC of the untagged and N-terminal tagged versions of Lpg2505. The peaks representing the monomer and dimer forms of each are indicated. (D) *In vitro* translation assay using RRL and *luc* control RNA to compare the ability of the N-terminally tagged Lpg2505 to rescue SidI-dependent translation inhibition with that of untagged Lpg2505. (The structure was determined by TaoTao Chen and Haidong Han of Xiamen University).

Lpg2505 directly interacts with SidI.

Because the later addition of Lpg2505 did not rescue SidI-dependent translation inhibition, I sought to determine if Lpg2505 inhibits SidI through a direct interaction. To do this, I performed a pulldown assay of the two purified proteins. After coincubation of tagless-Lpg2505 with either His_6-SidI or His_6-MvcA (Gan, Nakayasu, et al., 2019), as a negative control, Ni^{2+} beads were used to purify the His_6-tagged proteins and potential retention of Lpg2505 was evaluated using PAGE and Coomassie staining. Ni^{2+} beads were also added to Lpg2505 alone as a control. Only when His_6-SidI was purified did I detect retention of Lpg2505 (**Fig. 3-3A**).

Next, I tested the ability of SidI and Lpg2505 to form a stable complex using SEC. I compared samples containing His_6-SidI or His_6-SUMO-Lpg2505 alone to one containing both proteins together. The sample containing the combination of SidI and Lpg2505 produced an additional peak at a higher mw elution volume, indicating the formation of a complex (**Fig. 3-3B**).

PAGE analysis and Coomassie staining revealed both SidI and Lpg2505 in the fractions coinciding with the larger mw peak (**Fig. 3-3C-D**). In addition, the fraction containing the complex was tested for translation inhibition and showed a rescue phenotype when compared to the fraction pertaining to the peak containing SidI alone (**Fig. 3-3E**).

I also examined the interaction between SidI and Lpg2505 using a bacterial two-hybrid assay, in which binding of the two proteins will restore the enzymatic activity of the catalytic domain of the *Bordetella pertussis* toxin adenylate cyclase, leading to the production of the signaling molecule cAMP (Karimova, Pidoux, Ullmann, & Ladant, 1998). When compared to the strains containing SidI and the empty vector (EV) or Lpg2505 and the EV, the strain containing both proteins showed a 40-fold increase in β-galactosidase activity (**Fig. 3-3F**). All these data substantiate the mechanism of Lpg2505 regulation to be one of SidI inhibition through direct interaction.

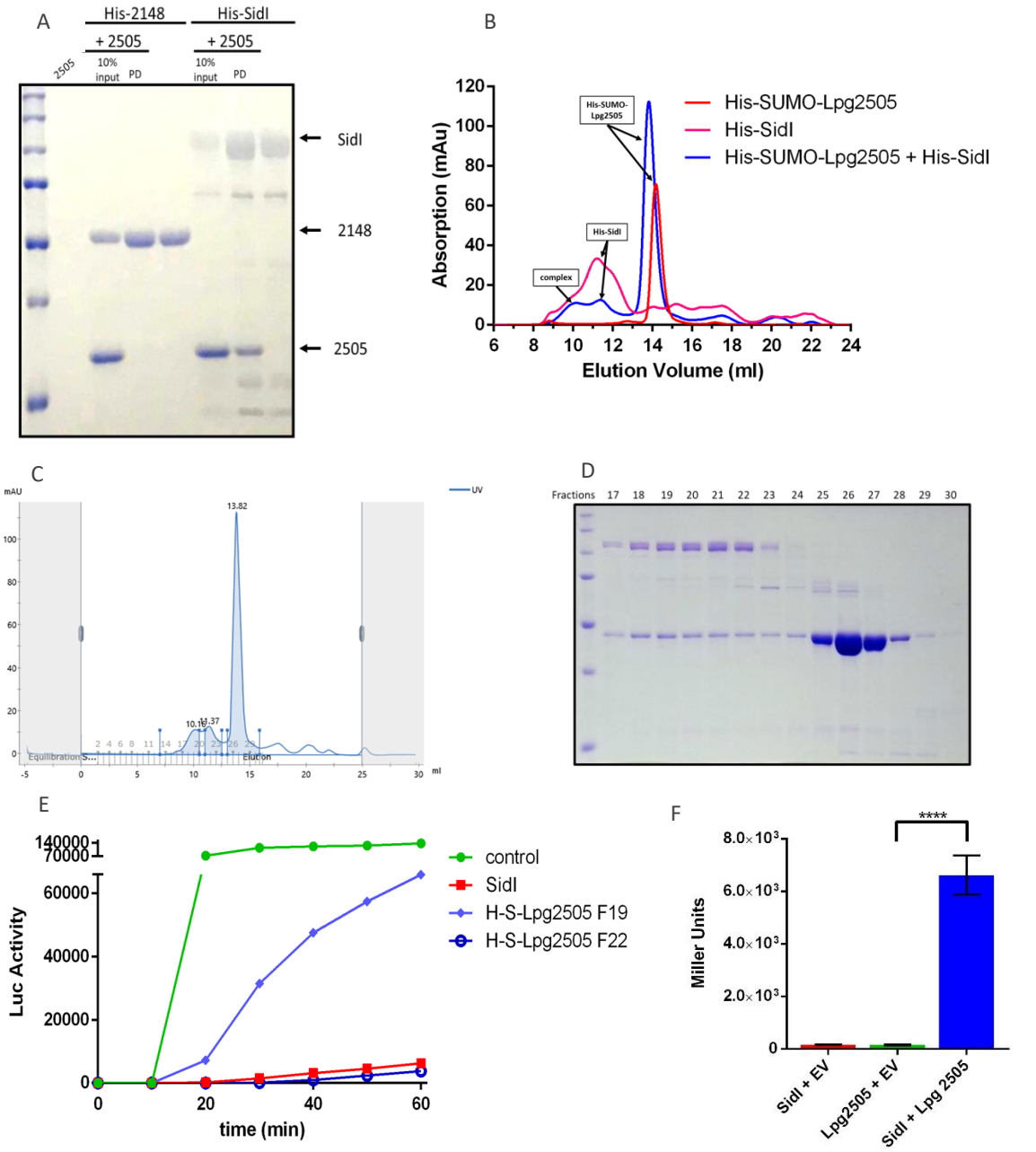

Figure 3-3. SidI and Lpg2505 form a stable complex. (A) A pure protein pulldown of Lpg2505 using His_6-SidI and His_6-MvcA. Proteins were combined and incubated at 30°C for one hour, incubated with Ni beads at 4°C for 30 minutes and after washing 5x with TBS + 1% NP40. The retention of Lpg2505 was assessed using PAGE followed by Coomassie staining and compared to the level seen in the 10% input. (B) SEC analysis of His_6-SidI alone, His_6-SUMO-Lpg2505 alone and coincubation of both proteins. Samples were run on an AKTA pure system (GE Healthcare) using a Superdex 200 increase 10/300 column (GE Healthcare) with a fractionation volume of 500 ul. (C,D) Chromatogram showing fractions pertaining to individual peaks produced during the SidI/Lpg2505 coincubation run and the Coomassie stained PAGE gel containing samples from the indicated fractions. (E) *In vitro* translation assay to assess the level of translation inhibition associated with each fraction. (F) Interaction between SidI and Lpg2505 determined by a bacterial two-hybrid system. Derivatives of BTH101 carrying the indicated plasmids were examined for galactosidase activity. Experiments were performed in triplicate with similar results obtained in all 3. Analysis was done using one-way ANOVA (****p<0.0001).

The interaction of SidI and Lpg2505 in *L. pneumophila*.

The detection pattern of SidI and Lpg2505 during growth in broth suggests that during the lag phase, both SidI and Lpg2505 are being expressed, although not at equally detectable levels. To determine if the two proteins interact within *L. pneumophila* prior to translocation into the host, I performed an immunoprecipitation (IP) assay using lysate from three different strains. Prior to lysis, cultures of Lp02, Δ*lpg2505* and Δ*sidI* were grown to 9 hrs. post-dilution, when both proteins are detectable. Using purified antibodies specific to Lpg2505 or SidI, I immunoprecipitated either SidI or Lpg2505 from all three strains and probed for the other protein to look for the specific interaction. After IP using α-Lpg2505 and only when Lpg2505 was present, in Lp02 and not in the Δ*lpg2505* strain, was SidI detected. Similarly, Lpg2505 was only detected in Lp02, after IP using α-SidI (**Fig. 3-4A**).

If the two effector proteins interact within the bacteria prior to introduction to the host, I wanted to know what effect, if any, the interaction has on the translocation of the two proteins. As mentioned previously, I was unable to detect translocation of the two proteins at endogenous levels using saponin fractionation and IP. Instead I employed exogenous expression of both SidI and Lpg2505 from plasmids in order to produce each protein at sufficient levels for detection using immunoblotting after saponin fractionation. I used this method to study any changes in the level of translocated SidI based on changes in the amount of produced Lpg2505. I expressed *sidI* on a plasmid under the control of the P_{BAD} promoter (Guzman, Belin, Carson, & Beckwith, 1995) in order to keep the expression level of SidI low and closer to endogenous levels, as well as distinct from Lpg2505 induction. I then altered the levels of Lpg2505 in strains containing P_{BAD}::*sidI* through either deletion of *lpg2505* or exogenously expressing *lpg2505* using IPTG induction. I was able to detect small amounts of SidI in the saponin soluble fraction only when the U937 cells were infected with the Δ*lpg2505* strain (**Fig. 3-4B**). These results indicate that Lpg2505 may interfere with SidI translocation, thereby limiting the amount of SidI that enters the host cell.

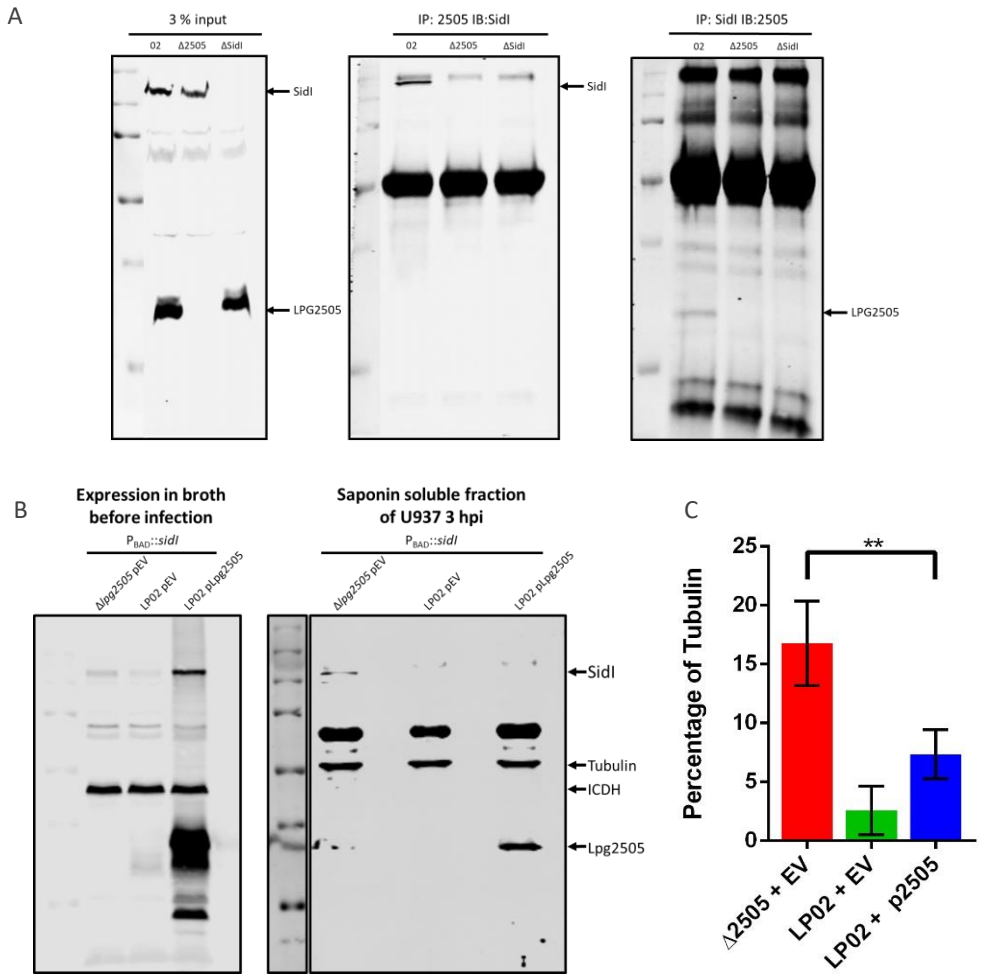

Figure 3-4. The interaction of SidI and Lpg2505 in *L. pneumophila*. (A) Immunoblots showing the association of endogenous SidI and Lpg2505 within *L. pneumophila*. The indicated strains were diluted 1:20 from an overnight culture and grown to 9 hpd. The cells were collected, and total protein samples were extracted from each using the Minute™ Total Protein Extraction Kit for Microbes with Thick Cell Walls from Invent Biotechnologies, Inc. (Cat # YT-015). Immunoprecipitation was performed on each sample using the indicated antibodies. Retention of either SidI or Lpg2505 was assessed using PAGE analysis and immunoblotting using the same indicated purified antibodies. (B) Translocation assay of ectopically expressed SidI based on altered amounts of Lpg2505 in U937 cells. Wild-type Lp02 or Δ*lpg2505* carrying pBBR1MCS1::P_{BAD}::*sidI* and pZL507 EV or pZL507::*lpg2505* were grown overnight with 1% arabinose and 0.1 mM IPTG in AYE broth. The induction of SidI and Lpg2505 within the bacteria was checked using immunoblotting and purified α-SidI and α-Lpg2505, with ICDH used as a loading control. The bacteria were then used to infect U937 cells at a MOI of 20 for 3 hours. The cells were collected, washed and fractionated using saponin. The saponin soluble fractions were then assayed for translocated proteins using immunoblotting, α-SidI and α-Lpg2505, with Tubulin as a loading control. (C) Quantification of translocated SidI as a percentage of Tubulin and normalized to expression in *L.p.* prior to infection. The values are from three separate experiments. Analysis was performed using one-way ANOVA (**p<0.05).

Lpg2505 residues 123-148 are required for SidI inhibition.

To further asses if the dimerization of Lpg2505 affected the inhibition of SidI activity, I constructed deletion mutants of Lpg2505 removing regions that potentially contribute to the dimer interface seen in the structure. More specifically, I removed the first 24 residues from the N-terminus ($Lpg2505_{\Delta N24}$) and residues 113-158 ($Lpg2505_{\Delta int46}$), corresponding to helices α1 and α2 and helices α8, α9 and α10, respectively (**Fig. 3-5A**). I began by testing these mutants for SidI translation inhibition rescue using the *in vitro* RRL translation assay. I found that although there was not a significant decrease in the ability of the $Lpg2505_{\Delta N24}$ to inhibit SidI function, $Lpg2505_{\Delta int46}$ showed a complete loss of SidI-inhibition function (**Fig. 3-5B**).

I also tested the mutants for the ability to rescue SidI-dependent toxicity in yeast. The N-terminal mutant showed rescue comparable to wild-type Lpg2505, but the internal deletion mutant, $Lpg2505_{\Delta int46}$, showed a complete loss of rescue even though the expression level of the mutant was higher than both the wild-type and $Lpg2505_{\Delta N24}$ (**Fig. 3-5C**).

To better define the region necessary for binding to and inhibiting SidI, I reduced the internal deletion region by 20 and 40 residues, deleting residues 113-148 ($Lpg2505_{\Delta int26}$) and 133-138 ($Lpg2505_{\Delta int6}$), respectively. When these mutants were tested for translation inhibition rescue using the RRL assay $Lpg2505_{\Delta int26}$, similar to $Lpg2505_{\Delta int46}$, was unable to rescue translation of Luciferase, but when only the 6 center residues were removed, SidI-dependent translation inhibition was fully rescued (**Fig. 3-5D**).

If the mechanism in which Lpg2505 inhibits SidI is through direct binding, the loss-of-function Lpg2505 mutants should no longer bind to SidI. When I tested the retention of all 4 mutants using His_6-SidI purification after coincubation, I saw a decrease in both $Lpg2505_{\Delta int26}$ and $Lpg2505_{\Delta int46}$ detection using immunoblotting compared to wild-type and $Lpg2505_{\Delta N24}$. Surprisingly, $Lpg2505_{\Delta int6}$ was not retained when His_6-SidI was purified, even though the mutant is still able to rescue translation inhibition in the RRL assay (**Fig. 3-5E**). Protein-protein interactions involve multiple residues and multiple non-covalent bonds. The mutant missing residues 133-138 may still have enough molecular interactions to bind to and inhibit SidI, but not enough to be retained during the extensive washing of the pure protein pulldown. Clearly the region of Lpg2505 residing from residues 123 to 148 is important for SidI inhibition and that function is dependent on the ability of Lpg2505 to interact with SidI.

Figure 3-5. Identification of Lpg2505 region necessary for binding to and thereby inhibiting SidI. (A) Diagram showing Lpg2505 dimer interface regions and residues deleted in $Lpg2505_{\Delta N24}$ and $Lpg2505_{\Delta int46}$. (B) RRL i*n vitro* translation assay evaluating the ability of $Lpg2505_{\Delta N24}$ and $Lpg2505_{\Delta int46}$ to rescue SidI-dependent translation inhibition and immunoblot showing amounts of protein added to each reaction. (C) Yeast spotting assay testing ability of $Lpg2505_{\Delta N24}$ and $Lpg2505_{\Delta int46}$ to rescue SidI-dependent toxicity. Yeast strain W303 carrying pSB157::*sidI* with a galactose inducible promoter was transformed with either p425GPD::*lpg2505*, p425GPD::$lpg2505_{\Delta N24}$ or p425GPD::$lpg2505_{\Delta int46}$ with constitutive expression. The strains were spotted on galactose to induce expression of SidI. To ensure the loss of rescue for the strain carrying p425GPD::$lpg2505_{\Delta int46}$ was not due to a lack of expression, the levels of detectable Lpg2505 was determined for each strain after growth on glucose. (D) RRL i*n vitro* translation assay evaluating the ability of $Lpg2505_{\Delta int26}$ and $Lpg2505_{\Delta int6}$ to rescue SidI-dependent translation inhibition and immunoblot showing amounts of protein added to each reaction. (E) Immunoblot of pure protein pulldown testing retention of Lpg2505 wild-type and deletion mutants after purifying His_6-SidI. Purified His_6-SidI was coincubated with the indicated purified versions of Lpg2505 for 1 hr. at 30°C, 10% was removed as the input samples followed by incubation with Ni beads at 4°C for 30 minutes. The beads were washed 5 times using TBS + 1% NP-40. SDS-PAGE and immunoblotting using α-SidI and α-Lpg2505 were used to compare the levels of Lpg2505 retained.

Figure 3-5.

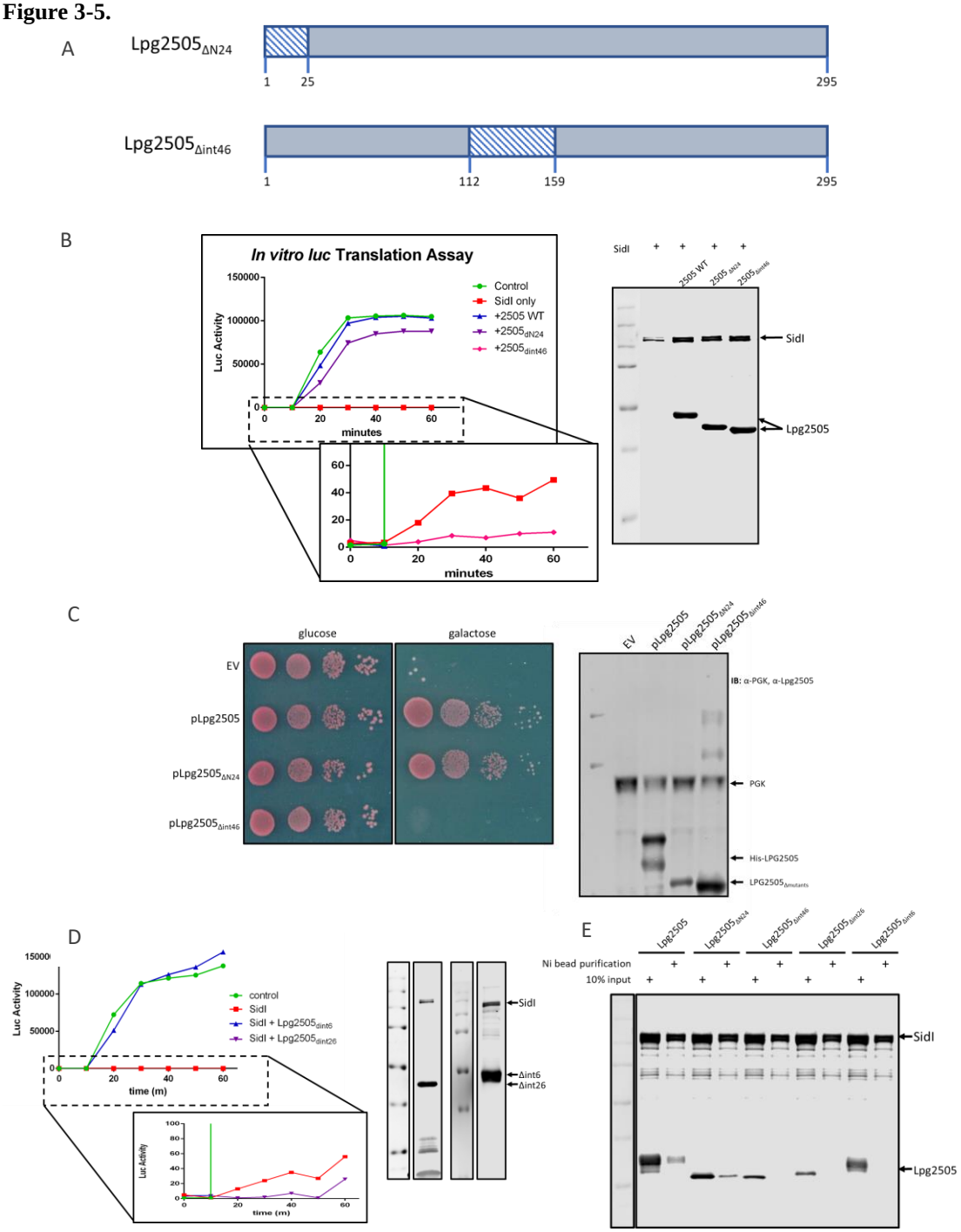
A
Lpg2505ΔN24
1
25
295
Lpg2505Δint46
1
112
159
295
B
In vitro luc Translation Assay
Luc Activity
minutes
Control
SidI only
+2505 WT
+2505ΔN24
+2505Δint46
SidI
Lpg2505
C
glucose
galactose
EV
pLpg2505
pLpg2505ΔN24
pLpg2505Δint46
IB: α-PGK, α-Lpg2505
PGK
His-LPG2505
LPG2505Δmutants
D
Luc Activity
time (m)
control
SidI
SidI + Lpg2505Δint6
SidI + Lpg2505Δint26
SidI
Δint6
Δint26
E
Ni bead purification
10% input
Lpg2505
Lpg2505ΔN24
Lpg2505Δint46
Lpg2505Δint26
Lpg2505Δint6
SidI
Lpg2505

Discussion

The study of *L. pneumophila*'s use of metaeffectors to tightly regulate virulence began with LubX and SidH in 2010, in which the idea was first introduced (Kubori et al., 2010). Since 2010, PTM abrogation pairs (SidM/SidD and AnkX/Lem3) (Tan et al., 2011; Tan & Luo, 2011), cognate effector modification pairs (SidH/LubX, LegC3/LupA and SidEs/SidJ) (Black et al., 2019; Gan, Zhen, et al., 2019; Kubori et al., 2010; Urbanus et al., 2016) and direct inactivation pairs (RavJ/LegL1 and now SidI/Lpg2505) have been characterized, with only a small number of examples each. In addition, the importance of metaeffector regulation can be surmised by both the evolutionary retention seen with the syntenic pairs and the negative effects seen when some metaeffectors are removed from the genome (Burstein et al., 2016; Yancheng Liu & Luo, 2007; Shames et al., 2017). Therefore, it is likely that other *Legionella* metaeffectors remain to be discovered and the use of metaeffectors by other intracellular pathogens will be seen as well.

The replication defect reported for the Δ*lpg2505* strain illustrates the importance of SidI regulation (Shames et al., 2017). Our study reveals the mechanism in which Lpg2505 performs this important regulation. What is interesting about the interaction between Lpg2505 and SidI is that it occurs within the bacteria itself. This is unexpected, as how would SidI function within the host cell if it is already bound to its inhibitor? It could be as simple as altering molecular amounts. When probing the levels of endogenous expression, we saw an elevation in Lpg2505 detection after SidI expression had waned. This would indicate a temporal control based on the varying amounts of SidI and Lpg2505 translocated into the host. I performed an *in vitro* translation assay in which I titrated the amount of Lpg2505 and recorded the level of rescue based on the molar ratio of SidI:Lpg2505. It took approximately 20x the amount of SidI, for Lpg2505 to fully rescue translation in the assay (**Fig. 3-6**), corroborating the idea that an increase in Lpg2505 production levels may be the way in which *L. pneumophila* limits SidI activity within the host cell. The increased amount of translocated SidI for the Δ*lpg2505* strain indicates that the interaction with Lpg2505 may interfere with secretion into the host. The level of detectable SidI from the strain overexpressing Lpg2505 within the bacteria was greater than the level of detectable SidI in the Δ*lpg2505* strain and yet no translocated SidI was detected. For that same strain, translocated Lpg2505 was detectable ensuring the lack of detectable SidI was not due to a problem with the infection. Perhaps this is a close resemblance to what occurs after the replicative phase, when the activity of SidI needs to be repressed. The increase in Lpg2505 production during that period might

lead to an increase in binding to SidI within the bacteria stopping translocation, but also increasing the amount of Lpg2505 in the host, effectively shutting down already translocated SidI.

I was able to identify a region of Lpg2505 that is necessary for inhibiting SidI. What remains to be discovered is the region of SidI that interacts with Lpg2505. Determining the location of SidI which is bound by Lpg2505 may shed some light on the catalytic function of SidI. Lpg2505 may bind to SidI in a manner similar to LegL1, in the catalytic pocket, thereby competitively inhibiting the enzymatic process. Based on my findings, however, I do not believe this to be the case. For one, the titration experiment shows the necessity of a greater than 1 stoichiometry between SidI and Lpg2505 for complete inhibition. Second, if Lpg2505 is already interacting with SidI within the *L. pneumophila* cell, it is difficult to imagine that an already tightly bound competitive inhibitor would release from the catalytic pocket when the function of SidI is needed. Our results also suggest that Lpg2505 has no enzymatic activity. First, there is no obvious enzymatic pocket within the structure. Second, I performed several extensive screenings to identify Lpg2505 substitution mutants that no longer inhibited SidI and no such mutants were obtained by chemical and error prone PCR mutagenesis, despite testing potentially millions of mutants (data not shown). Finally, I was unable to separate SidI from Lpg2505 to determine if there was a Lpg2505-dependent modification on SidI (data not shown), indicating a very strong interaction, not a transient one like those typically seen with enzyme and substrate.

Previously characterized effectors and metaeffectors require the presence of a host factor that is absent within *L. pneumophila*, thereby preventing any activity until translocation into the host. For example, most effectors target proteins only found in Eukaryotes, such as small GTPases, ubiquitin ligases, immune response regulators, etc. (Qiu & Luo, 2017). As for metaeffectors, LubX requires ubiquitin and the host proteasome while SidJ requires calmodulin (Black et al., 2019; Gan, Zhen, et al., 2019; Kubori et al., 2010). For Lpg2505 however, this seems to not be the case. What remains to be determined is the identification of some host factor required for a change in the activity of Lpg2505, if there is one, although our data suggest there is not one. It would be interesting to see if other effector/metaeffector pairs interact before translocation and if so, how does the interaction affect translocation or activity once in the host.

Based on the results of this study, I believe the inhibition of SidI activity within the host cell is likely dependent on the molecular ratio of SidI to Lpg2505. I suggest this simple model: During the initial stages of infection, the expression of SidI increases, making the SidI:Lpg2505

ratio greater than 1. This allows the movement of SidI into the host to inhibit protein translation, thereby freeing up essential nutrients for the replicative phase. Once replication begins to slow and inhibition of host translation is no longer needed, the expression of SidI decreases while the expression of Lpg2505 increases, decreasing the ratio to less than 1. The increased amount of Lpg2505 binds to the SidI remaining in the bacteria, halting translocation, and at the same time, moves into the host to bind to and shut down the already translocated SidI. By relying simply on changes in expression levels, *L. pneumophila* can maintain a finite regulation of SidI activity. A more sensitive method to detect the levels of translocated endogenous SidI and Lpg2505 throughout the infection cycle would be useful in determining the validity of the proposed model.

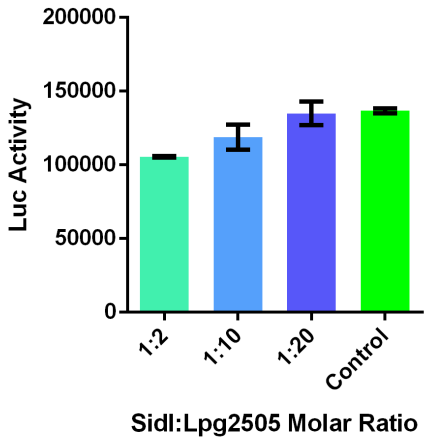

Figure 3-6. RRL *in vitro* translation assay comparing varied molar ratios of SidI and Lpg2505. Four different identical *luc* translation reactions were prepared. 50ng of His_6-SidI and increasing amounts of His_6-SUMO-Lpg2505, to achieve the molar ratios indicated, were added to three of the reactions. No proteins were added to one for a positive control. The reactions were incubated at 30°C for 1 hour. The luminescence for each reaction was then measured. The assay was performed in duplicate with error bars indicating the variability between the two experiments.

CHAPTER 4. MATERIALS AND METHODS

Media, bacterial strains, plasmid construction and cell culturing/transfection.

The bacterial and yeast strains used in these studies are listed in Table A-1, plasmids and primers are listed in Table A-2. All *L. pneumophila* strains used were derivatives of the Philadelphia 1 strain Lp02 (Karen H Berger & Isberg, 1993). *E. coli* strains were grown and maintained on LB agar with the addition of antibiotics when necessary. Strains of *L. pneumophila* were grown and maintained on CYE agar or in AYE broth as previously described (Karen H Berger & Isberg, 1993). The Lp02Δ*setA*, Lp02Δ*lpg2505* strains were constructed as previously described (Luo & Isberg, 2004). Briefly, the flanking regions on either side of *setA* were amplified using the primer sets setAKO-up-F-SalI/setAKO-up-R-BamHI and setAKO-down-F-BamHI/setAKO-down-R-SacI. The DNA fragments were then inserted into the R6K vector pSR47s (Merriam, Mathur, Maxfield-Boumil, & Isberg, 1997) using three-way ligation. The construct was introduced to strain Lp02 using tri-parental mating and clones carrying the vector backbone containing the flanking region inserts were selected for using CYE with kanamycin and streptomycin (Luo & Isberg, 2004). The clones were then passaged on CYE with 5% sucrose to select for bacterial cells that no longer carried the vector backbone. Finally, mutants carrying the deletion were identified by PCR. *Lpg2505* was deleted in the same fashion using the primer sets lpg2505KO-up-F-SalI/ lpg2505KO-up-R-BglII and lpg2505KO-down-F-BglII/lpg2505KO-down-R-SacI. For complementation experiments, Lp02 genes, and their mutants, were expressed from the RSF1010-derived plasmid pZL507 (Xu et al., 2010) using thymidine auxotrophic selection. To construct a plasmid for expression in *L. pneumophila* under arabinose control, *sidI* was inserted into the vector pBAD22, containing the arabinose inducible P_{BAD} promoter (Guzman et al., 1995) using the primer set pBAD22-sidI-NcoI-F/pBAD22-sidI-SalI-R. Then the region of pBAD22::*sidI* beginning with *araC* and ending with the ribosomal *rrnB* terminator was cloned into the broad host range plasmid pBBR1MCS (Kovach, Phillips, Elzer, & Peterson, 1994) using the primer set pBAD-up-of-*araC*-XbaI-F/pBAD-down-of-term-XhoI-R. Antibiotics were added as required with the following final concentrations: streptomycin, 30 μg/mL (*E. coli*); ampicillin, 50 μg/mL (*E. coli*); kanamycin, 50 μg/mL (*E. coli*); chloramphenicol, 5 μg/mL (*L. pneumophila*).

HEK293T cells were cultured in Dulbecco's Modified Eagle Medium (DMEM) supplemented with 10% (v/v) fetal bovine serum (FBS) under an atmosphere of 5% CO2 at 37°C. For transfection, HEK293T cells were seeded at a density of $6x10^5$ cells per 10 cm dish and cultured for 24 h. For cross-linking and immunoprecipitation experiments, 15 µg of plasmid DNA expressing HA- and FLAG-tagged SetA or SopD2 were transfected into cells of 80% confluence. After 24 h cultivation, cells were lysed for *in vivo* formaldehyde cross-linking reactions and further immunoprecipitation. To examine whether the identified Rab GTPases are glucosylation targets of SetA, 10 µg of plasmids expressing HA- and FLAG-tagged SetA or $SetA_{D134,136A}$ were co-transfected with 5 µg of plasmids expressing HA- and FLAG-tagged Rab1, Rab5c or Rab7 respectively. The Rab GTPases were further immunoprecipitated for the glucosylation assays. To examine whether SetA has a preference for a GTP-bound or GDP-bound form of Rab1, 10 µg of plasmids expressing HA- and FLAG-tagged SetA were co-transfected with 5 µg of plasmids expressing HA- and FLAG-tagged $Rab1_{Q70L}$ or $Rab1_{S25N}$, respectively. Each form of Rab1 was then affinity purified for LC-MS analyses to determine the rates of modification. For analyzing the binding ability of unmodified or modified Rab1 to GDI1 or SidM, 10 µg of plasmids expressing FLAG-tagged SetA or $SetA_{D134,136A}$ were co-transfected with 5 µg of plasmids expressing HA-tagged Rab1. GDI1 or SidM bound to Rab1 were co-precipitated and analyzed by LC-MS.

In vivo formaldehyde cross-linking

HEK293T cells expressing HA- and FLAG-tagged SetA or SopD2 were trypsinized and pelleted in 1.5 mL reaction tubes. The pellets were washed once in PBS and resuspended in 1 mL of PBS. *In vivo* formaldehyde cross-linking of intact cells was carried out in PBS buffer by adding 27 µl of 37% formaldehyde at 37°C for 10 min. The cross-linking reaction was quenched for 10 min at 30°C by the addition of 0.125 M glycine. After cross-linking, cells were pelleted and washed once with PBS. Then cells were lysed for further immunoprecipitation and LC-MS analyses.

Immunoprecipitation

For immunoprecipitation, cells expressing bait proteins were lysed in 1 mL of lysis buffer containing 150 mM Tris-HCl (pH 7.5), 150 mM NaCl, and 1% Triton. The lysates were clarified at 12,000 × g for 15 min to remove cell debris and the supernatants were incubated with anti-HA or anti-FLAG agarose beads (Sigma-Aldrich) overnight at 4°C. For cross-linking

immunoprecipitation, we used anti-HA agarose beads to minimize the adverse impact of cross-linking on the affinity between antibodies and bait proteins. The beads with bound proteins were washed four times with 1 mL of lysis buffer. Finally, the bound proteins were eluted by FLAG or HA peptides and boiled for 5 min in SDS-PAGE sample buffer containing 60 mM Tris-HCl (pH 6.8), 1.7% (w/v) SDS, 6% (v/v) glycerol, 100 mM dithiothreitol (DTT), and 0.002% (w/v) bromophenol blue. The eluted samples were then stored at -20°C for further analyses.

Bacterial infection

HEK293T cells were transfected with plasmids containing the gene for the FCγII receptor or the gene 4×FLAG-Rab1 using Lipofectamine 3000 (Life Technology) according to the manufacturer's instructions. After 24 h, the cells were infected with *L. pneumophila* strains Lp02, Lp02Δ*setA*, Lp02Δ*setA*(pSetA) and Lp02Δ*setA*(pSetA$_{D134,136A}$) opsonized with rabbit anti-*Legionella* antibodies at 1:500 for 1 h at a MOI of 100. The infection was allowed to proceed for 30 min, after which the cells were collected, lysed in RIPA buffer (Thermo Fisher Scientific) and the 4×FLAG-Rab1 was immunoprecipitated using FLAG beads (Sigma-Aldrich). The M2 beads were then washed three times with RIPA buffer and three times with TBS (20 mM Tris-HCl PH=8.0, 150 mM NaCl). The 4×FLAG-Rab1 was competitively eluted from the FLAG beads using 3×FLAG peptide at a concentration of 500 μg/mL. The eluted protein was concentrated, treated with SDS-PAGE sample buffer, boiled for 10 min and separated by SDS-PAGE. Samples (Coomassie stained gel slices) were further processed for LC-MS analysis.

Immunoblotting analysis and antibodies

Rabbit polyclonal serum against SetA was produced by Jiaxuan Biotech Company (Shanghai, China). Antibody-containing serum was further affinity-purified against SetA covalently coupled to an Affigel matrix (Bio-Rad) using standard protocols (Duménil & Isberg, 2001). Polyclonal antibodies against SidI and Lpg2505 were generated at the Pocono Rabbit Farm and Laboratory using recombinant His$_6$-tagged SidI and untagged Lpg2505 purified from *E. coli* to immunize the rabbits. The α-SidI and α-Lpg2505 antibodies were affinity purified following a standard protocol (Andree Hubber et al., 2014). For immunoblotting, the protein samples were separated by SDS-PAGE and transferred onto polyvinylidene difluoride (PVDF) or nitrocellulose (NC) membranes. After blocking with 5% milk for 1 h, membranes were incubated with the

appropriate primary antibodies: anti-SetA (1:2,000), anti-SidI (1:3,000), anti-Lpg2505 (1:3,000), anti-FLAG (Cwbio, China, 1:2,500), anti-HA (Cwbio, China, 1:2,500), anti-His (Cwbio, China, 1:2,500), anti-GDI1 (abcom, China, 1:2500), anti-ICDH (Xu et al., 2010) overnight at 4°C. Then the membranes were washed 3 times with Tris-buffered saline containing 0.1% (v/v) Tween 20 (TBST) and incubated with horseradish peroxidase (HRP)-conjugated (Cwbio, China, 1:5,000) or fluorescence dye-conjugated secondary antibodies for 1 h at room temperature. After washing four 4 times with TBST, antibody bands were visualized with the enhanced chemiluminescent (ECL) reagents (Tanon, China) by using a Tanon-5200 Image System (Tanon, China) or on an Odyssey detection system (Li-Cor).

Protein purification

The *E. coli* strain BL21(DE3) was used as the host for expression and purification of recombinant proteins. Rab1, $Rab1_{S25N}$ and $Rab1_{Q70L}$ were purified as GST-fusion proteins; SetA, $SetA_{D134,136A}$, AnkX, SidM and LepB were purified as His_6-fusion proteins. For protein purification, 10 mL of the overnight culture of the *E. coli* strain harboring the appropriate plasmids was transferred to 500 mL of fresh LB medium and grown at 37°C until the OD600 value reached 0.6–0.8. The bacterial culture was allowed to cool down to 16°C before the addition of isopropyl β-D-1-thiogalactopyranoside (IPTG) at a final concentration of 0.2 mM to induce protein expression. After overnight incubation (16~18 h) at 16°C, bacterial cells were harvested by spinning at 5,000 × g for 10 min and the pellets were resuspended in 30 mL of Tris-HCl buffer (25 mM, pH 7.5) containing 150 mM NaCl. Then bacterial cells were lysed by sonication on ice for 30 min. The lysates were centrifuged at 12,000 × g for 15 min to remove cellular debris and the supernatants were incubated for 2 h with either Ni-NTA or glutathione resins (GenScript) at 4°C with gentle rotation. The protein-bound beads were washed three times with Tris-HCl buffer (25 mM, pH 7.5) containing 150 mM NaCl. Elution was carried out with 300 mM imidazole for His_6-tagged proteins and 25 mM reduced glutathione for GST fusion proteins. To produce guanine nucleotide-free Rab1 for *in vitro* GTP-loading and GTPase activity assays, GST-Rab1 was washed with PBS containing 20 mM EDTA before elution with 25 mM reduced glutathione. Eluted proteins were further dialyzed twice in a buffer containing 25 mM Tris-HCl (pH 7.5), 150 mM NaCl, 5% (vol/vol) glycerol, and 1 mM dithiothreitol (DTT).

Preparation of the active and inactive forms of GST-Rab1

The active form GST-Rab1:GTP were obtained using the nucleotide exchange method (Christoforidis & Zerial, 2000). Briefly, 20 µL of GST-Rab1 attached to glutathione beads were washed with 100 µL of nucleotide exchange buffer (NE buffer: 20 mM HEPES, 100 mM NaCl, 10 mM EDTA, 5 mM MgCl2, 1 mM DTT, pH 7.5) containing 10 µM non-hydrolyzable GTP analog GTPγS and incubated for 10 min at room temperature in a 0.5 mL tube. The sample was centrifuged, and the NE buffer was removed. Then 100 µL of NE buffer containing 1 mM GTPγS was added and incubated for 30 min under rotation. Subsequently, the NE buffer was removed and the above procedure was repeated twice. Then the beads were washed with 100 µL of nucleotide stabilization buffer (NS buffer: 20 mM HEPES, 100 mM NaCl, 5 mM MgCl2, 1 mM DTT, pH 7.5) containing 10 µM GTPγS and further incubated with 100 µL of NS buffer in the presence of 1 mM GTPγS for 20 min at room temperature under rotation. For consistency, the GST-Rab1:GDP was obtained exactly as above except that the NE and NS buffers contained the same concentration of GDP instead of GTPγS. Finally, 10 µL of beads bound with GST-Rab1:GTP or GST-Rab1:GDP were used for *in vitro* glucosylation reactions.

***In vitro* glucosylation reactions**

1.4 µM of recombinant His_6-SetA or His_6-$SetA_{D134,136A}$ was incubated for 1 h at 37°C with 1 µM of GST-Rab1 in 20 µL of the reaction buffer containing 50 µM UDP-glucose, 1 mM MnCl2, 20 mM Tris-HCl (PH 7.5) and 150 mM NaCl. For the analysis of substrate preference between two nucleotide-binding states, 1.4 µM of recombinant His_6-SetA was incubated with 1 µM of GST-Rab1S25N or GST-Rab1Q70L under the same reaction conditions. Glucosylation reactions were terminated by boiling at 95°C for 5 min in SDS-PAGE sample buffer. The reaction mixtures were separated by 10% SDS-PAGE and the corresponding Rab1 bands were processed for LC-MS/MS analysis.

GTPase activity assay

GTPase activity was assayed by measuring the liberated phosphate from GTP hydrolysis using the malachite green method (Xu et al., 2010). Briefly, 1 mM purified Rab1 (either glucosylated or unmodified) from SetA- or $SetA_{D134,136A}$-expressing *E. coli* cells was incubated for

2 h at room temperature with 50 µL of GTPase reaction buffer (1 mM GTP, 10 mM HEPES, 125 mM KCl, 5 mM MgCl2, PH = 7.0) with or without the addition of 0.1 mM LepB. Then 200 µL of the malachite green reagent (2 volumes of 0.0812% malachite green, 1 volume of 5.72% ammonium molybdate dissolved in 6 M HCl, 1 volume of 2.32% polyvinyl alcohol and 2 volumes of distilled water) was added. The reactions were allowed to proceed for 2 min and were terminated by the addition of 25 µL of 34% sodium citrate. After 30 min incubation, the absorbance at 620 nm was measured. A control with no enzymes was used as a blank.

GTP-loading assay

GST-Rab1 was overexpressed in *E. coli* together with His_6-SetA or His_6-$SetA_{D134,136A}$. The modification rates of affinity purified Rab1 were analyzed via mass spectrometry before testing the ability of each to load 35SγGTP (a non-hydrolyzable GTP analog). Nucleotide-free modified and unmodified GST-Rab1 (6.6 µM) were incubated in 100 µL nucleotide exchange buffer containing 25 mM Tris-HCl (pH 7.5), 50 mM NaCl, 5 mM MgCl2, and 0.1 mM EDTA with 5 mM unlabeled GDP for 2 hours at room temperature. 15 µCi 35SγGTP (Perkin-Elmer) in 50 µL nucleotide exchange buffer was added to the samples. Reaction aliquots were withdrawn at indicated time points, placed onto nitrocellulose membrane filters (VSWP02500; Millipore) atop a vacuum platform attached to a waste liquid container. Membranes were washed three times using nucleotide exchange buffer to remove the free nucleotides and were then transferred into scintillation vials containing 8 mL scintillation fluid (Beckman). Incorporated 35SγGTP was measured by a scintillation counter at 1 min per count.

In-gel digestion and LC-MS/MS analysis

Upon SDS-PAGE fractionation, the band of interest was excised and subjected to in-gel trypsin digestion as previously described (Hu, Liu, Yu, & Liu, 2014). LC-MS analyses of protein digests were carried out on a hybrid ion trap-Orbitrap mass spectrometer (LTQ Orbitrap Velos, Thermo Scientific) coupled with nanoflow reversed-phase liquid chromatography (EASY-nLC 1000, Thermo Scientific). The capillary column (75 µm × 150 mm) with a laser-pulled electrospray tip (Model P-2000, Sutter instruments) was home-packed with 4 µm, 100 Å Magic C18AQ silica-based particles (Michrom BioResources Inc., Auburn, CA) and run at 250 nL/min with the following mobile phases (A: 97% water, 3% acetonitrile, and 0.1% formic acid; B: 90%

acetonitrile, 10% water, and 0.1% formic acid). The LC gradient started at 7% B for 3 min and then was linearly increased to 37% in 40 min. Next, the gradient was quickly ramped to 90% in 2 min and stayed there for 10 min. The gradient was then switched back to 100% solvent A for column equilibration. Eluted peptides from the capillary column were electrosprayed directly onto the mass spectrometer for MS and MS/MS analyses in a data-dependent acquisition mode. One full MS scan (m/z 350–1500) was acquired by the Orbitrap mass analyzer with R = 60,000 and simultaneously the ten most intense ions were selected for fragmentation under collision-induced dissociation (CID) or electron transfer dissociation (ETD). Dynamic exclusion was set with repeat duration of 30 s and exclusion duration of 12 s.

SidI and Lpg2505 translocation by *L. pneumophila*

Bacteria of relevant *L. pneumophila* strains were grown overnight with or without 1% arabinose and/or 0.1 mM IPTG. The bacteria were used to infect activated U937 cultures at a MOI of 20 for 3 hrs. Infected cells were lysed with 0.02% saponin, which lyses membranes of mammalian cells but not of bacterial cells, for 1 hr on ice. The soluble lysates were either probed directly for SidI and Lpg2505 using the specific antibodies or immunoprecipitated using the specific antibodies and protein G beads (Thermo Fisher) and then probed using specific antibodies.

Intracellular growth assay

For infection experiments, *L. pneumophila* strains were grown to the post-exponential phase as measured by optical density of the culture (OD600 = 3.3–3.8) and judged by an increase in bacterial motility. For the *L. pneumophila* intracellular growth assay, 4×10^5 bone marrow-derived mouse macrophages were seeded on glass coverslips in a 24-well plate. The cells were then infected with the indicated *L. pneumophila* strains expressing GFP from pAM239 (Derré & Isberg, 2005) at a MOI of 0.5 and grown at 37°C in the presence of 5% CO_2. After 2 hrs, the infection was synchronized by washing the monolayers three times with warmed, sterile PBS. At 14 hpi, cells attached to coverslips were washed 3 times with PBS and fixed using 4% paraformaldehyde at room temperature for 20 minutes. The coverslips were mounted and imaged using an IX-81 Olympus fluorescence microscope and the bacteria per vacuole were enumerated for each strain.

In vitro translation assay

To assay the ability of SidI to inhibit host translation, ½ reactions of Rabbit Reticulocyte Lysate System, Nuclease Treated (Promega, # L4960) were set up using the provided protocol. Indicated amounts (50ng of His_6-SidI, 100ng of His_6-SUMO-Lpg2505, or 75ng untagged Lpg2505 if not specified) of purified protein was added. Reactions with nothing added were used as the positive control. The reactions were incubated at 30°C for 60-100 minutes with 2.5 µl aliquots of each reaction assayed at the indicated time points. The aliquots were dispensed into a white 96 well plate, 50 µl of luciferase assay reagent (LAR) (Promega, # E1500) was added to each well and the luminescence was measured using a BioTek Synergy 2 microplate reader.

Lpg2505 crystal structure determination

For preparation and purification, *E. coli* BL21 strains harboring the encoding *lpg2505* gene plasmids were grown in LB (Luria-Bertani) medium supplemented with 100 mg/mL ampicillin and induced at an OD_{600} of 0.8-1.0 by 0.4 mM isopropyl-β-D-thiogalactopyranoside (IPTG) for 12-16 hours at 18˚C. For selenomethionine-substituted lpg2505 (SeMet-2505), *E. coli* BL21 strains harboring the plasmid encoded *lpg2505* were grown in M9 medium supplemented with 2 mM $MgSO_4$, 2 mM $CaCl_2$, 0.25 mg/mL Vitamin B, 100 mg/mL ampicillin, 2 g/L D-Glucose, 1 g/L NHCl, 40 mg/L selenomethionine-substituted, and nineteen amino acids (40 mg/per). All following purification steps were performed at 4˚C. The concentration of the purified protein was calculated using the theoretical extinction coefficient.

His_6-tagged proteins were purified using the following protocol. The cell pellets were suspended in lysis buffer containing 50 mM Tris pH 8, 500 mM NaCl, 10% (v/v) glycerol, 5 mM β-mercaptoethanol, 20 mM imidazole, and protease inhibitors, and lysed using sonication. The cell lysate was centrifuged at 18,000 rpm for 30 min and the supernatant was collected and incubated with nickel-sepharose beads for 2 hours at 4 ˚C. The beads were washed by lysis buffer and eluted by lysis buffer containing a concentration gradient of imidazole: 50 mM, 100 mM, 200 mM, and 500 mM. Proteins of interest were pooled, concentrated, and ran through a Superdex 200 16/60 size-exclusion column (GE Healthcare) in 20 mM Tris-HCl pH 8.0, 200 mM NaCl, 2 mM DTT. The fractions of interest were pooled, concentrated to 15 mg/mL with an Amicon Centrifugal filter (Millipore), flash-frozen in liquid nitrogen, and stored at -80˚C.

Crystals of His_6-Lpg2505 were obtained at 25˚C using the sitting-drop diffusion method by mixing 0.4 µL of protein (15 mg/mL) with an equal volume of reservoir solution containing 0.1 M HEPES pH 7.5 and 25% PEG 3350. The crystals were observed within 24 hours. The crystals were cryoprotected by briefly soaking in a buffer containing 15-30% (v/v) glycerol and flash cooled in liquid nitrogen. For phase determination, the crystals of SeMet-substituted Lpg2505 were obtained using the same conditions as native crystals. Diffractions of native and SeMet-substituted crystals were collected at Shanghai Synchrotron Radiation Facility (SSRF) (Shanghai, China). Data sets were indexed, integrated, and scaled with HKL2000. The crystals belong to the space group P1211 with unit cell dimensions a=106.542, b=50.448, c=122.029, α=γ=90.0°, β=109.065°. There are four protein molecules in the asymmetric unit. The structure was determined by single-wavelength anomalous dispersion phasing using a selenomethionine-substituted Lpg2505 crystal with the program AutoSol. The diffraction resolution is approximately 2.54 Å, but to distinguish anomalous signals, we cut off the resolution at 2.6 Å. Model building and refinement were performed using the software COOT and PHENIX. Crystallographic data statistics are summarized in Table A-3.

Size Exclusion Chromatography

After purification using the method described above, proteins were concentrated to approximately 10 mg/mL with an Amicon Centrifugal filter (Millipore) and then injected into a Superdex 200 increase 10/300 column (GE Healthcare) with washing buffer consisting of 20 mM Tris-HCl pH 8.0 and 150 mM NaCl on an AKTA Pure system (GE Healthcare).

Bacterial two-hybrid assay

A Cya-reconstitution based two-hybrid system was used to evaluate the relationship between SidI and Lpg2505 using the methods described previously (Karimova et al., 1998). Specifically, *sidI* was fused to the T25 fragment in pKT25 and *lpg2505* was fused to the T18 fragment in pUT18c. After verification of expression in DH5α cells, the individual plasmids were mixed and co-transformed into BTH101 cells. Mixtures of the individual plasmids along with empty vector versions of the complimentary plasmids were also introduced to BTH101 as negative controls. The interaction was initially evaluated on LB plates containing X-gal and 0.2 mM IPTG.

Clones that formed blue colonies, indicating X-gal hydrolysis, were further analyzed using β-galactosidase activity measurements.

Yeast toxicity spotting assay

To evaluate the ability of Lpg2505 mutants to rescue SidI-dependent toxicity in yeast, *sidI* was cloned into the vector pSB157 under galactose-inducible control and *lpg2505* was cloned into p425GPD under constitutive expression. W303 clones containing both plasmids were spotted on both glucose and galactose to show the ability of Lpg2505 to allow growth under SidI expressing conditions. The expression of Lpg2505 was confirmed using immunoblotting and α-Lpg2505 antibodies.

CHAPTER 5. GENERAL DISCUSSION AND FUTURE DIRECTIONS

The work presented in this dissertation summarizes and contributes to the overall understanding of *L. pneumophila* pathogenesis. There have been many significant and novel discoveries associated with the study of this intracellular pathogen. For example, the ability of the SidE family enzymes to ubiquitinate their target without the use of an E1 or E2 enzyme (Qiu et al., 2016). Also, the identification of previously unidentified catalytic mechanisms, such as AMPylation by SidM, deAMPylation by SidD, phosphorylcholination by AnkX, de-phosphorylcholination by Lem3 and glutamylation by SidJ (Black et al., 2019; Gan, Zhen, et al., 2019; Müller et al., 2010; Tan et al., 2011; Tan & Luo, 2011). These among others were discussed in detail in chapter 1. *L. pneumophila* is also an effective model of intracellular bacterial replication.

One of the most unique aspects of *L. pneumophila* infection is the large number of effector proteins with redundant activities, making them dispensable for replication in laboratory models. This of course makes the study of each effector more difficult. The most widely accepted theory as to the reason such redundancy is maintained is the large variety in *L. pneumophila* hosts, which may require the bacterium to use different sets of effectors for the modulation of their cellular processes. In support of the theory, when entire regions of the *L. pneumophila* chromosome were deleted, associated variations in intracellular replication in amoebal species were observed (O'Connor et al., 2011). Two additional theories proposed are: 1) an unidentified need for a complex regulatory approach during infection requires a large and seemingly redundant effector pool or 2) a low selective pressure allows for an abundance of effector DNA accumulation from eukaryotic hosts without an evolutionary cost (Ensminger, 2016).

The complexity in *L. pneumophila* host regulation is demonstrated nicely in the number of identified effectors targeting Rab1, the small GTPase essential in many phases of vesicle trafficking. Manipulation of the entire GTPase cycle is achieved through the GDF and GEF activities of SidM (Machner & Isberg, 2006, 2007) and the GAP activity of LepB (Ingmundson et al., 2007). Multiple post-translational modifications are attached to Rab1 by *L. pneumophila* effectors, including, those listed previously for novel catalytic motifs as well as the glucosylation of Rab1 by the effector SetA. In chapter 2, the specifics of SetA-dependent glucosylation of Rab1 were presented. SetA preferentially modifies GDP-Rab1, glucosylation of Rab1 by SetA interferes

with the association of GDI1. Whereas glucosylation does not perturb GTP loading, it does interfere with GTP hydrolysis. Furthermore, glucosylation does not affect AMPylation or phosphorylcholination of Rab1, but initial AMPylation and phosphorylcholination do restrict subsequent glucosylation, suggesting that during infection SetA likely accesses Rab1 that has either not yet been modified or after the modifications were removed. Together, these findings lead to a proposed model in which SetA works to increase the pool of free Rab1, preventing association with GDIs while allowing Rab1 activation and further modification. One remaining problem is the cycle disruption caused by glucosylation, which restricts GTP hydrolysis and prevents further work by other effectors. This could ultimately restrict *L. pneumophila* growth. This may be remedied in a manner similar to AMPylation and phosphorylcholination, whereby a second effector specifically removes the glucose moiety placed by SetA. Identification of a SetA metaeffector which removes the glucose and allows continuation of the Rab1 cycle would aid in understanding the exact role of SetA in contributing to *L. pneumophila* regulation of Rab1.

The important roles of *L. pneumophila* metaeffectors were further highlighted in chapter 3, which focuses on the mechanism of Lpg2505-mediated regulation of SidI. When *lpg2505* is removed from the chromosome, the *L. pneumophila* replication efficiency is significantly reduced and that reduction is dependent on a catalytically active SidI (Shames et al., 2017). Using SEC, *in vitro* binding assays with purified proteins and a bacterial two-hybrid assay, we found that Lpg2505 regulates the activity of SidI by direct binding. Furthermore, overexpression of Lpg2505 led to inhibition of SidI translocation into the host cell, supporting the formation of a complex by these two proteins in the bacterial cells. This in conjunction with an expression pattern where SidI levels increase during early stages of infection, followed by an increase in Lpg2505 levels, suggesting a temporal-based control that relies on differing amounts of the interacting proteins for SidI activity regulation.

One important question that remains to be answered is the exact enzymatic function of SidI. Although host targets have been discovered, single residues important for the function of SidI have been identified, and some homology between SidI and bacterial glycosyltransferase enzymes has been established, we still do not know how SidI inhibits host translation. It is possible that Lpg2505 may not be the only effector involved in SidI regulation. If SidI interferes with host translation by modifying one or both of the elongation factors known to associate with SidI, perhaps there is another *L. pneumophila* effector that subsequently removes the modification, akin

to SidD and Lem3 (Tan et al., 2011; Tan & Luo, 2011). If such a metaeffector does exist and can be identified, this finding could lead to finally discovering the catalytic function of SidI.

The complexity of *L. pneumophila* infection lends difficulty to determining the exact role played by individual components during infection, but it also means an abundance of avenues to pursue and many fascinating questions left unanswered. There is still much to be gained in studying the interaction between *L. pneumophila* and its many hosts, for example more novel catalytic motifs with the potential for human therapies. Because the evolution of this pathogen is not believed to be driven by mammalian hosts, robust immune responses are more likely detectable in its interaction with humans and other mammals, which provide an infection model for revealing novel immune response mechanisms. My own research on *L. pneumophila* has not been easy, but it has been extremely rewarding and the knowledge I have gained will aid me greatly in my future endeavors.

REFERENCES

Abu-Zant, A., Jones, S., Asare, R., Suttles, J., Price, C., Graham, J., & Kwaik, Y. A. (2007). Anti-apoptotic signalling by the Dot/Icm secretion system of L. pneumophila. *Cellular microbiology, 9*(1), 246-264.

Anand, C. M., Skinner, A. R., Malic, A., & Kurtz, J. B. (1983). Interaction of L. pneumophilia and a free living amoeba (Acanthamoeba palestinensis). *J Hyg (Lond), 91*(2), 167-178. doi:10.1017/s0022172400060174

Andrews, H. L., Vogel, J. P., & Isberg, R. R. (1998). Identification of linked Legionella pneumophila genes essential for intracellular growth and evasion of the endocytic pathway. *Infect Immun, 66*(3), 950-958.

Angot, A., Vergunst, A., Genin, S., & Peeters, N. (2007). Exploitation of eukaryotic ubiquitin signaling pathways by effectors translocated by bacterial type III and type IV secretion systems. *PLoS pathogens, 3*(1), e3.

Banga, S., Gao, P., Shen, X., Fiscus, V., Zong, W.-X., Chen, L., & Luo, Z.-Q. (2007). Legionella pneumophila inhibits macrophage apoptosis by targeting pro-death members of the Bcl2 protein family. *Proceedings of the National Academy of Sciences, 104*(12), 5121-5126.

Bärlocher, K., Hutter, C. A., Swart, A. L., Steiner, B., Welin, A., Hohl, M., . . . Hilbi, H. (2017). Structural insights into Legionella RidL-Vps29 retromer subunit interaction reveal displacement of the regulator TBC1D5. *Nature communications, 8*(1), 1543.

Bartfeld, S., Engels, C., Bauer, B., Aurass, P., Flieger, A., Brüggemann, H., & Meyer, T. F. (2009). Temporal resolution of two-tracked NF-κB activation by Legionella pneumophila. *Cellular microbiology, 11*(11), 1638-1651.

Behnia, R., & Munro, S. (2005). Organelle identity and the signposts for membrane traffic. *Nature, 438*(7068), 597.

Belyi, Y., Niggeweg, R., Opitz, B., Vogelsgesang, M., Hippenstiel, S., Wilm, M., & Aktories, K. (2006). Legionella pneumophila glucosyltransferase inhibits host elongation factor 1A. *Proceedings of the National Academy of Sciences, 103*(45), 16953-16958.

Belyi, Y., Stahl, M., Sovkova, I., Kaden, P., Luy, B., & Aktories, K. (2009). Region of Elongation Factor 1A1 Involved in Substrate Recognition by Legionella pneumophila Glucosyltransferase Lgt1 IDENTIFICATION OF Lgt1 AS A RETAINING GLUCOSYLTRANSFERASE. *Journal of Biological Chemistry, 284*(30), 20167-20174.

Belyi, Y., Tabakova, I., Stahl, M., & Aktories, K. (2008). Lgt: a family of cytotoxic glucosyltransferases produced by Legionella pneumophila. *Journal of bacteriology, 190*(8), 3026-3035.

Berger, K. H., & Isberg, R. R. (1993). Two distinct defects in intracellular growth complemented by a single genetic locus in Legionella pneumophila. *Mol Microbiol, 7*(1), 7-19.

Berger, K. H., Merriam, J. J., & Isberg, R. R. (1994). Altered intracellular targeting properties associated with mutations in the Legionella pneumophila dotA gene. *Mol Microbiol, 14*(4), 809-822.

Berk, S. G., Ting, R. S., Turner, G. W., & Ashburn, R. J. (1998). Production of respirable vesicles containing live Legionella pneumophila cells by two Acanthamoeba spp. *Appl Environ Microbiol, 64*(1), 279-286.

Bhogaraju, S., Kalayil, S., Liu, Y., Bonn, F., Colby, T., Matic, I., & Dikic, I. (2016). Phosphoribosylation of ubiquitin promotes serine ubiquitination and impairs conventional ubiquitination. *Cell, 167*(6), 1636-1649. e1613.

Bhuin, T., & Roy, J. K. (2014). Rab proteins: the key regulators of intracellular vesicle transport. *Experimental cell research, 328*(1), 1-19.

Black, M. H., Osinski, A., Gradowski, M., Servage, K. A., Pawlowski, K., Tomchick, D. R., & Tagliabracci, V. S. (2019). Bacterial pseudokinase catalyzes protein polyglutamylation to inhibit the SidE-family ubiquitin ligases. *Science, 364*(6442), 787-792. doi:10.1126/science.aaw7446

Bourne, H. R. (1988). Do GTPases direct membrane traffic in secretion? *Cell, 53*(5), 669-671.

Brand, B. C., Sadosky, A. B., & Shuman, H. A. (1994). The Legionella pneumophila icm locus: a set of genes required for intracellular multiplication in human macrophages. *Mol Microbiol, 14*(4), 797-808.

Brenner, D. J., Steigerwalt, A. G., & McDade, J. E. (1979). Classification of the Legionnaires' disease bacterium: Legionella pneumophila, genus novum, species nova, of the family Legionellaceae, familia nova. *Ann Intern Med, 90*(4), 656-658.

Burstein, D., Amaro, F., Zusman, T., Lifshitz, Z., Cohen, O., Gilbert, J. A., . . . Segal, G. (2016). Genomic analysis of 38 Legionella species identifies large and diverse effector repertoires. *Nature genetics, 48*(2), 167.

Burstein, D., Zusman, T., Degtyar, E., Viner, R., Segal, G., & Pupko, T. (2009). Genome-scale identification of Legionella pneumophila effectors using a machine learning approach. *PLoS pathogens, 5*(7), e1000508.

Buscher, B. A., Conover, G. M., Miller, J. L., Vogel, S. A., Meyers, S. N., Isberg, R. R., & Vogel, J. P. (2005). The DotL protein, a member of the TraG-coupling protein family, is essential for viability of Legionella pneumophila strain Lp02. *Journal of bacteriology, 187*(9), 2927-2938.

Campodonico, E. M., Chesnel, L., & Roy, C. R. (2005). A yeast genetic system for the identification and characterization of substrate proteins transferred into host cells by the Legionella pneumophila Dot/Icm system. *Mol Microbiol, 56*(4), 918-933.

Chen, J., de Felipe, K. S., Clarke, M., Lu, H., Anderson, O. R., Segal, G., & Shuman, H. A. (2004). Legionella effectors that promote nonlytic release from protozoa. *Science, 303*(5662), 1358-1361. doi:10.1126/science.1094226

Cherfils, J., & Zeghouf, M. (2013). Regulation of small gtpases by gefs, gaps, and gdis. *Physiological reviews, 93*(1), 269-309.

Chetrit, D., Hu, B., Christie, P. J., Roy, C. R., & Liu, J. (2018). A unique cytoplasmic ATPase complex defines the Legionella pneumophila type IV secretion channel. *Nature microbiology, 3*(6), 678.

Chien, M., Morozova, I., Shi, S., Sheng, H., Chen, J., Gomez, S. M., . . . Feder, M. (2004). The genomic sequence of the accidental pathogen Legionella pneumophila. *Science, 305*(5692), 1966-1968.

Choy, A., Dancourt, J., Mugo, B., O'Connor, T. J., Isberg, R. R., Melia, T. J., & Roy, C. R. (2012). The Legionella effector RavZ inhibits host autophagy through irreversible Atg8 deconjugation. *Science, 338*(6110), 1072-1076.

Christoforidis, S., & Zerial, M. (2000). Purification and identification of novel Rab effectors using affinity chromatography. *Methods, 20*(4), 403-410.

Cirillo, J. D., Cirillo, S. L., Yan, L., Bermudez, L. E., Falkow, S., & Tompkins, L. S. (1999). Intracellular growth in Acanthamoeba castellanii affects monocyte entry mechanisms and enhances virulence of Legionella pneumophila. *Infect Immun, 67*(9), 4427-4434.

Cirillo, J. D., Falkow, S., & Tompkins, L. S. (1994). Growth of Legionella pneumophila in Acanthamoeba castellanii enhances invasion. *Infect Immun, 62*(8), 3254-3261.

Correia, A. M., Ferreira, J. S., Borges, V., Nunes, A., Gomes, B., Capucho, R., . . . Gomes, J. P. (2016). Probable Person-to-Person Transmission of Legionnaires' Disease. *N Engl J Med, 374*(5), 497-498. doi:10.1056/NEJMc1505356

Cory, S., Huang, D. C., & Adams, J. M. (2003). The Bcl-2 family: roles in cell survival and oncogenesis. *Oncogene, 22*(53), 8590.

Creasey, E. A., & Isberg, R. R. (2012). The protein SdhA maintains the integrity of the Legionella-containing vacuole. *Proceedings of the National Academy of Sciences, 109*(9), 3481-3486.

Cunha, B. A., Burillo, A., & Bouza, E. (2016). Legionnaires' disease. *Lancet, 387*(10016), 376-385. doi:10.1016/s0140-6736(15)60078-2

D'Costa, V. M., Braun, V., Landekic, M., Shi, R., Proteau, A., McDonald, L., . . . Brumell, J. H. (2015). Salmonella disrupts host endocytic trafficking by SopD2-mediated inhibition of Rab7. *Cell reports, 12*(9), 1508-1518.

de Felipe, K. S., Pampou, S., Jovanovic, O. S., Pericone, C. D., Senna, F. Y., Kalachikov, S., & Shuman, H. A. (2005). Evidence for acquisition of Legionella type IV secretion substrates via interdomain horizontal gene transfer. *Journal of bacteriology, 187*(22), 7716-7726.

De Leon, J. A., Qiu, J., Nicolai, C. J., Counihan, J. L., Barry, K. C., Xu, L., . . . Nomura, D. K. (2017). Positive and negative regulation of the master metabolic regulator mTORC1 by two families of Legionella pneumophila effectors. *Cell reports, 21*(8), 2031-2038.

Derré, I., & Isberg, R. R. (2005). LidA, a translocated substrate of the Legionella pneumophila type IV secretion system, interferes with the early secretory pathway. *Infect Immun, 73*(7), 4370-4380.

Diederen, B. (2008). Legionella spp. and Legionnaires' disease. *Journal of infection, 56*(1), 1-12.

Donaldson, J. G., & Jackson, C. L. (2000). Regulators and effectors of the ARF GTPases. *Current opinion in cell biology, 12*(4), 475-482.

Dong, N., Niu, M., Hu, L., Yao, Q., Zhou, R., & Shao, F. (2017). Modulation of membrane phosphoinositide dynamics by the phosphatidylinositide 4-kinase activity of the Legionella LepB effector. *Nature microbiology, 2*(3), 16236.

Dorer, M. S., Kirton, D., Bader, J. S., & Isberg, R. R. (2006). RNA interference analysis of Legionella in Drosophila cells: exploitation of early secretory apparatus dynamics. *PLoS pathogens, 2*(4), e34.

Duménil, G., & Isberg, R. R. (2001). The Legionella pneumophila IcmR protein exhibits chaperone activity for IcmQ by preventing its participation in high-molecular-weight complexes. *Mol Microbiol, 40*(5), 1113-1127.

Eisenreich, W., & Heuner, K. (2016). The life stage-specific pathometabolism of Legionella pneumophila. *FEBS Lett, 590*(21), 3868-3886. doi:10.1002/1873-3468.12326

Ensminger, A. W. (2016). Legionella pneumophila, armed to the hilt: justifying the largest arsenal of effectors in the bacterial world. *Current opinion in microbiology, 29*, 74-80.

Ensminger, A. W., & Isberg, R. R. (2010). E3 ubiquitin ligase activity and targeting of BAT3 by multiple Legionella pneumophila translocated substrates. *Infect Immun, 78*(9), 3905-3919.

Eylert, E., Herrmann, V., Jules, M., Gillmaier, N., Lautner, M., Buchrieser, C., . . . Heuner, K. (2010). Isotopologue Profiling of Legionella pneumophila ROLE OF SERINE AND GLUCOSE AS CARBON SUBSTRATES. *Journal of Biological Chemistry, 285*(29), 22232-22243.

Fan, H.-Y., Cheng, K. K., & Klein, H. L. (1996). Mutations in the rna polymerase ii transcription machinery suppress the hyperrecombination mutant hpr1 δ of saccharomyces cerevisiae. *Genetics, 142*(3), 749-759.

Fazzio, T. G., & Tsukiyama, T. (2003). Chromatin remodeling in vivo: evidence for a nucleosome sliding mechanism. *Molecular cell, 12*(5), 1333-1340.

Fields, B. S. (1996). The molecular ecology of legionellae. *Trends in microbiology, 4*(7), 286-290. Retrieved from https://www.sciencedirect.com/science/article/pii/0966842X9610041X?via%3Dihub

Finsel, I., Ragaz, C., Hoffmann, C., Harrison, C. F., Weber, S., van Rahden, V. A., . . . Hilbi, H. (2013). The Legionella effector RidL inhibits retrograde trafficking to promote intracellular replication. *Cell host & microbe, 14*(1), 38-50.

Fliermans, C. B., Cherry, W. B., Orrison, L. H., Smith, S. J., Tison, D. L., & Pope, D. H. (1981). Ecological distribution of Legionella pneumophila. *Appl Environ Microbiol, 41*(1), 9-16.

Fontana, M. F., Banga, S., Barry, K. C., Shen, X., Tan, Y., Luo, Z.-Q., & Vance, R. E. (2011). Secreted bacterial effectors that inhibit host protein synthesis are critical for induction of the innate immune response to virulent Legionella pneumophila. *PLoS pathogens, 7*(2), e1001289.

Franco, I. S., Shohdy, N., & Shuman, H. A. (2012). The Legionella pneumophila effector VipA is an actin nucleator that alters host cell organelle trafficking. *PLoS pathogens, 8*(2), e1002546.

Fraser, D. W., Tsai, T. R., Orenstein, W., Parkin, W. E., Beecham, H. J., Sharrar, R. G., . . . Brachman, P. S. (1977). Legionnaires' disease: description of an epidemic of pneumonia. *N Engl J Med, 297*(22), 1189-1197. doi:10.1056/nejm197712012972201

From the Centers for Disease Control and Prevention. Legionnaires' disease associated with cooling towers--Massachusetts, Michigan, and Rhode Island, 1993. (1994). *Jama, 272*(6), 426, 428.

Gan, N., Nakayasu, E. S., Hollenbeck, P. J., & Luo, Z.-Q. (2019). Legionella pneumophila inhibits immune signalling via MavC-mediated transglutaminase-induced ubiquitination of UBE2N. *Nature microbiology, 4*(1), 134.

Gan, N., Zhen, X., Liu, Y., Xu, X., He, C., Qiu, J., . . . Zhou, B. (2019). Regulation of phosphoribosyl ubiquitination by a calmodulin-dependent glutamylase. *Nature, 572*(7769), 387-391.

Gaspar, A. H., & Machner, M. P. (2014). VipD is a Rab5-activated phospholipase A1 that protects Legionella pneumophila from endosomal fusion. *Proceedings of the National Academy of Sciences, 111*(12), 4560-4565.

Ge, J., Gong, Y.-N., Xu, Y., & Shao, F. (2012). Preventing bacterial DNA release and absent in melanoma 2 inflammasome activation by a Legionella effector functioning in membrane trafficking. *Proceedings of the National Academy of Sciences, 109*(16), 6193-6198.

Ge, J., Xu, H., Li, T., Zhou, Y., Zhang, Z., Li, S., . . . Shao, F. (2009). A Legionella type IV effector activates the NF-κB pathway by phosphorylating the IκB family of inhibitors. *Proceedings of the National Academy of Sciences, 106*(33), 13725-13730.

Ghosal, D., Chang, Y. W., Jeong, K. C., Vogel, J. P., & Jensen, G. J. (2017). In situ structure of the Legionella Dot/Icm type IV secretion system by electron cryotomography. *EMBO reports, 18*(5), 726-732.

Gomez-Valero, L., & Buchrieser, C. (2019). Intracellular parasitism, the driving force of evolution of Legionella pneumophila and the genus Legionella. *Genes & Immunity*, 1.

Gomez-Valero, L., Rusniok, C., Carson, D., Mondino, S., Pérez-Cobas, A. E., Rolando, M., . . . Crumbach, J. (2019). More than 18,000 effectors in the Legionella genus genome provide multiple, independent combinations for replication in human cells. *Proceedings of the National Academy of Sciences, 116*(6), 2265-2273.

Gomez-Valero, L., Rusniok, C., Jarraud, S., Vacherie, B., Rouy, Z., Barbe, V., . . . Buchrieser, C. (2011). Extensive recombination events and horizontal gene transfer shaped the Legionella pneumophila genomes. *BMC genomics, 12*(1), 536.

Grosshans, B. L., Ortiz, D., & Novick, P. (2006). Rabs and their effectors: achieving specificity in membrane traffic. *Proceedings of the National Academy of Sciences, 103*(32), 11821-11827.

Gruenberg, J., & Maxfield, F. R. (1995). Membrane transport in the endocytic pathway. *Current opinion in cell biology, 7*(4), 552-563.

Gudiol, C., Verdaguer, R., Angeles Dominguez, M., Fernandez-Sevilla, A., & Carratala, J. (2007). Outbreak of Legionnaires' disease in immunosuppressed patients at a cancer centre: usefulness of universal urine antigen testing and early levofloxacin therapy. *Clin Microbiol Infect, 13*(11), 1125-1128. doi:10.1111/j.1469-0691.2007.01805.x

Guo, Z., Stephenson, R., Qiu, J., Zheng, S., & Luo, Z.-Q. (2014). A Legionella effector modulates host cytoskeletal structure by inhibiting actin polymerization. *Microbes Infect, 16*(3), 225-236.

Guzman, L.-M., Belin, D., Carson, M. J., & Beckwith, J. (1995). Tight regulation, modulation, and high-level expression by vectors containing the arabinose PBAD promoter. *Journal of bacteriology, 177*(14), 4121-4130.

Hayward, A. P., & Dinesh-Kumar, S. (2011). What can plant autophagy do for an innate immune response? *Annual review of phytopathology, 49*, 557-576.

Heidtman, M., Chen, E. J., Moy, M. Y., & Isberg, R. R. (2009). Large-scale identification of Legionella pneumophila Dot/Icm substrates that modulate host cell vesicle trafficking pathways. *Cellular microbiology, 11*(2), 230-248.

Hempstead, A. D., & Isberg, R. R. (2015). Inhibition of host cell translation elongation by Legionella pneumophila blocks the host cell unfolded protein response. *Proceedings of the National Academy of Sciences, 112*(49), E6790-E6797.

Hilbi, H., Hoffmann, C., & Harrison, C. F. (2011). Legionella spp. outdoors: colonization, communication and persistence. *Environ Microbiol Rep, 3*(3), 286-296. doi:10.1111/j.1758-2229.2011.00247.x

Hoffmann, C., Harrison, C. F., & Hilbi, H. (2014). The natural alternative: protozoa as cellular models for L egionella infection. *Cellular microbiology, 16*(1), 15-26. Retrieved from https://onlinelibrary.wiley.com/doi/pdf/10.1111/cmi.12235

Horwitz, M. A. (1987). Characterization of avirulent mutant Legionella pneumophila that survive but do not multiply within human monocytes. *J Exp Med, 166*(5), 1310-1328. doi:10.1084/jem.166.5.1310

Hsu, F., Luo, X., Qiu, J., Teng, Y.-B., Jin, J., Smolka, M. B., . . . Mao, Y. (2014). The Legionella effector SidC defines a unique family of ubiquitin ligases important for bacterial phagosomal remodeling. *Proceedings of the National Academy of Sciences, 111*(29), 10538-10543.

Hsu, F., Zhu, W., Brennan, L., Tao, L., Luo, Z.-Q., & Mao, Y. (2012). Structural basis for substrate recognition by a unique Legionella phosphoinositide phosphatase. *Proceedings of the National Academy of Sciences, 109*(34), 13567-13572.

Hu, M., Liu, Y., Yu, K., & Liu, X. (2014). Decreasing the amount of trypsin in in-gel digestion leads to diminished chemical noise and improved protein identifications. *Journal of proteomics, 109*, 16-25.

Huang, L., Boyd, D., Amyot, W. M., Hempstead, A. D., Luo, Z. Q., O'connor, T. J., . . . Isberg, R. R. (2011). The E Block motif is associated with Legionella pneumophila translocated substrates. *Cellular microbiology, 13*(2), 227-245.

Hubber, A., Arasaki, K., Nakatsu, F., Hardiman, C., Lambright, D., De Camilli, P., . . . Roy, C. R. (2014). The machinery at endoplasmic reticulum-plasma membrane contact sites contributes to spatial regulation of multiple Legionella effector proteins. *PLoS pathogens, 10*(7), e1004222.

Hubber, A., & Roy, C. R. (2010). Modulation of host cell function by Legionella pneumophila type IV effectors. *Annu Rev Cell Dev Biol, 26*, 261-283. doi:10.1146/annurev-cellbio-100109-104034

Hurtado-Lorenzo, A., Skinner, M., El Annan, J., Futai, M., Sun-Wada, G.-H., Bourgoin, S., . . . Ausiello, D. A. (2006). V-ATPase interacts with ARNO and Arf6 in early endosomes and regulates the protein degradative pathway. *Nature cell biology, 8*(2), 124.

Ichimura, Y., Kirisako, T., Takao, T., Satomi, Y., Shimonishi, Y., Ishihara, N., . . . Ohsumi, M. (2000). A ubiquitin-like system mediates protein lipidation. *Nature, 408*(6811), 488.

Ingmundson, A., Delprato, A., Lambright, D. G., & Roy, C. R. (2007). Legionella pneumophila proteins that regulate Rab1 membrane cycling. *Nature, 450*(7168), 365.

Isberg, R. R., O'Connor, T. J., & Heidtman, M. (2009). The Legionella pneumophila replication vacuole: making a cosy niche inside host cells. *Nat Rev Microbiol, 7*(1), 13-24. doi:10.1038/nrmicro1967

Jank, T., Böhmer, K. E., Tzivelekidis, T., Schwan, C., Belyi, Y., & Aktories, K. (2012). Domain organization of Legionella effector SetA. *Cellular microbiology, 14*(6), 852-868.

Jeong, K. C., Ghosal, D., Chang, Y.-W., Jensen, G. J., & Vogel, J. P. (2017). Polar delivery of Legionella type IV secretion system substrates is essential for virulence. *Proceedings of the National Academy of Sciences, 114*(30), 8077-8082.

Just, I., Selzer, J., Wilm, M., Von Eichel-Streiber, C., Mann, M., & Aktories, K. (1995). Glucosylation of Rho proteins by Clostridium difficile toxin B. *Nature, 375*(6531), 500.

Just, I., Wilm, M., Selzer, J., Rex, G., von Eichel-Streiber, C., Mann, M., & Aktories, K. (1995). The enterotoxin from Clostridium difficile (ToxA) monoglucosylates the Rho proteins. *Journal of Biological Chemistry, 270*(23), 13932-13936.

Kagan, J. C., & Roy, C. R. (2002). Legionella phagosomes intercept vesicular traffic from endoplasmic reticulum exit sites. *Nature cell biology, 4*(12), 945.

Kagan, J. C., Stein, M. P., Pypaert, M., & Roy, C. R. (2004). Legionella subvert the functions of Rab1 and Sec22b to create a replicative organelle. *J Exp Med, 199*(9), 1201-1211. doi:10.1084/jem.20031706

Kanamori, H., Weber, D. J., & Rutala, W. A. (2016). Healthcare Outbreaks Associated With a Water Reservoir and Infection Prevention Strategies. *Clin Infect Dis, 62*(11), 1423-1435. doi:10.1093/cid/ciw122

Karimova, G., Pidoux, J., Ullmann, A., & Ladant, D. (1998). A bacterial two-hybrid system based on a reconstituted signal transduction pathway. *Proceedings of the National Academy of Sciences, 95*(10), 5752-5756.

Khodr, A., Kay, E., Gomez-Valero, L., Ginevra, C., Doublet, P., Buchrieser, C., & Jarraud, S. (2016). Molecular epidemiology, phylogeny and evolution of Legionella. *Infection, genetics and evolution, 43*, 108-122.

Komano, T., Yoshida, T., Narahara, K., & Furuya, N. (2000). The transfer region of IncI1 plasmid R64: similarities between R64 tra and Legionella icm/dot genes. *Mol Microbiol, 35*(6), 1348-1359.

Kovach, M., Phillips, R., Elzer, P., & Peterson, K. (1994). pBBR1MCS: a broad-host-range cloning vector. *BioTechniques, 16*(5), 800-802.

Kuballa, P., Nolte, W. M., Castoreno, A. B., & Xavier, R. J. (2012). Autophagy and the immune system. *Annual review of immunology, 30*, 611-646.

Kubori, T., Hyakutake, A., & Nagai, H. (2008). Legionella translocates an E3 ubiquitin ligase that has multiple U-boxes with distinct functions. *Mol Microbiol, 67*(6), 1307-1319.

Kubori, T., Shinzawa, N., Kanuka, H., & Nagai, H. (2010). Legionella metaeffector exploits host proteasome to temporally regulate cognate effector. *PLoS pathogens, 6*(12), e1001216.

Laguna, R. K., Creasey, E. A., Li, Z., Valtz, N., & Isberg, R. R. (2006). A Legionella pneumophila-translocated substrate that is required for growth within macrophages and protection from host cell death. *Proceedings of the National Academy of Sciences, 103*(49), 18745-18750.

Lanternier, F., Tubach, F., Ravaud, P., Salmon, D., Dellamonica, P., Bretagne, S., . . . Lortholary, O. (2013). Incidence and risk factors of Legionella pneumophila pneumonia during anti-tumor necrosis factor therapy: a prospective French study. *Chest, 144*(3), 990-998. doi:10.1378/chest.12-2820

Lanzetti, L. (2007). Actin in membrane trafficking. *Current opinion in cell biology, 19*(4), 453-458.

Lee, P.-C., & Machner, M. P. (2018). The Legionella effector kinase LegK7 hijacks the host Hippo pathway to promote infection. *Cell host & microbe, 24*(3), 429-438. e426.

Levin, R. S., Hertz, N. T., Burlingame, A. L., Shokat, K. M., & Mukherjee, S. (2016). Innate immunity kinase TAK1 phosphorylates Rab1 on a hotspot for posttranslational modifications by host and pathogen. *Proceedings of the National Academy of Sciences, 113*(33), E4776-E4783.

Li, S., Zhang, L., Yao, Q., Li, L., Dong, N., Rong, J., . . . Chen, X. (2013). Pathogen blocks host death receptor signalling by arginine GlcNAcylation of death domains. *Nature, 501*(7466), 242.

Li, T., Lu, Q., Wang, G., Xu, H., Huang, H., Cai, T., . . . Shao, F. (2013). SET-domain bacterial effectors target heterochromatin protein 1 to activate host rDNA transcription. *EMBO reports, 14*(8), 733-740.

Lin, Y.-H., Doms, A. G., Cheng, E., Kim, B., Evans, T. R., & Machner, M. P. (2015). Host cell-catalyzed S-palmitoylation mediates Golgi targeting of the Legionella ubiquitin ligase GobX. *Journal of Biological Chemistry, 290*(42), 25766-25781.

Liu, Y., & Luo, Z.-Q. (2007). The Legionella pneumophila effector SidJ is required for efficient recruitment of endoplasmic reticulum proteins to the bacterial phagosome. *Infect Immun, 75*(2), 592-603.

Liu, Y., Zhu, W., Tan, Y., Nakayasu, E. S., Staiger, C. J., & Luo, Z.-Q. (2017). A Legionella effector disrupts host cytoskeletal structure by cleaving actin. *PLoS pathogens, 13*(1), e1006186.

Lomma, á., Dervins-Ravault, D., Rolando, M., Nora, T., Newton, H., Sansom, F., . . . Hartland, E. (2010). The Legionella pneumophila F-box protein Lpp2082 (AnkB) modulates ubiquitination of the host protein parvin B and promotes intracellular replication. *Cellular microbiology, 12*(9), 1272-1291.

Losick, V. P., Haenssler, E., Moy, M. Y., & Isberg, R. R. (2010). LnaB: a Legionella pneumophila activator of NF-κB. *Cellular microbiology, 12*(8), 1083-1097.

Losick, V. P., & Isberg, R. R. (2006). NF-κB translocation prevents host cell death after low-dose challenge by Legionella pneumophila. *Journal of Experimental Medicine, 203*(9), 2177-2189.

Lu, Q., Yao, Q., Xu, Y., Li, L., Li, S., Liu, Y., . . . Ben-Nissan, G. (2014). An iron-containing dodecameric heptosyltransferase family modifies bacterial autotransporters in pathogenesis. *Cell host & microbe, 16*(3), 351-363.

Luo, Z.-Q., & Isberg, R. R. (2004). Multiple substrates of the Legionella pneumophila Dot/Icm system identified by interbacterial protein transfer. *Proceedings of the National Academy of Sciences, 101*(3), 841-846.

Machner, M. P., & Isberg, R. R. (2006). Targeting of host Rab GTPase function by the intravacuolar pathogen Legionella pneumophila. *Developmental cell, 11*(1), 47-56.

Machner, M. P., & Isberg, R. R. (2007). A bifunctional bacterial protein links GDI displacement to Rab1 activation. *Science, 318*(5852), 974-977.

Maculins, T., Fiskin, E., Bhogaraju, S., & Dikic, I. (2016). Bacteria-host relationship: ubiquitin ligases as weapons of invasion. *Cell research, 26*(4), 499.

Marra, A., Blander, S. J., Horwitz, M. A., & Shuman, H. A. (1992). Identification of a Legionella pneumophila locus required for intracellular multiplication in human macrophages. *Proc Natl Acad Sci U S A, 89*(20), 9607-9611. doi:10.1073/pnas.89.20.9607

McDade, J. E., Shepard, C. C., Fraser, D. W., Tsai, T. R., Redus, M. A., & Dowdle, W. R. (1977). Legionnaires' disease: isolation of a bacterium and demonstration of its role in other respiratory disease. *N Engl J Med, 297*(22), 1197-1203. doi:10.1056/nejm197712012972202

Meng, Z., Moroishi, T., & Guan, K.-L. (2016). Mechanisms of Hippo pathway regulation. *Genes & development, 30*(1), 1-17.

Merriam, J. J., Mathur, R., Maxfield-Boumil, R., & Isberg, R. R. (1997). Analysis of the Legionella pneumophila fliI gene: intracellular growth of a defined mutant defective for flagellum biosynthesis. *Infect Immun, 65*(6), 2497-2501.

Michard, C., Sperandio, D., Baïlo, N., Pizarro-Cerdá, J., LeClaire, L., Chadeau-Argaud, E., . . . Gilbert, C. (2015). The Legionella kinase LegK2 targets the ARP2/3 complex to inhibit actin nucleation on phagosomes and allow bacterial evasion of the late endocytic pathway. *MBio, 6*(3), e00354-00315.

Molmeret, M., Bitar, D. M., Han, L., & Kwaik, Y. A. (2004). Cell biology of the intracellular infection by Legionella pneumophila. *Microbes Infect, 6*(1), 129-139.

Mukherjee, S., Liu, X., Arasaki, K., McDonough, J., Galán, J. E., & Roy, C. R. (2011). Modulation of Rab GTPase function by a protein phosphocholine transferase. *Nature, 477*(7362), 103.

Müller, M. P., Peters, H., Blümer, J., Blankenfeldt, W., Goody, R. S., & Itzen, A. (2010). The Legionella effector protein DrrA AMPylates the membrane traffic regulator Rab1b. *Science, 329*(5994), 946-949.

Mumberg, D., Müller, R., & Funk, M. (1995). Yeast vectors for the controlled expression of heterologous proteins in different genetic backgrounds. *Gene, 156*(1), 119-122.

Murata, T., Delprato, A., Ingmundson, A., Toomre, D. K., Lambright, D. G., & Roy, C. R. (2006). The Legionella pneumophila effector protein DrrA is a Rab1 guanine nucleotide-exchange factor. *Nature cell biology, 8*(9), 971.

Nagai, H., Kagan, J. C., Zhu, X., Kahn, R. A., & Roy, C. R. (2002). A bacterial guanine nucleotide exchange factor activates ARF on Legionella phagosomes. *Science, 295*(5555), 679-682.

Neunuebel, M. R., Chen, Y., Gaspar, A. H., Backlund, P. S., Yergey, A., & Machner, M. P. (2011). De-AMPylation of the small GTPase Rab1 by the pathogen Legionella pneumophila. *Science, 333*(6041), 453-456.

Newton, H. J., Ang, D. K., van Driel, I. R., & Hartland, E. L. (2010). Molecular pathogenesis of infections caused by Legionella pneumophila. *Clinical microbiology reviews, 23*(2), 274-298. Retrieved from https://www.ncbi.nlm.nih.gov/pmc/articles/PMC2863363/pdf/0052-09.pdf

Ninio, S., Zuckman-Cholon, D. M., Cambronne, E. D., & Roy, C. R. (2005). The Legionella IcmS–IcmW protein complex is important for Dot/Icm-mediated protein translocation. *Mol Microbiol, 55*(3), 912-926.

Nuoffer, C., Davidson, H. W., Matteson, J., Meinkoth, J., & Balch, W. E. (1994). A GDP-bound of rab1 inhibits protein export from the endoplasmic reticulum and transport between Golgi compartments. *The Journal of Cell Biology, 125*(2), 225-237.

O'Connor, T. J., Zheng, H., VanRheenen, S. M., Ghosh, S., Cianciotto, N. P., & Isberg, R. R. (2016). Iron Limitation Triggers Early Egress by the Intracellular Bacterial Pathogen Legionella pneumophila. *Infect Immun, 84*(8), 2185-2197. doi:10.1128/iai.01306-15

O'Connor, T. J., Adepoju, Y., Boyd, D., & Isberg, R. R. (2011). Minimization of the Legionella pneumophila genome reveals chromosomal regions involved in host range expansion. *Proceedings of the National Academy of Sciences, 108*(36), 14733-14740.

O'Connor, T. J., Boyd, D., Dorer, M. S., & Isberg, R. R. (2012). Aggravating genetic interactions allow a solution to redundancy in a bacterial pathogen. *Science, 338*(6113), 1440-1444.

Oesterlin, L. K., Goody, R. S., & Itzen, A. (2012). Posttranslational modifications of Rab proteins cause effective displacement of GDP dissociation inhibitor. *Proceedings of the National Academy of Sciences, 109*(15), 5621-5626.

Pearson, J. S., Giogha, C., Ong, S. Y., Kennedy, C. L., Kelly, M., Robinson, K. S., . . . Oates, C. V. (2013). A type III effector antagonizes death receptor signalling during bacterial gut infection. *Nature, 501*(7466), 247.

Pfeffer, S. R. (2001). Rab GTPases: specifying and deciphering organelle identity and function. *Trends in cell biology, 11*(12), 487-491.

Pike, C. M., Boyer-Andersen, R., Kinch, L. N., Caplan, J. L., & Neunuebel, M. R. (2019). The Legionella effector RavD binds phosphatidylinositol-3-phosphate and helps suppress endolysosomal maturation of the Legionella-containing vacuole. *J Biol Chem, 294*(16), 6405-6415. doi:10.1074/jbc.RA118.007086

Porter, A. G., & Jänicke, R. U. (1999). Emerging roles of caspase-3 in apoptosis. *Cell death and differentiation, 6*(2), 99.

Price, C. T., Al-Khodor, S., Al-Quadan, T., Santic, M., Habyarimana, F., Kalia, A., & Kwaik, Y. A. (2009). Molecular mimicry by an F-box effector of Legionella pneumophila hijacks a conserved polyubiquitination machinery within macrophages and protozoa. *PLoS pathogens, 5*(12), e1000704.

Qiu, J., & Luo, Z.-Q. (2017). Legionella and Coxiella effectors: strength in diversity and activity. *Nature Reviews Microbiology, 15*(10), 591.

Qiu, J., Sheedlo, M. J., Yu, K., Tan, Y., Nakayasu, E. S., Das, C., . . . Luo, Z.-Q. (2016). Ubiquitination independent of E1 and E2 enzymes by bacterial effectors. *Nature, 533*(7601), 120.

Ragaz, C., Pietsch, H., Urwyler, S., Tiaden, A., Weber, S. S., & Hilbi, H. (2008). The Legionella pneumophila phosphatidylinositol-4 phosphate-binding type IV substrate SidC recruits endoplasmic reticulum vesicles to a replication-permissive vacuole. *Cellular microbiology, 10*(12), 2416-2433.

Rolando, M., Escoll, P., Nora, T., Botti, J., Boitez, V., Bedia, C., . . . Skarina, T. (2016). Legionella pneumophila S1P-lyase targets host sphingolipid metabolism and restrains autophagy. *Proceedings of the National Academy of Sciences, 113*(7), 1901-1906.

Rolando, M., Sanulli, S., Rusniok, C., Gomez-Valero, L., Bertholet, C., Sahr, T., . . . Buchrieser, C. (2013). Legionella pneumophila effector RomA uniquely modifies host chromatin to repress gene expression and promote intracellular bacterial replication. *Cell host & microbe, 13*(4), 395-405.

Rothman, J. E., & Orci, L. (1992). Molecular dissection of the secretory pathway. *Nature, 355*(6359), 409.

Rothmeier, E., Pfaffinger, G., Hoffmann, C., Harrison, C. F., Grabmayr, H., Repnik, U., . . . Griffiths, G. (2013). Activation of Ran GTPase by a Legionella effector promotes microtubule polymerization, pathogen vacuole motility and infection. *PLoS pathogens, 9*(9), e1003598.

Rowbotham, T. J. (1980). Preliminary report on the pathogenicity of Legionella pneumophila for freshwater and soil amoebae. *Journal of clinical pathology, 33*(12), 1179-1183. Retrieved from https://jcp.bmj.com/content/jclinpath/33/12/1179.full.pdf

Rubin, R. (2017). Most Drinking Water-Associated Disease Outbreaks Linked to Legionella. *Jama, 318*(24), 2420. doi:10.1001/jama.2017.19202

Sandkovsky, U., Sandkovsky, G., Suh, J., Smith, B., Sharp, V., & Polsky, B. (2008). Legionella pneumonia and HIV: case reports and review of the literature. *AIDS Patient Care STDS, 22*(6), 473-481. doi:10.1089/apc.2007.0111

Schoebel, S., Oesterlin, L. K., Blankenfeldt, W., Goody, R. S., & Itzen, A. (2009). RabGDI displacement by DrrA from Legionella is a consequence of its guanine nucleotide exchange activity. *Molecular cell, 36*(6), 1060-1072.

Schuelein, R., Spencer, H., Dagley, L. F., Li, P. F., Luo, L., Stow, J. L., . . . Buchrieser, C. (2018). Targeting of RNA Polymerase II by a nuclear Legionella pneumophila Dot/Icm effector SnpL. *Cellular microbiology, 20*(9), e12852.

Seaman, M. N. (2005). Recycle your receptors with retromer. *Trends in cell biology, 15*(2), 68-75.

Segal, G., Purcell, M., & Shuman, H. A. (1998). Host cell killing and bacterial conjugation require overlapping sets of genes within a 22-kb region of the Legionella pneumophila genome. *Proceedings of the National Academy of Sciences, 95*(4), 1669-1674.

Segal, G., & Shuman, H. A. (1997). Characterization of a new region required for macrophage killing by Legionella pneumophila. *Infect Immun, 65*(12), 5057-5066.

Shames, S. R., Liu, L., Havey, J. C., Schofield, W. B., Goodman, A. L., & Roy, C. R. (2017). Multiple Legionella pneumophila effector virulence phenotypes revealed through high-throughput analysis of targeted mutant libraries. *Proc Natl Acad Sci U S A, 114*(48), E10446-e10454. doi:10.1073/pnas.1708553114

Shen, X., Banga, S., Liu, Y., Xu, L., Gao, P., Shamovsky, I., . . . Luo, Z. Q. (2009). Targeting eEF1A by a Legionella pneumophila effector leads to inhibition of protein synthesis and induction of host stress response. *Cell Microbiol, 11*(6), 911-926. doi:10.1111/j.1462-5822.2009.01301.x

Shohdy, N., Efe, J. A., Emr, S. D., & Shuman, H. A. (2005). Pathogen effector protein screening in yeast identifies Legionella factors that interfere with membrane trafficking. *Proceedings of the National Academy of Sciences, 102*(13), 4866-4871.

Silveira, T. N., & Zamboni, D. S. (2010). Pore formation triggered by Legionella spp. is an Nlrc4 inflammasome-dependent host cell response that precedes pyroptosis. *Infect Immun, 78*(3), 1403-1413. doi:10.1128/iai.00905-09

Simon, S., Wagner, M. A., Rothmeier, E., Müller-Taubenberger, A., & Hilbi, H. (2014). Icm/Dot-dependent inhibition of phagocyte migration by L egionella is antagonized by a translocated Ran GTPase activator. *Cellular microbiology, 16*(7), 977-992.

Singh, N., Stout, J. E., & Yu, V. L. (2004). Prevention of Legionnaires' disease in transplant recipients: recommendations for a standardized approach. *Transpl Infect Dis, 6*(2), 58-62. doi:10.1111/j.1399-3062.2004.062_2.x

Sol, A., Lipo, E., de Jesús-Díaz, D. A., Murphy, C., Devereux, M., & Isberg, R. R. (2019). Legionella pneumophila translocated translation inhibitors are required for bacterial-induced host cell cycle arrest. *Proceedings of the National Academy of Sciences, 116*(8), 3221-3228.

Son, J., Jo, C. H., Murugan, R. N., Bang, J. K., Hwang, K. Y., & Lee, W. C. (2015). Crystal structure of Legionella pneumophila type IV secretion system effector LegAS4. *Biochemical and biophysical research communications, 465*(4), 817-824.

Spanò, S., Gao, X., Hannemann, S., Lara-Tejero, M., & Galán, J. E. (2016). A bacterial pathogen targets a host Rab-family GTPase defense pathway with a GAP. *Cell host & microbe, 19*(2), 216-226.

Tan, Y., Arnold, R. J., & Luo, Z.-Q. (2011). Legionella pneumophila regulates the small GTPase Rab1 activity by reversible phosphorylcholination. *Proceedings of the National Academy of Sciences, 108*(52), 21212-21217.

Tan, Y., & Luo, Z.-Q. (2011). Legionella pneumophila SidD is a deAMPylase that modifies Rab1. *Nature, 475*(7357), 506.

Teo, W. X., Yang, Z., Kerr, M. C., Luo, L., Guo, Z., Alexandrov, K., . . . Teasdale, R. D. (2017). Salmonella effector SopD2 interferes with Rab34 function. *Cell biology international, 41*(4), 433-446.

Tilney, L. G., Harb, O. S., Connelly, P. S., Robinson, C. G., & Roy, C. R. (2001). How the parasitic bacterium Legionella pneumophila modifies its phagosome and transforms it into rough ER: implications for conversion of plasma membrane to the ER membrane. *J Cell Sci, 114*(Pt 24), 4637-4650.

Tisdale, E. J., Bourne, J. R., Khosravi-Far, R., Der, C. J., & Balch, W. (1992). GTP-binding mutants of rab1 and rab2 are potent inhibitors of vesicular transport from the endoplasmic reticulum to the Golgi complex. *The Journal of Cell Biology, 119*(4), 749-761.

Toulabi, L., Wu, X., Cheng, Y., & Mao, Y. (2013). Identification and structural characterization of a Legionella phosphoinositide phosphatase. *Journal of Biological Chemistry, 288*(34), 24518-24527.

Urbanus, M. L., Quaile, A. T., Stogios, P. J., Morar, M., Rao, C., Di Leo, R., . . . Cuff, M. E. (2016). Diverse mechanisms of metaeffector activity in an intracellular bacterial pathogen, Legionella pneumophila. *Molecular systems biology, 12*(12), 893.

Urwyler, S., Nyfeler, Y., Ragaz, C., Lee, H., Mueller, L. N., Aebersold, R., & Hilbi, H. (2009). Proteome analysis of Legionella vacuoles purified by magnetic immunoseparation reveals secretory and endosomal GTPases. *Traffic, 10*(1), 76-87.

Vincent, C. D., Friedman, J. R., Jeong, K. C., Buford, E. C., Miller, J. L., & Vogel, J. P. (2006). Identification of the core transmembrane complex of the Legionella Dot/Icm type IV secretion system. *Mol Microbiol, 62*(5), 1278-1291.

Viner, R., Chetrit, D., Ehrlich, M., & Segal, G. (2012). Identification of two Legionella pneumophila effectors that manipulate host phospholipids biosynthesis. *PLoS pathogens, 8*(11), e1002988.

Vogel, J. P., Andrews, H. L., Wong, S. K., & Isberg, R. R. (1998). Conjugative transfer by the virulence system of Legionella pneumophila. *Science, 279*(5352), 873-876.

Vogel, J. P., & Isberg, R. R. (1999). Cell biology of Legionella pneumophila. *Current opinion in microbiology, 2*(1), 30-34.

Wan, M., Wang, X., Huang, C., Xu, D., Wang, Z., Zhou, Y., & Zhu, Y. (2019). A bacterial effector deubiquitinase specifically hydrolyses linear ubiquitin chains to inhibit host inflammatory signalling. *Nature microbiology*, 1.

Wang, C.-Y., Mayo, M. W., Korneluk, R. G., Goeddel, D. V., & Baldwin, A. S. (1998). NF-κB antiapoptosis: induction of TRAF1 and TRAF2 and c-IAP1 and c-IAP2 to suppress caspase-8 activation. *Science, 281*(5383), 1680-1683.

Wang, Z., McCloskey, A., Cheng, S., Wu, M., Xue, C., Yu, Z., . . . Liu, X. (2018). Regulation of the small GTPase Rab1 function by a bacterial glucosyltransferase. *Cell discovery, 4*(1), 53.

Weber, S. S., Ragaz, C., & Hilbi, H. (2009). Pathogen trafficking pathways and host phosphoinositide metabolism. *Mol Microbiol, 71*(6), 1341-1352.

Worby, C. A., Mattoo, S., Kruger, R. P., Corbeil, L. B., Koller, A., Mendez, J. C., . . . Dixon, J. E. (2009). The fic domain: regulation of cell signaling by adenylylation. *Molecular cell, 34*(1), 93-103.

Xie, Z., & Klionsky, D. J. (2007). Autophagosome formation: core machinery and adaptations. *Nature cell biology, 9*(10), 1102.

Xu, L., Shen, X., Bryan, A., Banga, S., Swanson, M. S., & Luo, Z.-Q. (2010). Inhibition of host vacuolar H+-ATPase activity by a Legionella pneumophila effector. *PLoS pathogens, 6*(3), e1000822.

Yao, J., Yang, F., Sun, X., Wang, S., Gan, N., Liu, Q., . . . Wei, Y. (2018). Mechanism of inhibition of retromer transport by the bacterial effector RidL. *Proceedings of the National Academy of Sciences, 115*(7), E1446-E1454.

Yau, R., & Rape, M. (2016). The increasing complexity of the ubiquitin code. *Nature cell biology, 18*(6), 579.

Zerial, M., & McBride, H. (2001). Rab proteins as membrane organizers. *Nature reviews Molecular cell biology, 2*(2), 107.

Zhu, W., Banga, S., Tan, Y., Zheng, C., Stephenson, R., Gately, J., & Luo, Z.-Q. (2011). Comprehensive identification of protein substrates of the Dot/Icm type IV transporter of Legionella pneumophila. *PloS one, 6*(3), e17638.

APPENDIX

Table A-1. Bacterial and yeast strains used in this study

Strains	Description	References/Sources
L. pneumophila		
Lp02	Wild type	(Merriam et al., 1997)
Lp03	*dotA*$^{-}$	(Merriam et al., 1997)
Lp02Δ*setA*		This study
Lp02Δ*setA*(pSetA)		This study
Lp02Δ*setA*(pSetA$_{D134,136A}$)		This study
Lp02Δ*lpg2505*		This study
Lp02Δ*sidI*		(Shen et al., 2009)
Lp02Δ*lpg2505*(P$_{BAD}$::*sidI*)		This study/(Guzman et al., 1995)
Lp02(P$_{BAD}$::*sidI*)		This study/(Guzman et al., 1995)
Lp02(P$_{BAD}$::*sidI*)(pLpg2505)		This study/(Guzman et al., 1995)
E. coli		
DH5α		TransGene Biotech
BL21-(DE3)		NEB
BTH101		(Karimova et al., 1998)
Saccharomyces cerevisiae		
W303		(Fan, Cheng, & Klein, 1996)

Table A-2. Plasmids and primers used in this study

Plasmids	**Properties**	**References or expressed proteins**
pET28a	For the expression of His_6-tagged proteins	SetA, $SetA_{D134,136A}$, SidM, AnkX, LepB
pcDNA4	Mammalian expression vector with N-terminal FLAG, HA, FLAG and HA tags	SetA, $SetA_{D134,136A}$, Rab1, $Rab1_{S25N}$, $Rab1_{Q70L,}$ Rab5c, Rab7, SopD2
pGEX-6p1	*E. coli* GST fusion vector	Rab1, $Rab1_{S25N}$, $Rab1_{Q70L}$
pZL507	Vector for His_6-tagged protein expression in *L. pneumophila*	(Xu et al., 2010)
pSB157-Flag	Low level expression in yeast under galactose induction	(Fazzio & Tsukiyama, 2003)
P425GPD	High level, constitutive expression in yeast	(Mumberg, Müller, & Funk, 1995)
pSetA	*setA* cloned into pZL507	This study
$pSetA_{D134,136A}$	$setA_{D134,136A}$ cloned into pZL507	This study
pSR47s	R6K vector for gene deletion	(Xu et al., 2010)
pQE30	For the expression of His_6-tagged proteins	SidI
pETSUMO	For the expression of His_6-SUMO-tagged proteins	Lpg2505
pAM239	Vector for GFP protein expression in *L. pneumophila*	(Dorer et al., 2006)
pLpg2505	*lpg2505* cloned into pZL507	This study
pBBR1MCS::P_{BAD}::*sidI*	*sidI* cloned into pBAD22 region and subcloned into pBBR1MCS	This study/(Guzman et al., 1995)/(Kovach et al., 1994)
Primer	**Sequence**	**Note**
setAKO-up-F-SalI	att**GTCGAC**agtgccgatcatgacgttattataa	To construct Δ*setA*
setAKO-up-R-BamHI	att**GGATCC**ttgagcctcttgaccagcctgtggt	To construct Δ*setA*
setAKO-down-F-BamHI	att**GGATCC**tcaaaggcaaccagaaaccgggcaa	To construct Δ*setA*
setAKO-down-R-SacI	att**GAGCTC**gcaccacaaaaaatcgccaaaaaat	To construct Δ*setA*
lpg2505KO-up-F-SalI	att**GTCGAC**ttgatcaaagataactccctttcta	To construct Δ*lpg2505*
lpg2505KO-up-R-BamHI	att**GGATCC**ttgcacatccttcagagagttgggc	To construct Δ*lpg2505*
lpg2505KO-down-F-BamHI	att**GGATCC**ggtaaagacgatgagcgcagtataa	To construct Δ*lpg2505*
lpg2505KO-down-R-SacI	att**GAGCTC**tacttccagccagcatgcgcatacc	To construct Δ*lpg2505*
SidI-BamHI-F	att**GGATCC**atgactaaaatatacttattaactg	For cloning ORF
SidI-SalI-R	att**GTCGAC**tcaaaataccagtatcgattcttta	For cloning ORF

Lpg2505-BglII-F	att**AGATCT**atgataaaaggaaaacttatgccca	For cloning ORF
Lpg2505-SalI-R	att**GTCGAC**ttataaaataattggtcgagttata	For cloning ORF
pKT25-sidI-PstI-F	att**CTGCAG**GGactaaaatatacttattaactg	For BacTH, 2 additional Gs to maintain frame
pKT25-sidI-BamHI-R	att**GGATCC**tcaaaataccagtatcgattcttta	For BacTH
pUT18c-lpg2505-PstI-F	att**CTGCAG**Gataaaaggaaaacttatgccca	For BacTH, 1 additional G to maintain frame
pUT18c-lpg2505-BglII-R	att**AGATCT**AGtaaaataattggtcgagttata	For BacTH
pBAD22-sidI-NcoI-F	att**CCATGG**ccatgactaaaatatacttattaactg	For cloning ORF into pBAD22
pBAD22-sidI-SalI-R	att**GTCGAC**tcaaaataccagtatcgattcttta	For cloning ORF into pBAD22
pBAD-up-of-araC-XbaI-F	att**TCTAGA**atcgatgcataatgtgcc	To clone into pBBR1MCS
pBAD-down-of-term-XhoI-R	att**CTCGAG**attgtctcatgagcggat	To clone into pBBR1MCS
Lpg2505t-25-295-BglII-F	att**AGATCT**atgaatgtaattacgactcta	To produce $Lpg2505_{\Delta N24}$
Lpg2505t-1-112-NotI-R	att**GCGGCCGC**ataactactgatttcttt	To produce $Lpg2505_{\Delta int46}$
Lpg2505t-159-295-NotI-F	att**GCGGCCGC**gcaaagcactcaaatacaa	To produce $Lpg2505_{\Delta int46}$
Lpg2505t-1-122-NotI-R	att**GCGGCCGCt**gttgtgaaggaaagatt	To produce $Lpg2505_{\Delta int26}$
Lpg2505t-149-295-NotI-F	att**GCGGCCGC**gatcgacctttatacaat	To produce $Lpg2505_{\Delta int26}$
Lpg2505t-1-132-NotI-R	att**GCGGCCGC**aatttcctgagccgcata	To produce $Lpg2505_{\Delta int6}$
Lpg2505t-139-295-NotI-F	att**GCGGCCGC**ggcttgtaagaatgacacc	To produce $Lpg2505_{\Delta int6}$

Table A-3. Lpg2505 data collection and refinement statistics

	lpg2505-SAD
Data Collection	
Space group	P1211
Cell dimensions	
a,b,c (Å)	106.542, 50.448, 122.029
α,β,γ (◦)	90, 109.065, 90
Wavelength (Å)	0.97919
Resolution (Å)	50-2.54 (2.63-2.54)
R_{merge}	0.143 (1.026)
I/σI	14.227 (2.174)
Completeness (%)	99.9 (91.3)
Redundancy	6.9 (7.2)
Refinement	
Resolution (Å)	50-2.54 (2.63-2.54)
No. reflections	38156 (3988)
R_{work}/R_{free} (%)	23.2/28.1
No. atoms	
Protein	8972
Ligands	24
water	146
B factors (Å^2)	
Protein	37.66
Ligands	33.35
R.m.s deviations	
Bond Lengths (Å)	0.008
Bond angles (◦)	1.30